

https://dspace.org/

A molecular mechanics study for selective complexation of metal ions in medical applications

Chantson, Tracy, Elizabeth

1994

http://hdl.handle.net/10539/22402

Chantson, Tracy, Elizabeth (1994) A molecular mechanics study for selective complexation of metal ions in medical applications, University of the Witwatersrand, Johannesburg, <http://hdl.handle.net/10539/22402>

Downloaded from a DSpace repository. https://dspace.org/

A MOLECULAR MECHANICS STUDY OF LIGANDS FOR SELECTIVE COMPLEXATION OF METAL IONS IN MEDICAL APPLICATIONS

Tracy Elizabeth Chantson

A dissertation submitted to the
Faculty of Science
University of the Witwatersrand, Johannesburg
for the degree of Master of Science

ABSTRACT

Molecular mechanics calculations are used to interpret and predict metal ion discrimination by coordinating ligands. Of particular interest are chelates exhibiting characteristics that single them out for potential medical application.

Selectivity patterns for several series of ligands are investigated with the help of strain energy profiles as a function of metal-donor atom bond distance. Ligands include simple, open-chain oxygen- and nitrogen-donors and triaza- and tetraazamacrocycles. Results are compared with X-ray crystallographic and solution data. Factors such as chelate ring size, conformational flexibility and preferred metal coordination geometry are found to influence metal specificity. Addition of pendent donor groups to macrocycles leads to rigid structures and selectivity predictions according to cavity size.

Interpretation of specific metal ion recognition by polyether antibiotics is attempted. Structural and steric factors are probed as possible determinants of metal choice. Both covalent and ionic bonding models are explored. The covalent approach results in predictions of metal selectivity which correlate with known selectivity patterns. Unfortunately, inability to optimise force field parameters in the ionic bonding approach forced us to abandon this model.

The main force field used is the TRIPOS (1992,1993) force field. It performs well in calculations involving a univariate scanning technique but has to be modified to obtain reasonable structure reproduction with the large antibiotics. Errors in thermodynamic data predictions are obtained, nonbonding parameters have yet to be properly parameterized and the allocation of partial atomic charges warrants closer examination. All of these factors contribute to the poor performance of the force field when ionic interactions between metal and donor atoms of the polyethers are assumed.

DECLARATION

I hereby declare that this dissertation represents my own work, supervised by Professor R.D. Hancock. This dissertation has not been submitted before for a higher degree at any other university.

T.E. Chantson
March, 1994.

ACKNOWLEDGEMENTS

The following contributions to this dissertation are gratefully acknowledged:

Professor R.D. Hancock, my supervisor, for advice and guidance throughout this project.

My family, who provided moral support.

Trudy Chantson, for extensive help with the word processing.

Peter Wade, for proofreading part of this dissertation.

The Research Grants Committees of the University of the Witwatersrand and the Foundation for Research and Development for financial support.

CONTENTS

		Page
List of Figures		ix
List of Tables		xiv
Abbreviations of Ligands		xvii
A.	INTRODUCTION	
A.1	Macrocyclic Ligands in Medicine	1
A.2	Polyether Antibiotics	2
A.3	Factors Determining Selectivity of Macrocyclic Ligands	3
	A.3.1 Effects of chelate ring size	3
	A.3.2 Flexibility of macrocycles	4
	A.3.3 Addition of pendant donor groups	6
	A.3.3.1 Preorganization	6
	A.3.3.2 N-substituted azamacrocycles	7
A.4	Factors Determining Selectivity of Polyether Antibiotics	9
	A.4.1 Monensin selectivity versus nigericin selectivity	9
	A.4.2 Conformational flexibility	11
	A.4.3 Thermodynamics of complexation	12
A.5	Application of Molecular Mechanics to Coordination Chemistry	14
	A.5.1 History and concepts	14

Page

A.5.2 The molecular mechanical potential 15
A.5.2.1 Parameterization 15
A.5.2.2 Minimization and conformational searching 16
A.5.2.3 Solvation 16
A.5.3 Molecular mechanics in coordination chemistry 17

A.6 The TRIPOS Force Field 18
A.6.1 Potential energy functions 18
A.6.2 Validation of the TRIPOS force field 21

A.7 Objectives of this Study 22

B. EXPERIMENTAL

B.1 Initial Coordinates 23

B.2 Molecular Dynamics 24

B.3 Determination of Cavity Size 24
B.3.1 Previous calculations 24
B.3.2 Univariate scans 27
B.3.3 Force field parameters for univariate scanning 27

B.4 Parameter Optimization 28

Page

C. RESULTS AND DISCUSSION

C.1 Four-Membered Chelate Rings 29
C.1.1 Coordination preferences of biologically interesting cations 29
C.1.2 Molecular mechanics calculations 35

C.2 Best-fit Sizes and Geometries of Metal Ions Coordinated to N-donor Macrocycles 39
C.2.1 Molecular mechanics calculations using constraints 40
C.2.2 9-aneN_3 and 12-aneN_3 complexes 41
C.2.3 12-aneN_4 complexes 49
C.2.4 13-aneN_4 complexes 55
C.2.5 14-aneN_4 complexes 59
C.2.6 15-aneN_4 complexes 64
C.2.7 16-aneN_4 complexes 67

C.3 Best-fit Sizes of Metal Ions Coordinated to N-functionalized N-donor Macrocycles 72
C.3.1 Open-chain ligands 74
C.3.1.1 EDTA and DTPA 74
C.3.1.2 NTA and analogues 76
C.3.2 Triacetate triazamacrocycles 78
C.3.2.1 TACNTA 78
C.3.2.2 TACDTA 81
C.3.3 Comparison of conformers for each N-functionalized azamacrocycle 82
C.3.3.1 DOTA and analogues 83
C.3.3.2 TETA and analogues 87
C.3.3.3 HETA and analogues 90

Page

C.3 4 Effect of pendent donor group - acetate, hydroxyphenyl, hydroxybenzyl 92

C.4 Structural Factors Affecting Selectivity in Monensin and Related Polyether Antibiotics 95

C.4.1 Previous molecular mechanics calculations 95

C.4.2 Optimization of TRIPOS force field 95

C.4.2.1 Covalent assumption 95

C.4.2.2 Ionic assumption 100

Electrostatic parameters 100

Nonbonding parameters 102

C.4.3 Comparison with previous molecular mechanics studies 104

C.4.3.1 18-crown-6 105

C.4.3.2 Valinomycin 107

C.4.4 Application to monensin and related polyether antibiotics 109

D. CONCLUSIONS 113

E. REFERENCES 115

F. CRYSTAL STRUCTURE REFERENCES 121

LIST OF FIGURES

Figure	Page
A.1 : The five conformers of 14-aneN$_4$. H-atoms above the plane of the page are designated with a +, while those below the plane of the page are designated with a -. The cis and trans prefixes indicate whether the two remaining ligand sites in octahedral coordination would be cis or trans to each other.	*4*
A.2 : The trans-I, trans-III and cis-V conformers of 14-aneN$_4$.	*5*
A.3 : Examples of highly preorganized ligands.	*7*
A.4 : Ligands with pendent donor groups.	*8*
A.5 : Structural formulae for monensin (A and B), nigericin, dianemycin and A2O4A.	*10*
A.6 : Components of intramolecular strain.	*18*
C.1 : The series of tetraaza macrocycles 12-aneN$_4$ through 16-aneN$_4$.	*25*
C.2 : Distribution of coordination number for Na-acetate complexes. Minimum Na-O bond length/ Å = 2.212 Maximum Na-O bond length/ Å = 2.765	*30*
C.3 : Distribution of coordination number for K-acetate complexes. Minimum K-O bond length/ Å = 2.572 Maximum K-O bond length/ Å = 3.000	*31*

C.4 : Distribution of coordination number for Mg-acetate complexes.
Minimum Mg-O bond length/ Å = 1.978
Maximum Mg-O bond length/ Å = 2.398 31

C.5 : Distribution of coordination number for Ca-acetate complexes.
Minimum Ca-O bond length/ Å = 2.250
Maximum Ca-O bond length/ Å = 2.862 32

C.6 : Distribution of coordination number for Mn-acetate complexes.
Minimum Mn-O bond length/ Å = 1.817
Maximum Mn-O bond length/ Å = 2.688 32

C.7 : Distribution of coordination number for Zn-acetate complexes.
Minimum Zn-O bond length/ Å = 1.718
Maximum Zn-O bond length/ Å = 2.564 33

C.8 : Strain energy, ΣU, of an isolated four-membered chelate ring involving acetate and nitrate as a function of metal-oxygen bond length and O-M-O bond angles appropriate to different coordination geometries. 36

C.9 : Strain energy, ΣU, of an isolated four-membered chelate ring involving phosphate as a function of metal-oxygen bond length and O-M-O bond angles appropriate to different coordination geometries. 37

C.10 : Strain energy, ΣU, of isolated acetate, nitrate and phosphate ligands as a function of metal-oxygen bond length and unconstrained O-M-O angles. 38

C.11 : Lowest strain energy geometry for (A) the four-membered chelate ring, (B) the five-membered chelate ring, and (C) the six-membered chelate ring. 39

C.12 : The six conformers of (a) 13-aneN$_4$, and (b) 15-aneN$_4$ with respect to the possible orientations of the N-H hydrogen atoms. H-atoms above the plane of the page are assigned +, while those below the plane of the page are assigned - . 41

C.13 : Triazamacrocycles discussed in this section. 42

C.14(a) : Total strain energy, ΣU, as a function of ideal M-N bond length for the +++ conformer of 9-aneN$_3$ and 12-aneN$_3$. Lowest energy structures for both are drawn. 43

C.14(b) : Total strain energy, ΣU, as a function of ideal M-N bond length for the chair-chair-chair and chair-chair-boat conformations of 12-aneN$_3$. M was constrained to be tetrahedral. 46

C.14(c) : Total strain energy, ΣU, as a function of ideal M-N bond length for the chair-chair-chair (i), chair-chair-boat and chair-chair-chair (ii) conformations of 12-aneN$_3$Br. M was constrained to be tetrahedral. 47

C.15 : Total strain energy, ΣU, as a function of ideal M-N bond length for the four conformers of 12-aneN$_4$. 50

C.16 : Variation of complex stability of the tetraazamacrocycles 12-aneN$_4$ through 16-aneN$_4$, relative to 12-aneN$_4$, as a function of macrocyclic ring size. The metal ions are represented as circles of radii proportional to their ionic radii. 53

C.17 : Stereoviews of lowest energy conformers of (a) 12-aneN$_4$, (b) 14-aneN$_4$ and (c) 16-aneN$_4$. 54

C.18 : Total strain energy, ΣU, as a function of ideal M-N bond length for the six conformers of 13-aneN$_4$ 57

C.19 : Total strain energy, ΣU, as a function of ideal M-N bond length for the five conformers of 14-aneN$_4$ 62

C.20 : Total strain energy, ΣU, as a function of ideal M-N bond length for the six conformers of 15-aneN$_4$ 65

C.21 : Total strain energy, ΣU, as a function of ideal M-N bond length for the four conformers of 16-aneN$_4$ 68

C.22 : Ligands N-functionalized with acetate, hydroxyphenyl and hydroxybenzyl groups. 73

C.23 : Total strain energy, ΣU, as a function of ideal M-L bond length for EDTA and DTPA. 75

C.24 : Total strain energy, ΣU, as a function of ideal M-L bond length for NTA, NTP, NTHP and NTHB. 77

C.25(a) : Total strain energy, ΣU, as a function of ideal M-L bond length for type I and type II configurations of TACNTA using angle constraints. 80

C.25(b) : Total strain energy, ΣU, as a function of ideal M-L bond length for unconstrained TACNTA and TACDTA. 82

C.26 : Stereoviews of lowest energy conformers of (a) DOTA, (b) S, and (c) X. 85

C.27 : The two isomers of DOTA differing in the orientation of the acetate arms. 86

C.28 : Stereoviews of lowest energy conformers of (a) TETA, (b) T, and (c) Y. 88

C.29 : Variation of log stability constants with various metal ions for the macrocyclic series DOTA, TRITA and TETA. 89

C.30 : Stereoviews of lowest energy conformers of (a) HETA, (b) U, and (c) Z. 91

C.31 : The K monensin crystal structure showing intramolecular hydrogen bonding and cation coordination. 97

C.32 : Total strain energy, ΣU, as a function of ideal M-O bond length for the polyether antibiotics, monensin and nigericin. Covalent bonding was assumed, electrostatics was ignored and hydrogen bonding was constrained. 98

C.33 : Stereoviews of initial and final energy minimized structures of (a) M^+-monensin and (b) M^+-nigericin. 99

C.34 : The structures of (a) 18-crown-6 and (b) valinomycin. 104

C.35 : Structures of (a) $[Na(18C6)]^+$ and (b) $[K(18C6)]^+$. The Na^+ complex is in the C_1 conformer, and the K^+ complex in the D_{3d} conformer. 105

C.36 : Stereoviews of initial and final energy minimized structures of (a) K^+-valinomycin and (b) Na^+-valinomycin. 108

LIST OF TABLES

Table — Page

C.1 : Molecular mechanics cavity size calculations for planar conformers. 25

C.2 : Distribution of coordination number for metal-nitrate complexes. 33

C.3 : Distribution of coordination number for metal-phosphate complexes. 34

C.4 : Best-fit M-N bond lengths for triaza- and tetraaza macrocycles constrained to be trigonal planar and square planar respectively. 40

C.5 : Crystallographic data on 9-aneN_3 (L1) and 12-aneN_3 (L2) complexes. 44

C.6 : Compilation of log K_1 values for complexes of the triazamacrocycles. 48

C.7 : Crystallographic data on 12-aneN_4 (L) complexes. 51

C.8 : Results from MM calculations on conformers of 12-aneN_4. 52

C.9 : Results from MM calculations on conformers of 13-aneN_4. 56

C.10 : Crystallographic data on 13-aneN_4 (L) complexes. L^1 is 1,4,7,10 - tetramethyl-13-aneN_4. 58

C.11 : Crystallographic data on 14-aneN_4 (L) complexes. X = Cl^-, Br^-, or NO_3^-. 60

C.12 : Results from MM calculations on conformers of 14-aneN_4. 63

C.13 : Results from MM calculations on conformers of 15-aneN$_4$ 66

C.14 : Crystallographic data on 15-aneN$_4$ (L) complexes. L^1 is 1,4,8,12 - tetramethyl-15-aneN$_4$ 67

C.15 : Results from MM calculations on conformers of 16-aneN$_4$ 69

C.16 : Crystallographic data on 16-aneN$_4$ (L) complexes. 70

C.17 : Strain energies for the conformers of Cu(16-aneN$_4$)$^{2+}$ and Pb(16-aneN$_4$)$^{2+}$. 71

C.18 : Crystallographic data on TACNTA complexes. 79

C.19 : Formation constants of the Ca(II) and Mg(II) complexes of a variety of ligands. 83

C.20 : Minimized strain energies (kcal.mol^{-1}) for conformers of N-functionalized tetraazamacrocycles. 84

C.21 : Comparison of ideal r(M-L) and θ(L-M-L) values for unsubstituted and substituted triazamacrocycles. Lowest energy conformer results. 93

C.22 : Comparison of ideal r(M-L) and θ(L-M-L) values for unsubstituted and substituted tetraazamacrocycles. Lowest energy conformer results. 94

C.23 : Complexed monensin minimization results as a function of M formal charge. 96

C.24 : K- and Na- monensin minimization results as a function of dielectric constant, D. 101

C.25 : Nonbonded parameters for Na and K, and corresponding monensin complex reproduction. 103

C.26 : Summary of total energies (kcal.mol^{-1}) of 18C6 uncomplexed and complexed. 106

C.27 : Calculated ΔG values for monensin and related polyether antibiotics. 110

C.28 : Calculated ΔE, RMSD and metal displacement values as a function of nonbonded parameters and dielectric constant, D. 112

ABBREVIATIONS OF LIGANDS

9-aneN$_3$	1,4,7-triazacyclononane
10-aneN$_3$	1,4,7-triazacyclodecane
12-aneN$_3$	1,5,9-triazacyclododecane
12-aneN$_4$ (CYCLEN)	1,4,7,10-tetraazacyclododecane
13-aneN$_4$	1,4,7,10-tetraazacyclotridecane
14-aneN$_4$ (CYCLAM)	1,4,8,11-tetraazacyclotetradecane
15-aneN$_4$	1,4,8,12-tetraazacyclopentadecane
16-aneN$_4$	1,5,9,13-tetraazacyclohexadecane
EN	ethylenediamine
TN	1,3-diaminopropane (trimethylenediamine)
EDTA	ethylenediaminetetraacetic acid
DTPA	diethylenetriaminepentaacetic acid
NTA	nitrilotriacetic acid
NTP	nitrilotripropionic acid
NTHP	nitrilotrihydroxyphenyl
NTHB	nitrilotrihydroxybenzyl
HBED	N,N^{I}-bis(2-hydroxybenzyl)ethylenediamine-N,N^{I}-diacetic acid
TACNTA/ NOTA	1,4,7-triazacyclononane-N,N^{I},N^{II}-triacetic acid
TACDTA	1,5,9-triazacyclododecane-N,N^{I},N^{II}-triacetic acid
DOTA	1,4,7,10-tetraazacyclododecane-N,N^{I},N^{II},N^{III}-tetraacetic acid
TRITA	1,4,7,10-tetraazacyclotridecane-N,N^{I},N^{II},N^{III}-tetraacetic acid
TETA	1,4,8,11-tetraazacyclotetradecane-N,N^{I},N^{II},N^{III}-tetraacetic acid
HETA	1,5,9,13-tetraazacyclohexadecane-N,N^{I},N^{II},N^{III}-tetraacetic acid
18C6 (18-crown-6)	1,4,7,10,13,16-hexaoxacyclooctadecane
18-azacrown-6	1,4,7,10,13,16-hexaazacyclooctadecane
DB18C6	dibenzo-18-crown-6
DB30C10	dibenzo-30-crown-10

A. INTRODUCTION

Over the past few years, the availability of more powerful computer hardware and software for CAMD (Computer Assisted Molecular Design) has changed the traditional hit-and-miss approach of synthetic chemists (Ripka, 1988). This is particularly true for those involved in pharmaceutical or medical research, where the main emphasis is on the design of drugs for therapeutic use. In certain applications, an important factor is the selectivity of the drug for specific metal ions. Thus the role of the coordination chemist in this research field.

The overall objective of this work was to use Molecular Mechanics to find factors governing metal selectivity with specific reference to medical applications.

A.1 MACROCYCLIC LIGANDS IN MEDICINE

Macrocyclic ligands which bind metal ions via nitrogen atoms in the ring have been studied extensively because of their relation to such naturally occurring complexes as the metalloporphyrins, vitamin B_{12} and chlorophyll (Cotton & Wilkinson, 1980). These nitrogen-donor macrocycles form strong complexes with transition metal ions while oxygen-donor macrocycles complex strongly to alkali and alkaline-earth metals. These coordinating preferences, in addition to the following characteristics of macrocyclic complexes: their marked kinetic inertness with regard to both metal-ligand complex formation and extrusion of the metal from the ligand, their ability to stabilize high oxidation states not readily attained, and their high thermodynamic stability due to the "macrocyclic effect" (Cabbiness *et al.*, 1969), have led to an interest in macrocycles for possible use in medicine. Two areas where chelating agents are already used are in the treatment of metal intoxication (May *et al.*, 1983) and in clinical diagnosis with imaging agents (Deutsch *et al.*, 1983).

A.2 POLYETHER ANTIBIOTICS

Antibiotic action is another area in which selective complexation of metals is encountered. Valinomycin is a cyclic depsipeptide antibiotic which is potassium-selective leading to its participation in uncoupling oxidative phosphorylation in mitochondria (McMurray *et al.*, 1959 and Pressman, 1965). Monensin is another antibiotic but belongs to a different class, that of polyether antibiotics. It is sodium-selective and is used extensively as an agricultural feed additive. It controls coccidiosis, a disease found in poultry, and promotes growth in ruminants such as cattle and sheep (Painter & Pressman, 1985). Monensin and its related structures have found no use as clinical antibacterial agents due to their high toxicity.

Polyether antibiotics is the term given to a group of monocarboxylic acid ionophores which contain several tetrahydrofurans and -pyrans in their structures. Westley (1977) further divided the group into four separate groups, namely (i) monovalent, (ii) monovalent monoglycoside, (iii) divalent, and (iv) divalent pyrrole. Classes (i) and (ii) transport monovalent cations while classes (iii) and (iv) transport divalent cations. This transportation occurs across lipophilic environments and is made possible by the ability of the antibiotics to form lipid-soluble complexes. Cation-binding properties in organic solvents have been determined for the more common polyether antibiotics and are reported by Painter and Pressman (1985). Only two antibiotics, monensin and dianemycin, display selectivity for sodium over potassium. The others are more selective for potassium.

A.3 FACTORS DETERMINING SELECTIVITY OF MACROCYCLIC LIGANDS

A considerable number of factors must be considered when designing ligands for selective complexation of metal ions in aqueous solution. Hancock and Martell (1989) discussed several of these factors in detail. These included the selection of suitable donor atoms, the effect of chelate ring size and macrocyclic ring size, the addition of substituent groups, preorganization and steric effects. Parameters influencing both enthalpy and entropy effects have been listed by Meyers (1978) and the importance of these effects in macrocyclic chemistry is illustrated by the large amount of thermodynamic data available for ion-macrocycle interactions (Izatt *et al.*, 1991). Hancock *et al.* (1983) have also investigated steric effects of coordinated solvent atoms, and Wade (1989) has reviewed the relation between ligand field strength and selectivity.

Selectivity-determining factors which are explored in this work are detailed below.

A.3.1. Effects of chelate ring size

An increase in chelate ring size from five-membered to six-membered has been found to increase the stability of complexes of smaller relative to larger metal ions (Hancock, 1986). Molecular Mechanics (MM) calculations are performed by Thöm and Hancock (1985) in an attempt to explain this observation. They found that for the five-membered chelate ring, lowest strain energy occurs when the metal ion is large with a metal-nitrogen (M-N) length of 2.5 Å and an N-M-N angle of 69°. For the six-membered chelate ring, minimum strain energy occurs at an M-N length of 1.6 Å and an N-M-N bond angle of 109.5°. A bite size (N-- N distance across the chelate ring) of 2.8 Å was measured for the five-membered chelate and 2.5° for the six-membered.

Similar studies on the four-membered chelate ring should yield even larger metal-donor atom (M-L) bond lengths than 2.5 Å and smaller L-M-L angles than 69°.

The "size-match selectivity" rule or "best-fit" hypothesis was first suggested by Pedersen (1967), and subsequently investigated by Martin *et al.* (1974) and Lindoy (1989). The rule states that a metal ion will complex most strongly with a macrocycle whose cavity size matches its ionic radius.

Thöm *et al.* (1985) tried to rationalise their observations with this hypothesis. They were correlating cavity sizes of the tetraazamacrocycles 12-aneN_4 through 16-aneN_4, as calculated by De Hayes and Busch (1973), with formation constants of these ligands with certain metal ions. Contrary to expectations, log K_1 values of large metals decreased with increasing hole size. The reason for this is that other conformers besides that of the trans-III, for which the above cavity sizes were measured, are observed for tetraazamacrocycles. The five conformations differ with respect to the orientation of the H-atoms attached to the nitrogens (Bosnich *et al.*, 1965) and are diagrammed below.

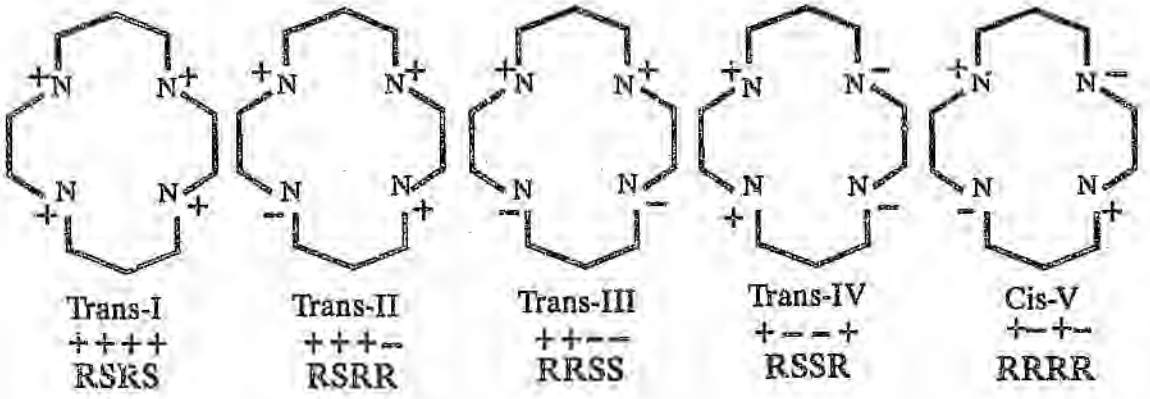

Figure A.1 : The five conformers of 14-aneN_4. H-atoms above the plane of the page are designated with a +, while those below the plane of the page are designated with a -. The cis and trans prefixes indicate whether the two remaining ligand sites in octahedral coordination would be cis or trans to each other.

MM calculations performed by Thöm, Fox *et al.* (1985) on 12-aneN$_4$ through 14-aneN$_4$ revealed that the type I configuration is adopted when the metal ion is too large for the macrocyclic cavity and also not obliged to be octahedral. The folded type V configuration is adopted to relieve steric strain when the metal has a strong preference for remaining octahedral. When type III configuration is forced, compression of M-N bonds occurs. With larger macrocycles 15-aneN$_4$ and 16-aneN$_4$, another consideration is the situation where cavity size is larger than the best-fit size for a particular metal ion. Ito *et al.* (1984a) found that for the octahedral high-spin Ni(II) complex of 16-aneN$_4$, the NiN$_4$ set distorts toward tetrahedral character. With the smaller macrocycles, Ni(II) remains in the plane of the N-donors.

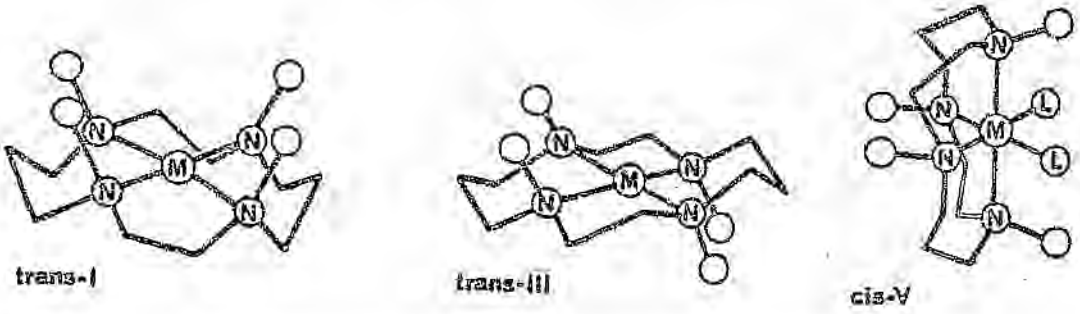

Figure A.2 : The trans-I, trans-III and cis-V conformers of 14-aneN$_4$

In this thesis, MM will be used to investigate the various configurations adopted by 15-aneN$_4$ and 16-aneN$_4$.

Conformers of azacycloalkanes can also be classified according to Dale's (1973) approach. He devised a scheme to select conformations of the C9 - C16 cycloalkanes and calculated their conformational energies. Although the difference in enthalpy between the lowest conformations in cyclododecane is high (4.4 kcal.mol^{-1}), differences in ΔH values for those of C13 - C16 are lower. This could be another reason for the flexibility encountered in macrocycles. Another contribution to macrocyclic complex flexibility is the variation in chelate ring orientations. Five-membered EN rings can adopt the envelope or half-chair form, while six-membered TN rings can assume the conformation of chair, boat or twist-boat (Ferguson, 1989).

A.3.3 Addition of pendent donor groups

A.3.3.1 Preorganization

It was noted in the previous section that macrocycles are too flexible to adhere to the "hole-size selectivity" rule. This complicates matters when using them in designing ligands for metal specificity. One solution is to synthesise macrocycles which are more rigid. Rigidity can be achieved by adding substituents to the ring such as pendent donor groups or bridging groups. In this way, the molecule becomes "preorganized".

Artz and Cram (1984) introduced the term "preorganization", the principle of which is that the formation constant for metal-ligand complexation is greatly increased if the free ligand is already in the conformation required for binding to the metal and is poorly solvated before complex formation. Preorganizing a ligand can thus improve its selectivity for one metal over another and minimise the change in strain upon complexation since no conformational adjustment need occur. For coordination to transition-metal ions, which display different geometry preferences, rigid ligands may be able to provide the required geometries. This "coordination-geometry selectivity" (Izatt *et al.*, 1991) was found by Shinkai *et al.* (1987) to occur for calixarene complexes with UO_2^{2+}. Other examples of highly preorganized ligands are cryptands (Lehn, 1978), sepulchrates (Sargeson, 1984) and spherands (Cram *et al.*, 1985). Another approach to greater ligand rigidity is reinforcement of macrocycles with bridges between the nitrogen donors (Hancock *et al.*, 1987).

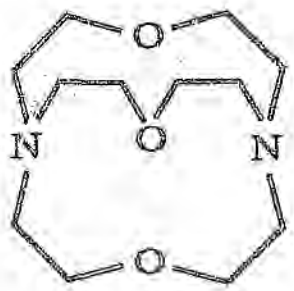

a cryptand

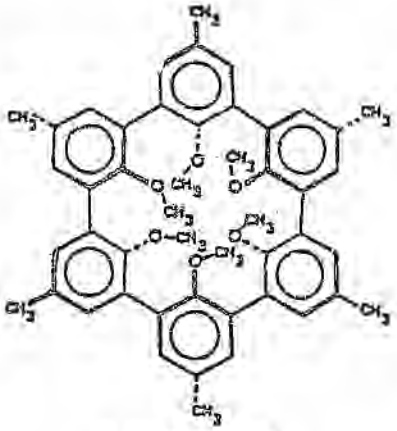

a spherand

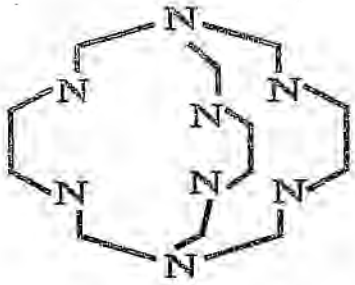

a sepulchrate

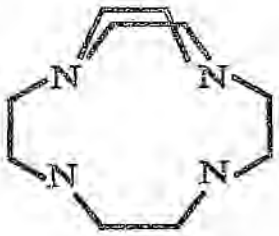

a reinforced macrocycle

Figure A.3 : Examples of highly preorganized ligands.

A.3.3.2 N-substituted azamacrocycles

Examples of less highly preorganized ligands are tetraazamacrocycles with four pendent donor N-acetate groups (Stetter & Frank, 1976). These ligands are ideal for larger metal ions such as the lanthanides and calcium, which are capable of expanding their coordination numbers. Because of the success of the Gd(III)-DOTA complex as a paramagnetic imaging agent (Lauffer, 1987), much interest has been directed towards similar complexes with a view to further medical application (Parker, 1990). Hancock and Martell (1989) concluded that such ligands with pendent donor groups display the best properties needed for complexes used as NMR contrast agents since they are non-labile, highly stable and form at reasonable rates.

Complexes of TACNTA with In(III) and Ga(III) have been studied for possible use as metal radionuclides (Broan *et al.*, 1991), and ligands containing N-bonded phenolate arms, such as HBED and derivatives thereof (Mathias *et al.*, 1990) have also been studied for this purpose. Workers like Moore *et al.* (1989) and Auerbach *et al.* (1990), combined the two ideas and synthesised ligands containing a TACNTA backbone with 2-hydroxybenzyl and similar groups as pendent arms. Clarke and Martell (1991b) found that Moore's (1989) ligand formed highly stable complexes with Ga(III), Fe(III) and In(III). The high basicity of phenolate O-atoms creates an advantage over the less basic O-atoms of acetate groups for coordination to these metals. The effect of the addition of these pendent donor groups to both triaza- and tetraazamacrocycles on steric strain will be evaluated via MM calculations.

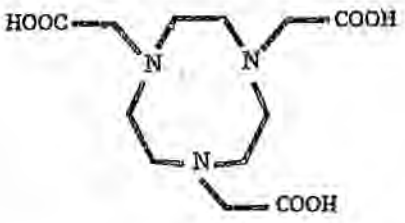

TACNTA

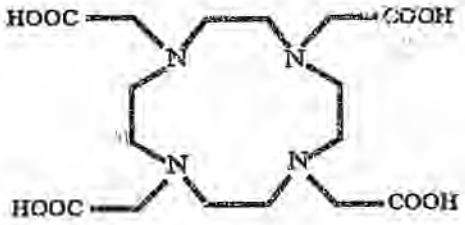

DOTA

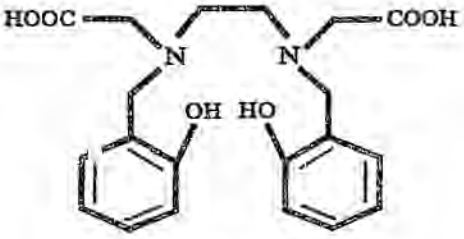

HBED

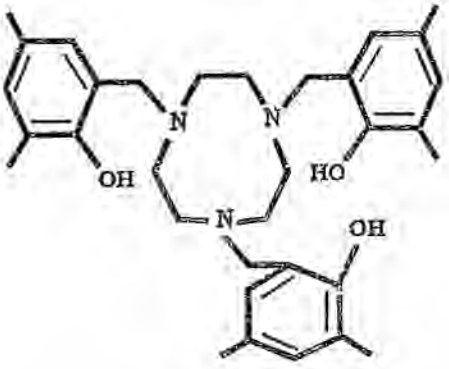

TX-TACNTA

Figure A.4 : Ligands with pendent donor groups.

A.4 FACTORS DETERMINING SELECTIVITY OF POLYETHER ANTIBIOTICS

A.4.1 Monensin selectivity versus nigericin selectivity

Cation selectivity of several polyether antibiotics indicates that monensin is the exception to the rule regarding its selectivity for sodium over potassium (Pressman *et al.*, 1975). Pinkerton and Steinrauf (1970) attributed the difference in cation binding between monensin and nigericin to the differences in molecule length and side groups. (See Figure A.5 for the structural formulae.) These antibiotics complex the particular cation by enclosing it with oxygen atoms situated at similar cation-oxygen distances. Nigericin, being the longer of the two molecules, would form a larger complexing ring thus allowing for binding to the larger potassium ion. Pinkerton *et al.* (1970) also concluded that side groups attached to rings in the molecules restrict rotation of the rings with respect to each other and therefore may also affect cation binding.

In further work, Steinrauf *et al.* (1971) compared the structures of monensin, nigericin and dianemycin to explain cation specificities. With monensin, both oxygens of the carboxylate group are firmly hydrogen-bonded and neither bond to the cation. With nigericin, the extra length of the carboxylate end enables it to reach and bond. Only one oxygen of the group is hydrogen-bonded. Rotation about the C-C bond depicted in red in Figure A.5 could allow movement of the oxygen so as to permit coordination to larger cations. The flexibility of the carboxylate end of dianemycin allows it to adopt conformations to form complexes of almost equal stability with sodium, potassium and rubidium.

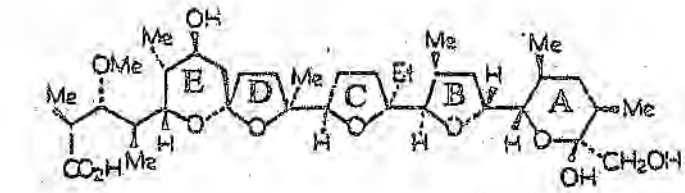

monensin A

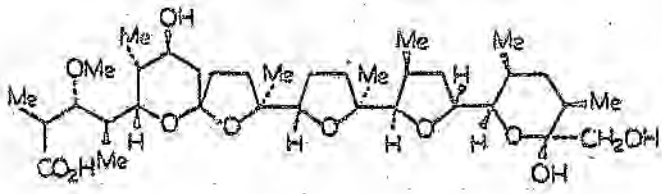

monensin B

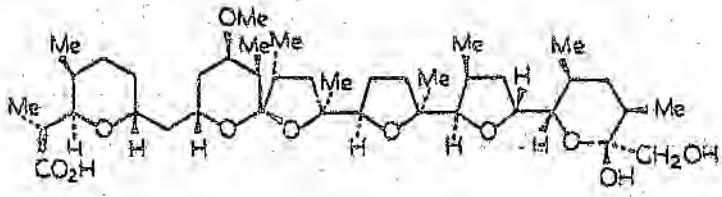

nigericin

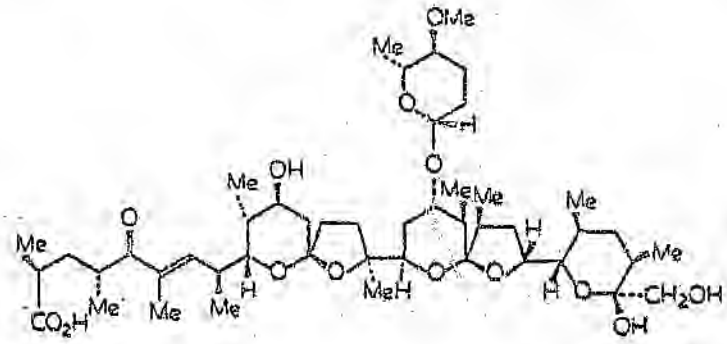

dianemycin

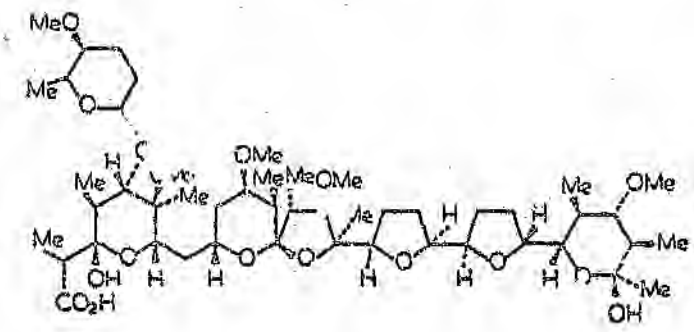

A204A

Figure A.5 : Structural formulae for monensin (A and B), nigericin, dianemycin and A204A.

Painter and Pressman (1985) reviewed the conformational aspects related to the capture and release of cations by carboxylic ionophores. Two proposed mechanisms of molecular rearrangement were examined. The first involves the existence of two radically different conformations: an open, acyclic form in the highly polar environment before ion capture, and a cyclic form during transport of the ion through low polarity biological membranes. "Hinges" (Goldman *et al.*, 1972) in the backbone of these molecules result in backbone flexibility. As expected, conformational equilibrium is dependent on solvent polarity. In low polarity solvents, intramolecular hydrogen bonding which closes the complexing ring can occur, while in highly polar solvents, hydrogen bonding is unlikely because of solvation of the relevant oxygen atoms.

The second mechanism postulated (Painter *et al.*, 1985) stems from available crystal structure data on several carboxylic ionophores. Their complexed and uncomplexed structures were found to be essentially isomorphic. The mechanism supports the idea that the liganding cavity is preformed and thus results in minimal conformational change when binding takes place. Examples of ionophores where comparisons between the free acid and its metal complexes have been made, are monensin A (Lutz *et al.*, 1971, Duax *et al.*, 1980, and Pangborn *et al.*, 1987a) and A204A (Smith *et al.*, 1978, Pangborn *et al.*, 1987b). Although similar conformations were observed in the case of each antibiotic, subtle changes also occurred. Variation in hydrogen bonding is in some cases not insignificant and rings C and D (see Figure A.5) differed for Na^+ and K^+ monensin. The reason for the presence of only one conformer of monensin was given by Smith and Still (1988) as being the avoidance of high-energy +gauche/ -gauche pentane interactions in the acyclic part of the molecule. Geddes *et al.* (1974) and Walba *et al.* (1986) also found small torsion angle differences between complexed structures of nigericin and monensin B respectively. These investigations indicated that the ion binding properties of these antibiotics probably result from an accumulation of small structural changes rather than large variations in conformational

energies.

A.4.3 Thermodynamics of complexation

Early thermodynamics work by Lutz and Früh (1971) on monensin and nigericin confirmed the selectivity preferences of these antibiotics for Na^+ and K^+ respectively. They accounted for the smaller ΔS values of the monensin system by assuming that less solvent molecules are liberated when monensin complexes with the cations than when nigericin complexes. Since the carboxylate anion of monensin is not bonded to the cation, greater charge separation exists in the complex leading to a higher degree of solvation. In the same way, Na^+ is more strongly solvated than K^+ and its complexation results in large ΔS values. These and other calorimetric measurements (Taylor *et al.*, 1982) were conducted in methanol.

In reality, monensin operates between an aqueous medium and membranes. This led Hebrant *et al.* (1991) to measure its complexation thermodynamics in heterogenous systems. Selectivity of sodium over potassium was again demonstrated in all tested environments, but was attributed to enthalpic effects. It was also shown that solubilities of the complexed monensin in water increase in the order $Na < K < Li$.

For the reaction,

$$M^+ + L^- \rightleftharpoons M^+L^- \qquad (1)$$

where M^+ = monovalent cation and L^- = carboxylic ionophore anion, the following equation can be used to describe complex stability and thus cation specificity (Painter & Pressman, 1985):

$$\Delta G_{ML} = \Delta G_{M(desolv)} + \Delta G_{L(desolv)} + \Delta G_{L(conf)} - \Delta G_{int} \qquad (2)$$

where $\Delta G_{M(desolv)}$ = nett free energy to transfer M^+ from bulk solvent to the lig

$\Delta G_{L(desolv)}$ = nett free energy to desolvate liganding heteroatoms,

$\Delta G_{L(conf)}$ = nett free energy to convert from uncomplexed conformation to complexed conformation,

ΔG_{int} = nett free energy of interaction between desolvated M^+ and L^-.

$\Delta G_{M(desolv)}$ can be taken from literature experimental values. In this work, attempts will be made to quantify the remaining factors for monensin and its Na^+ and K^+ complexes.

In conclusion, the discrimination between cations by polyether antibiotic is a result of several parameters. The most important appear to be ionophore backbone flexibility, conformational variation and solvation. These will be addressed in my investigation of monensin selectivity.

A.5 APPLICATION OF MOLECULAR MECHANICS TO COORDINATION CHEMISTRY

Many reviews on molecular mechanics (MM) dealing with its history, background, concepts, force fields and parameterization already exist (Allinger, 1976; Burkert & Allinger, 1982; White *et al.*, 1989; Seibel & Kollman, 1990; and Bowen & Cory, 1991). Only a brief summary of these aspects will thus be given in the following sections.

A.5.1 History and concepts

As early as 1946, three sets of workers (Westheimer *et al.*, Hill, and Döstrovsky *et al.*) applied "classical" mechanical concepts to chemical problems. Their papers formed the basis for future research development in molecular mechanics, which only really gathered momentum in the 1950's with the advent of computers. Today, the MM or force-field method, also known as the Westheimer method, is considered one of the standard techniques of structural chemistry. Continuing advances in computer hardware, graphics and software technology are allowing scientists to investigate molecular modeling of larger structures, as well as more complex, realistic systems.

MM is a structural method of calculating potential energies of molecules or systems of interacting molecules as a function of their nuclear coordinates. The Börn-Oppenheimer approximation, which treats nuclear and electronic motions separately, is assumed. Unlike quantum mechanics, where electronic behaviour in a fixed nuclear field is described, MM solves for the positions of the nuclei, the electronic distribution being implicit in the force-field. The force-field consists of "classical" equations and constants that describe this resultant potential energy surface of the molecule.

"Classical" equations are used since the MM model considers molecules as a system of points held together by elastic forces. Any deformation of this ball-and-spring

model from its "natural" bond lengths, angles and torsions results in strain and a corresponding increase in internal energy.

A.5.2 The molecular mechanical potential

In general, the total energy of a molecule may be regarded as the sum of potential energy terms due to bond stretching, angle bending, torsions, van der Waals interactions and electrostatic interactions (Seibel *et al.*, 1990).

$$E_{total} = E_{bond} + E_{angle} + E_{torsion} + E_{vdW} + E_{elec}$$

Other energy terms, for example E_{oop} (out-of -plane distortion) and E_{hyd} (hydrogen bonds), may also be added. The individual functions differ from one force field to another and will be detailed under the discussion of the TRIPOS force field.

A.5.2.1 Parameterization

The quality of a MM field depends both on the potential energy equations and the parameter values or force constants used (Burkert *et al.*, 1982). Since a specific force field is parameterized against experimental data for a given set of molecules, parameters are usually not transferable from one field to another. Force field derivation by linear least-squares method was proposed by Lifson and Warshel (1968) where parameters are fitted to a large set of data. Alternative methods are simplex optimization (Wade, 1989) and optimization by trial-and-error. This complex problem of assigning force constants has, as yet, found no universally accepted solution.

A.5.2.2 Minimization and conformational searching

To obtain the structure geometry where its energy is at a minimum, the function describing its potential energy must be minimised. MM energy minimization involves successive iterative computations, beginning with the initial molecule conformation. White (1977) delineated the classes of practical algorithms used: (a) search procedures not requiring derivative evaluation guarantee minimisation and are conceptually simple, (b) procedures requiring evaluation of potential derivatives, such as steepest descents, (c) variants of the general Newton iteration, such as the Newton-Raphson, which require evaluation of both first and second partial derivatives.

The minimized molecule corresponds to the first local minimum encountered in the potential energy surface and may not be the absolute lowest energy structure - the global minimum (Cohen *et al.*, 1990). To find the global minimum in simple systems, conformational space must be searched. Search methods include Monte Carlo (Paine & Scheraga, 1985), distance geometry (Weiner *et al.*, 1983) and molecular dynamics. Molecular dynamics (MD) simulations describe the trajectory of a system by applying Newton's equations of motion (Bowen & Cory, 1991) and is able to climb small barriers and thus locate deep local minima.

A.5.2.3 Solvation

Seibel and Kollman (1990) stressed the importance of solvent effects in their review on molecular mechanics and the modeling of drugs. Because of the high dielectric constant of water, they recommend the use of solvent environments when calculating MM on polar molecules. Monte Carlo and molecular dynamics are two methods offering such a treatment. A much easier solvent treatment although not aesthetically pleasing, is the use of a modified dielectric. The dielectric can be a constant, which is normally set to unity with gas-phase calculations, or a function of distance. Wade (1989) examined work done by several researchers who applied dielectric variance to their calculations and concluded that the choice of dielectric was circumstantial.

All the most extensively tested force fields, MM2 (Burkert & Allinger, 1982), AMBER (Weiner & Kollman, 1981) CHARMM (Brooks *et al.*, 1983), and ECEPP (Momany *et al.*, 1975) have been derived for organic molecules. Applications of MM to inorganic chemistry problems have been fewer due to difficulties encountered with metal parameterization. Corey and Bailer (1959) were the first to perform calculations on transition metal systems, followed by Gollogly and Hawkins (1969). Since then, conformation analysis has become well established in the field of coordination chemistry (Brubaker & Johnson, 1984; Hancock, 1989; and Comba, 1993).

Force field optimization for transition metals is complicated by the number of varied coordination geometries assumed by these metals. Hancock and coworkers (1989) have reproduced structures successfully by using separate parameters for the two spin-states of a metal, eg. low-spin and high-spin Ni(II), and also by using parameters specific to the observed metal geometry, eg. square planar Cu(II). Comba (1993) suggested that the replacement of L-M-L angle bending terms by 1,3-nonbonded interactions would simplify optimization and thus lead to better accuracy. Examples given in his review substantiate this approach.

With alkali-metal ions and lanthanide(III) ions, the ionic character of the M-L bonds do not allow for coordination geometry definition. Here, the ionic bond model, as opposed to the covalent bond model, would be employed where no L-M-L angles are defined and geometry is dictated by the ligand and L-L nonbonded interactions (Hancock, 1989). Electrostatic interactions must also be accounted for when metal ions complex with ligands, especially charged ligands. However, difficulties encountered with the determination of partial charges on atoms have made incorporation of these electrostatic effects into force fields problematic. Partial atomic charges are usually derived from quantum mechanical calculations.

Molecular mechanics can be used to calculate vibrational spectra, optimize structural geometries and predict thermodynamics by comparing minimized strain energies. It is thus invaluable to research areas such as drug design, the study of biochemical phenomena and metal ion selectivity in coordination chemistry.

A.6 THE TRIPOS FORCE FIELD

The SYBYL molecular modeling package (TRIPOS, 1992,1993) incorporating the TRIPOS force field was used in this work.

A.6.1 Potential energy functions

The types of interactions between atoms that are modelled by force fields are shown in the following diagram.

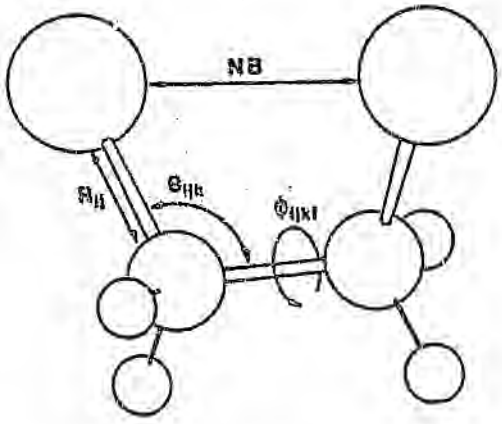

$$U_{total} = U_{bonded} + U_{angles} + U_{torsion} + U_{non\ bonded}$$

Figure A.6 : Components of intramolecular strain.
Redrawn from Brubaker and Johnson (1984).

Energy functions employed in the TRIPOS force field are described below.

(a) Bond stretching

The energy stretching or compressing function is described by the harmonic potential,

$$E = 1/2\ k_{ij}\ (d_{ij} - d_{ij}^{0})^2,$$

where k_{ij} is the force constant (kcal/mol.Å^2), d_{ij} the actual bond length (Å) between atoms i and j, and d_{ij}^{0} the equilibrium or unstrained bond length (Å).

(b) Angle bending

The harmonic potential also describes this term,

$$E = 1/2\ k_{ijk}\ (\theta - \theta^{0})^2,$$

where k_{ijk} is the force constant (kcal/mol.°^{2}), θ the angle (°) between atoms i, j and k, and θ^0 the equilibrium angle (°).

(c) Out-of-plane bending

This energy accounts for the bending of planar atoms out of the plane.

$$E = 1/2\ k_i d_i^2,$$

where k_i is the out-of-plane bending force constant (kcal/mol.Å^2) for atom i, and d_i the distance (Å) from atom i to the plane defined by its three attached atoms. For example,

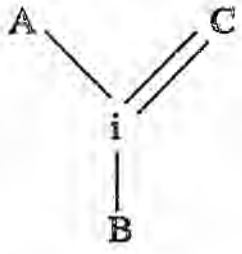

A, B and C will define the plane.

(d) Torsional potential

For four consecutively bonded atoms i, j, k, l,

$$E = 1/2\ k_{ijkl}\ (\ 1 + S \cos (\ |n|\ .\ \Phi\ )\ ).$$

k is the torsional barrier (kcal.mol), n is the periodicity around the bond and Φ is the torsion angle (°).

S = +1 in staggered conformation, and S = -1 in eclipsed conformation.

(e) Van der Waals

This nonbonded term associates any pair of atoms which are not directly bonded to a common atom. It is depicted with a form of the 6-12 Lennard-Jones potential.

$$E = \varepsilon_{ij}\ (1.0 / a^{12} - 2.0 / a^{6}),$$

where ε_{ij} is the van der Waals constant or potential well depth (kcal.mol^{-1}) which equals $\sqrt{\varepsilon_i\ \varepsilon_j}$, and a is the distance (Å) between atoms i and j divided by the sum of their radii. The first term in the equation represents an attractive force, while the second represents a repulsion.

(f) Hydrogen bonding

Unlike the Weiner *et al.* (1983) force field which uses a 10-12 hydrogen bonding potential, the TRIPOS force field does not include an explicit hydrogen bonding term. Instead, it treats hydrogen bonds with the same function as the van der Waals interactions. In earlier SYBYL versions (5.4 and lower), hydrogens involved in hydrogen bonding were given zero size which probably resulted in very large nonbonded strain. Version 5.5 and higher account for H-bond energies by scaling the van der Waals interactions between H-bond acceptors and hydrogens attached to H-bond donors.

(g) Electrostatic

The point charge approach is used and the form of the Coulomb potential function is

$$E = 332.17\ (\ Q_iQ_j\ /\ D_{ij}r_{ij}\ ),$$

where D_{ij} is the dielectric function for atoms i and j, Q_i is the nett atomic

charge (e^-) at atom i, and r_{ij} is the distance (Å) between the two atoms. The dielectric function may either be a constant or distance dependent. This electrostatic potential term is optional.

A.6.2 Validation of the TRIPOS force field

The test of a good force field is its ability to reproduce crystal structures for a diverse selection of molecules. The TRIPOS 5.2 force field has been tested by Clarke *et al.* (1989) of "TRIPOS Associates". They assessed model geometries produced by their force field by minimizing 80 crystallographic structures, all organic in nature. Differences between initial and final structures were analyzed with both rms heavy atom movements and internal coordinated deviations. The results on crambin and three proteins were compared to those from the AMBER (Weiner *et al.*, 1984) and AMBER/OPLS (Jorgensen *et al.*, 1988) force fields. Relative energies produced by TRIPOS were assessed by calculating conformational energy differences and torsional barriers, and then comparing values with both experimental and MM2 (Burkert *et al.*, 1982). Results confirmed the validity of the TRIPOS force field.

Gundertofte *et al.* (1991) further compared conformational energies calculated with SYBYL 5.1 and SYBYL 5.21 to those calculated with two other MM methods and two semiempirical methods. Molecules with different functional groups were chosen as test compounds. All methods reproduced the experimentally determined conformational energies reasonably well, with MM2(85) (Burkert *et al.*, 1982) delivering the closest results.

A.7 OBJECTIVES OF THIS STUDY

Molecular mechanics will be used in an attempt to achieve the following objectives:

(1) To examine the role of the four-membered chelate ring in coordination chemistry.

(2) To determine ideal M-N bond lengths and coordination geometries for all conformers of the triaza- and tetraazamacrocycles.

(3) To determine ideal M-N bond lengths, M-O bond lengths and coordination geometries for all conformers of the triaza- and tetraazamacrocycles bearing pendent oxygen-donor groups.

(4) To quantify the differences in selectivity exhibited by monensin and other related polyether antibiotics.

(5) To evaluate the performance of the TRIPOS force field in the above-mentioned applications.

B. EXPERIMENTAL

All molecular mechanics calculations were performed on a Silicon Graphics INDIGO (R3000) computer. The SYBYL Versions 5.5 and 6.0 program, available from TRIPOS Associates, was used. Differences between the two versions which are applicable to this study include the implementation of a molecular spreadsheet to allow for easy manipulation and analysis of data, a change in default from energy change to gradient termination option for minimization and the treatment of hydrogen bonds. Both versions treat hydrogen bonds as non-directional and electrostatic in nature. Version 5.5 accounts for H-bond energies by omitting the van der Waals interactions between the H-bond acceptors (nitrogen, oxygen, fluorine) and hydrogens bonded to H-bond donors (nitrogen, oxygen, fluorine). In Version 6.0, H-bond energies are accounted for by scaling these van der Waals interactions to the van der Waals radii. No changes in force field parameter values relevant to this study occur.

B.1 INITIAL COORDINATES

Starting coordinates for the calculations were either taken from crystallographic data, which was obtained from the Cambridge Crystallographic Database (1992) or from relevant papers, or from molecules built with the SKETCH option available in the SYBYL package. Actual crystal structures were used as the bases in molecule construction. For simplification purposes, crystal structures cited in the text will be referred to numerically. (See section F.)

B.2 MOLECULAR DYNAMICS

Molecular dynamics, another option within SYBYL, was applied to conformers in an attempt to overcome the problem of local energy minima. Simulated annealing runs were performed. Each molecule, minimized first to a RMS gradient of less than 1.000 kcal/mol.Å, was held at a "plateau" temperature of 800 K for 1000 fs, then annealed over 500 fs to 0 K in five annealing steps. Five cycles were executed for each conformer. After the dynamics run, the low temperature "annealed" configurations were saved to a database. The resultant molecule database was then searched for lowest energy structures. These were in turn minimized with molecular mechanics and the resulting most stable conformer assumed to be the global minimum.

B.3 DETERMINATION OF CAVITY SIZE

B.3.1 Previous calculations

The interest in correlating macrocycle "hole" size with metal ion radius has led to several methods cited in the literature for the calculation of these cavity sizes.

Henrick *et al.* (1985) postulated the simplest method. Using crystal structure data, the hole radius of the macrocycle was determined by the mean distance of the donor atom positions from their centroid. The main problem with this method is its disregard for macrocycle flexibility.

Busch and coworkers (Martin *et al.*, 1974) performed MM calculations on the tetraaza macrocycle series 12-aneN_4 through 16-aneN_4. The M-N stretching force constant was set to zero so that the M-N bond length would be entirely determined by the ligand. Their resultant ideal bond lengths are given in Table C.1. Ligands used were in the correct stereochemistry for essentially planar chelation. Hancock and McDougall

(1980) scanned the same conformations of 12-aneN$_4$ through 14-aneN$_4$. The minima in their strain energy versus unstrained bond length curves agreed closely with Busch's work.

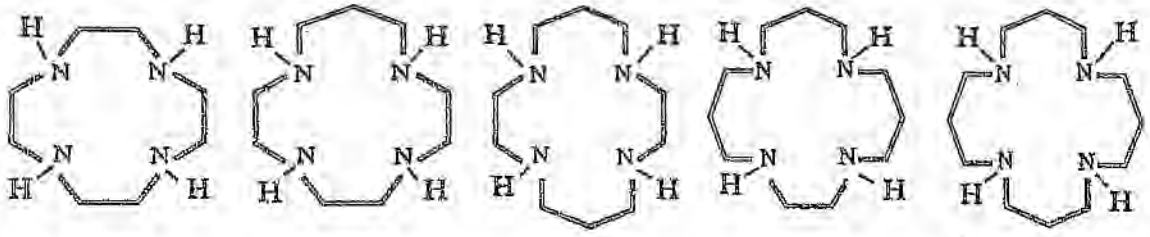

12-aneN$_4$ 13-aneN$_4$ 14-aneN$_4$ 15-aneN$_4$ 16-aneN$_4$

Figure C.1 : The series of tetraaza macrocycles 12-aneN$_4$ through 16-aneN$_4$.

Table C.1 : Molecular mechanics cavity size calculations for planar conformers.

Macrocycle	Cavity Size / Å	
	Busch *et al.* (1974)	Hancock *et al.* (1980)
12-aneN$_4$	1.83	1.81
13-aneN$_4$	1.92	1.92
14-aneN$_4$	2.07	2.05
15-aneN$_4$	2.22	
16-aneN$_4$	2.38	

Hancock and coworkers (Thöm *et al.*, 1984) further proceeded with MM calculations on other conformers besides that of the planar or trans-III. It was concluded that selectivities of the tetraazamacrocycles are governed by relative stabilities of two or more conformers with differing preferences for metal ion size. The size-match

selectivity concept thus does not apply. During the scans, all parameters involving the metal ion, except for the strain-free M-N length, were kept constant at values previously optimised for high spin Ni(II) (McDougall *et al.*, 1978).

Drew *et al.* (1985) described a method of cavity size determination similar to that of Hancock *et al.* (1980) in that ideal bond lengths were plotted against strain energy. The difference between the two methods is the value of the force constant for M-N, K_r(M-N). Drew uses an exceedingly high value to force the molecule to vary its conformation and accommodate the new bond length. This approach claimed to be independent of accurate force field parameters, thereby making it transferable to any system.

"Sphere-radius" calculations on macrocycles have been carried out by Bernhardt and Comba (1991). Strain energy of molecules was again plotted as a function of M-N bond length. Their metal-ligand distance was however fixed mathematically, thus excluding K_r and r_0 from the force field (Bernhardt & Comba, 1992). The L-M-L bending potential function was also replaced with 1.3-repulsion of the donor atoms. Here, the calculated hole size is made completely independent of the metal ion to be coordinated. Configurational isomers of Co(II) amine complexes have also been theoretically studied in this manner by Bond *et al.* (1985, 1987).

In recent work, Drew and Santos (1993) calculated the hole sizes of various conformations of 18-azacrown-6 using both Drew's above-mentioned method and Comba's method. The increased M-N bond lengths obtained with the latter were ascribed to an increase in the allowed flexibility of the metal within the coordination sphere. They concluded that the method of using 1,3-nonbonded interactions was unsuitable for smaller than 7 coordination number environments.

Bivariate scanning is another technique that could be used to probe different coordination preferences of metals. Wade (1989) scanned strain energy as a function of both unstrained M-L bond length and L-M-L angle.

B.3.2 Univariate scans

Univariate scanning was employed in the investigation of macrocycles. Strain energies (ΣU) of metal complexes were calculated as a function of ideal metal-ligand bond length (r_0). The approach of Hancock *et al.* (1980), where the M-L bond length was varied and a small K_r(M-L) constant was retained, was adopted. Macro programs using SYBYL'S programming language (SPL) were written to scan molecules. The minima in the resulting curves, which were taken as the best-fit M-L size, were obtained with the aid of the statistical regression analysis option in the AXUM package. A third-order polynomial function was fitted to the data sets and its coefficients determined. The point where the first derivative of the function equals zero was then located. Force field parameters used in this work will be discussed in the relevant sections.

B.3.3 Force field parameters for univariate scanning

For a completely rigorous molecular mechanics investigation, calculations with force field constants appropriate to each metal ion of interest should be done. A simpler approach is to keep all the constants involving the metal fixed at those for one metal ion. The Ni(II) ion was chosen since it is an "average" ion, with M-L bonds that are neither very strong nor very weak and neither very ionic nor very covalent.

Thus nickel was added to the ATOM_DEF file in SYBYL's Tripos force field. It was assigned a coordination number of four, an unclassified geometry and a +2 charge. In this force field, if a metal is defined to have a valency less than or equal to four, angle bending constants, L-M-L, come into operation. If a coordination of greater than four is specified, 1-3 nonbonded interactions between L--L pairs are utilised.

The value of 0.68 mdyne.Å^{-1} for the bond stretching force constant K_r(Ni(II)-L), where Ni is high-spin, used by McDougall *et al.* (1978) in their MHB force field was transported to the Tripos force field by the appropriate conversion factor. Thus K_r(M-L) in the TAFF_BOND_STRETCH file was assigned the value 98.0 kcal/mol.Å^2.

In previous scanning methods, described in section B.3.1, if the angle bending function L-M-L was used, angles subtended at the metal were constrained in particular geometries by assigning angle bending force constants, K_b. In this work, to permit the coordination geometry of the metal to be controlled entirely by the ligand, no constraints, ie. K_b equals zero, were placed on the L-M-L and M-L-C angles. The ideal angle dependence about the metal ions was thus removed.

Force constants involving torsions about the metal-ligand bonds, i.e. L-M-L-X, were set to zero. No electrostatics or bond dipoles were applied. Unless otherwise stated in the results section, default organic parameter sets for the purely organic interactions and default settings in the minimization procedure (Powell minimization method, 100 maximum iterations, RMS gradient termination option of 0.05 kcal/mol.Å, nonbonding atoms cutoff radius of 8.0 Å) were employed.

B.4 PARAMETER OPTIMIZATION

Molecular mechanics calculations on the polyether antibiotics involved optimization of the force fields so as to produce a minimized structure geometry as close as possible to the original. These attempts at optimization are reported in detail at a later stage. In order to assess force field accuracy, minimized and initial structures were compared by statistical analysis. RMS deviations, standard deviations, mean deviations and maximum deviations of internal coordinates, bond lengths, bond angles and torsions were evaluated.

C. RESULTS AND DISCUSSION

C.1 FOUR-MEMBERED CHELATE RINGS

The role played by chelate ring size in metal ion recognition (Hancock, 1990) prompted investigation of the effect of the four-membered chelate ring. Examples of multidentate ligands forming four-membered rings upon complexation are carboxylate, acetate, nitrate and phosphate. The coordination of carboxylate groups of proteins and phosphate groups of nucleotides to biologically important metal ions is of interest here.

C.1.1 Coordination preferences of biologically interesting cations

The functions of Groups IA and IIA cations are vital in biological chemistry (Hughes & Birch, 1982). Na^+, K^+, Mg^{2+} and Ca^{2+} are selectively distributed throughout the body. This selectivity enables them to perform their respective roles. For example, Ca^{2+} rather than Mg^{2+} stabilises cell walls because of its more effective binding to sites of high coordination number supplied by carboxylate groups. Calcium ions also play a central part in the conveyance of intracellular messages by way of regulatory Ca^{2+} - binding proteins (Ahlström *et al.*, 1989). These proteins undergo conformational changes in response to increases in intracellular Ca^{2+} concentrations. Studies on several Ca^{2+} - binding proteins have indicated that coordination to the ion occurs via carboxyl and carbonyl oxygen atoms. Oxygen binding to cations also occurs through phosphate groups of ATP and ADP, which play pivotal roles in regulating metabolic reactions.

Other metal ions involved in biochemical processes include Zn, Cu, Ni, Co, Fe and Mn. Williams (1983) researched the binding of these metals to proteins. Coordination number preferences and chemical nature of ligand donors on the proteins are major considerations. Cu(II), Ni(II) and Zn(II) are selected by sites of low coordination number and strong donors, while Mn(II) and Fe(II) complex better

with sites of higher coordination number and poor donor strength.

A preliminary study was conducted on preferred coordination numbers of univalent Na and K and divalent Mg, Ca, Mn and Zn, where oxygen is the major donor atom. The Cambridge Structural Database Version 5.1 (1992) was searched with QUEST (92) for complexes of each metal bound to acetate, nitrate and phosphate. Atoms situated within a distance of 3.0 Å from the metal were then tabulated with GSTAT (92) for every complex. Perusal of the resultant files led to the findings shown in Figures C.2 to C.7 and Tables C.2 and C.3. Only one metal-nitrate structure occurred with each of the metals Na, K and Mg.

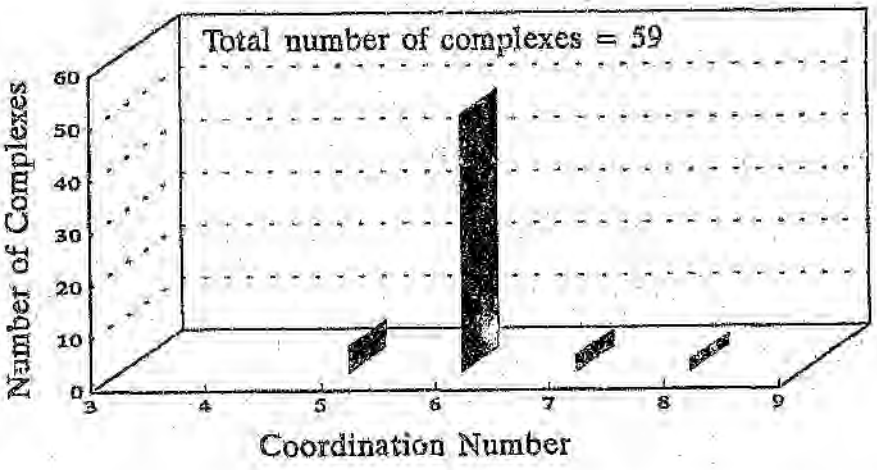

Figure C.2 : Distribution of coordination number for Na-acetate complexes.
Minimum Na-O bond length/ Å = 2.212
Maximum Na-O bond length/ Å = 2.765

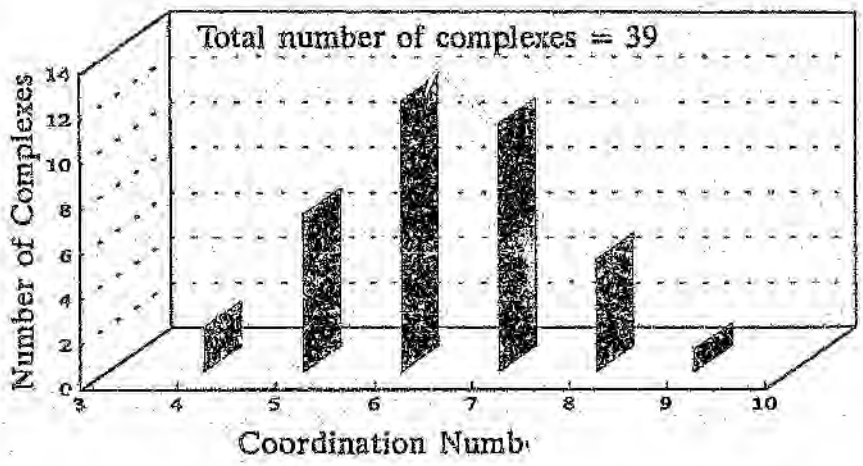

Figure C.3 : Distribution of coordination number for K-acetate complexes.
Minimum K-O bond length/ Å = 2.572
Maximum K-O bond length/ Å = 3.000

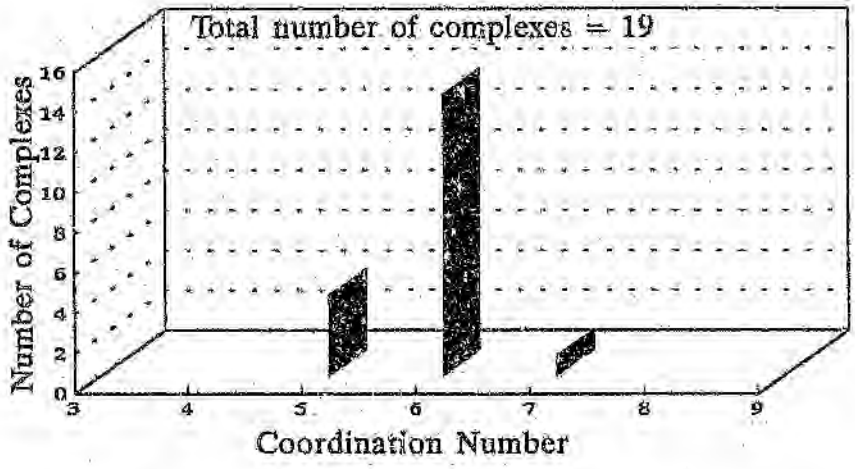

Figure C.4 : Distribution of coordination number for Mg-acetate complexes.
Minimum Mg-O bond length/ Å = 1.978
Maximum Mg-O bond length/ Å = 2.398

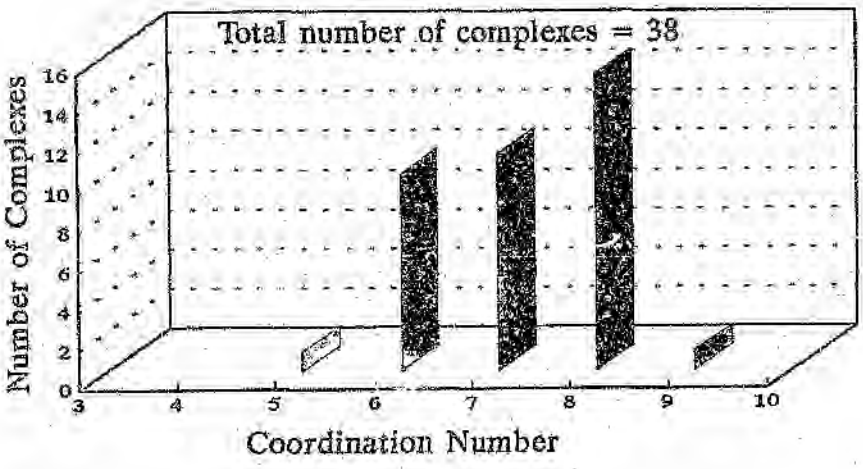

Figure C.5 : Distribution of coordination number for Ca-acetate complexes.
Minimum Ca-O bond length/ Å = 2.250
Maximum Ca-O bond length/ Å = 2.862

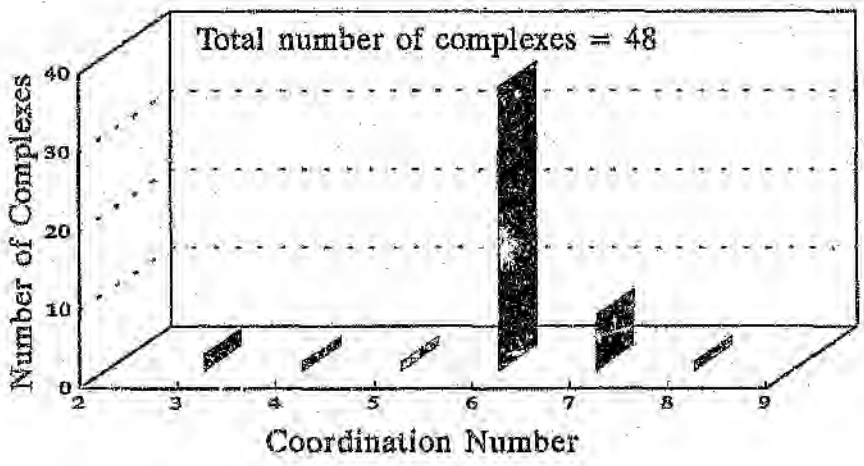

Figure C.6 : Distribution of coordination number for Mn-acetate complexes.
Minimum Mn-O bond length/ Å = 1.817
Maximum Mn-O bond length/ Å = 2.688

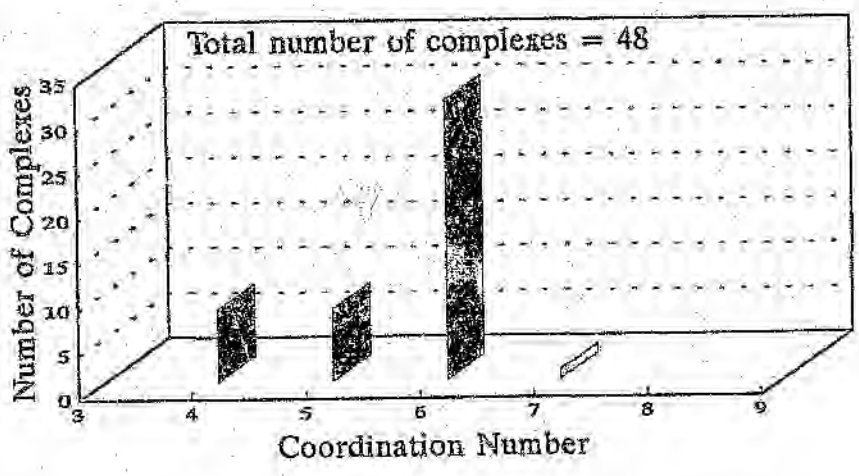

Figure C.7 : Distribution of coordination number for Zn-acetate complexes.
Minimum Zn-O bond length/ Å = 1.718
Maximum Zn-O bond length/ Å = 2.564

Table C.2 : Distribution of coordination number for metal-nitrate complexes.

Metal (M)	Coordination Number					Total No. of Complexes	Minimum M-O /Å	Maximum M-O /Å
	4	5	6	7	8			
Ca	-	-	-	-	5	5	2.247	2.684
Mn	1	1	8	1	2	13	1.818	2.517
Zn	6	1	13	2	-	22	1.896	2.525

Table C.3 : Distribution of coordinati number for metal-phosphate complexes.

Metal (M)	Coordination Number					Total No. of Complexes	Minimum M-O /Å	Maximum M-O /Å
	4	5	6	7	8			
Na	-	10	18	3	-	31	2.219	2.704
K	-	-	5	1	-	7	2.559	2.980
Mg	1	-	2	-	-	3	1.897	2.176
Ca	-	-	5	5	-	10	2.196	2.650
Mn	-	-	3	-	-	3	1.784	2.348
Zn	5	1	-	-	-	6	1.872	2.140

It appears that coordination of six is most popular with all the metal ions, except Ca. Na, Mg and Mn display an average 74% tendency towards complexation with six donor atoms. The larger group IA cation, K, also coordinates readily with seven donor atoms, while the larger Group IIA cation, Ca, has, as expected, a slight preference for eight-coordination over that of six and seven. This can be seen in Figure C.5. The trend towards four- and five-coordination with Zn, the smaller of the two transition metals, is not surprising.

The trend observed for maximum and average M-O bond lengths, ie. a decrease in values of the order K > Na > Ca > Mn > Zn > Mg, correlates with the 6-coordination effective ionic radii of the metals as given by Shannon (1976).

C.1.2 Molecular mechanics calculations

In general, as metal ions increase in size, their coordination number increases, resulting in smaller ligand-metal-ligand (L-M-L) angles. Molecular mechanics calculations showed this to be true for isolated chelate rings, five-membered involving EN and six-membered involving TN (Hancock & Martell, 1989). Strain energies, ΣU, were plotted against varying M-N length with M, a generalized metal ion and L-M-L angles set to different values. 109.5° was used for tetrahedral coordination, 90° for octahedral, and 70° for cubic 8-coordination. The five-membered chelate ring showed an increasing preference for geometry from cubic to octahedral to tetrahedral, while the six-membered ring showed a decreasing preference for the same order. The ability of four-membered chelate rings to [illegible] coordination numbers and long M-L bond lengths derives largely from its [illegible] size than the five or six-membered rings resulting in more efficient packing of chelates around a metal ion. This ability was investigated using the same molecular mechanics technique described above.

Acetate, nitrate and phosphate groups were isolated from pertinent crystal structures. The two oxygens bound to the metal as part of the chelate ring were defined as carboxylate and phosphate oxygens in SYBYL. To constrain the complexes in particular geometries, the K_b (L-M-L) constant was set to 3.0 kcal.mol^{-1}.deg^{-1}, and the L-M-L angles to 50°, 70° and 90°. These were the only parameter settings changed from those described in section B.3.3. For the M-O-N, M-O-C and M-O-P bending interactions, the Tripos force field used the relevant angle of the chosen crystal structure and the default K_b(M-O-X), where X = N, C, P, of 0.02 kcal.mol^{-1}.deg^{-1}. Default assignments for the M-O-X-X, where X = any other atom, torsional interactions were used. The curves from these scans are shown in Figures C.8 and C.9.

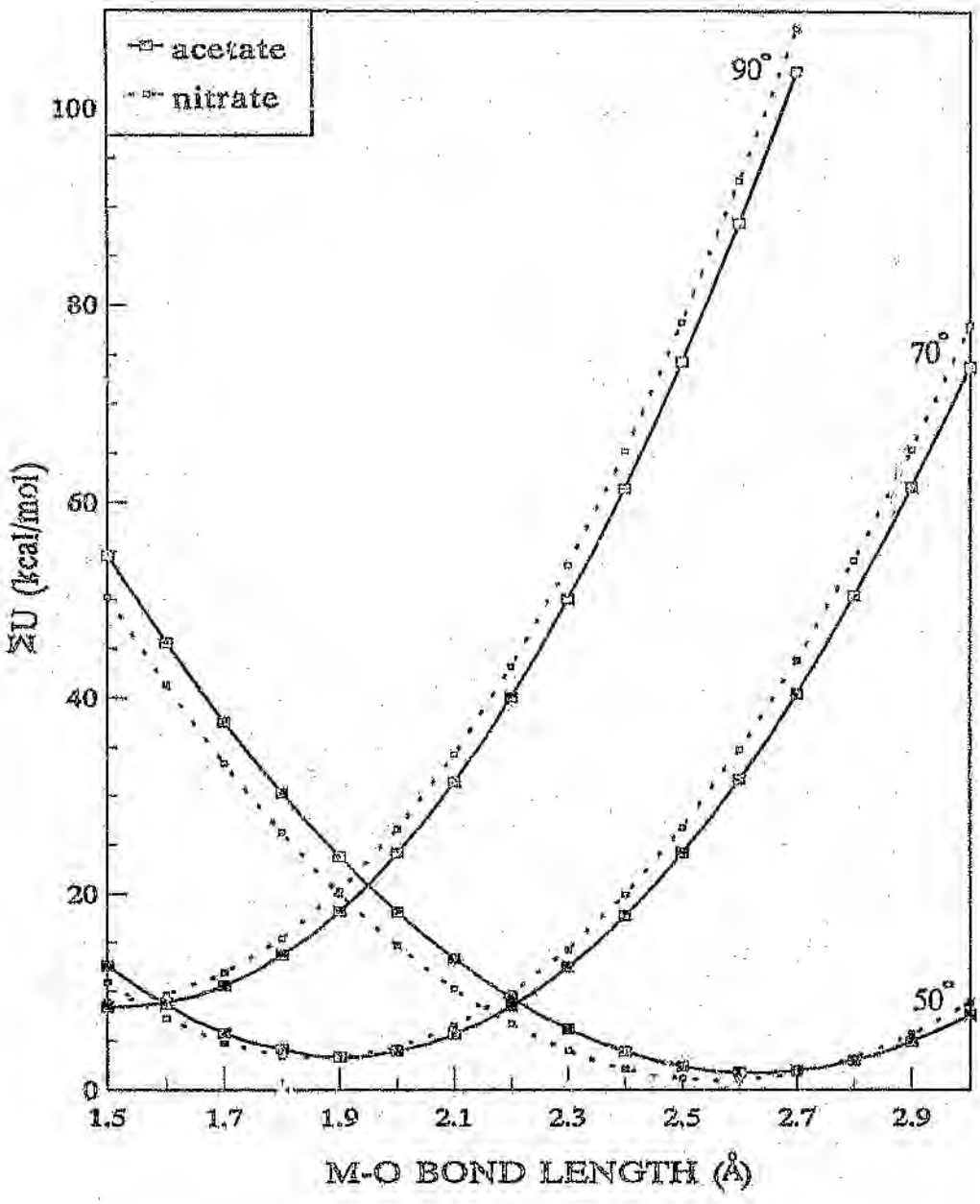

Figure C.8 : Strain energy, ΣU, of an isolated four-membered chelate ring involving acetate and nitrate as a function of metal-oxygen bond length and O-M-O bond angles appropriate to different coordination geometries.

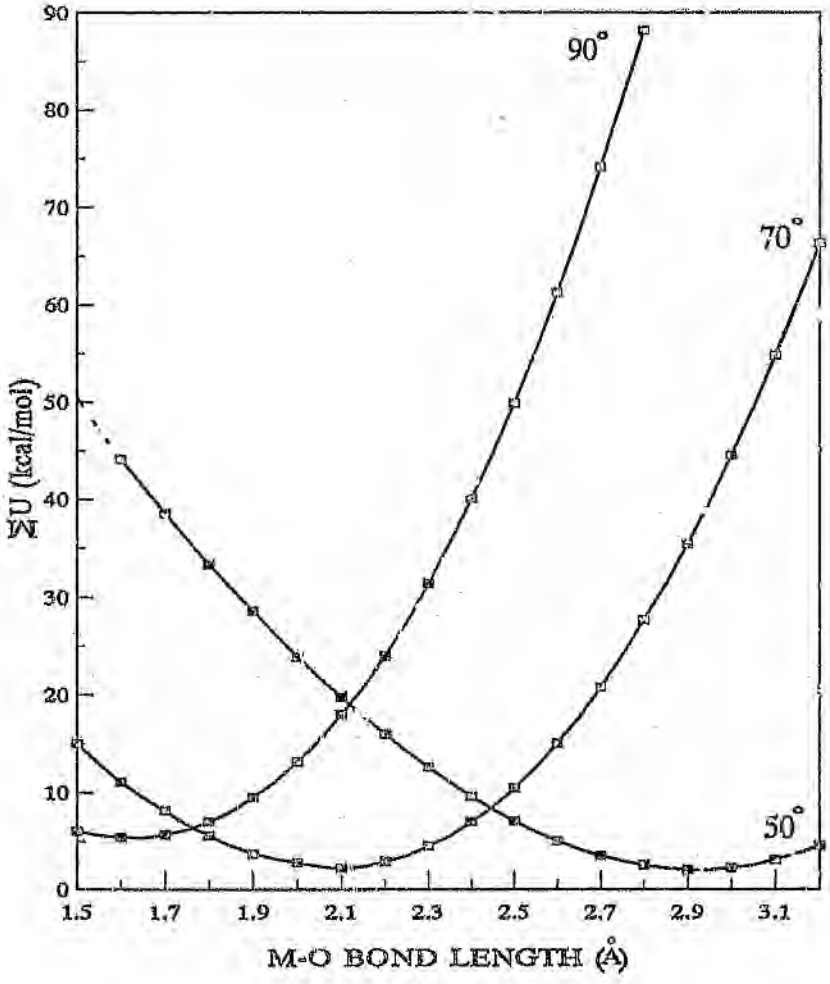

Figure C.9 : Strain energy, ΣU, of an isolated four-membered chelate ring involving phosphate as a function of metal-oxygen bond length and O-M-O bond angles appropriate to different coordination geometries.

Although the curve for phosphate differs from those of acetate and nitrate, it can be clearly predicted that four-membered chelate rings will be most stable at longer M-O bond lengths with smaller O-M-O angles.

These isolated groups were also scanned with no constraints placed on coordination geometry. See Figure C.10. Variances in best-fit M-O lengths, O-M-O angles and O...O bite sizes for the three complexed ligands can probably be attributed to the differing atom sets attached to the O-donors. For nitrate, M-O = 2.74 Å, ∠ O-M-O = 47°, ∠ M-O-N = 97°, ∠ O-N-O = 120° and O...O = 2.17 Å, and for phosphate, M-O = 2.53 Å , ∠ O-M-O = 57°, ∠ M-O-P = 97°, ∠ O-P-O = 109° and O...O = 2.43 Å. Results obtained for the lowest energy structure of metal-acetate were compared to those obtained with five- and six-membered chelate rings (Figure C.11).

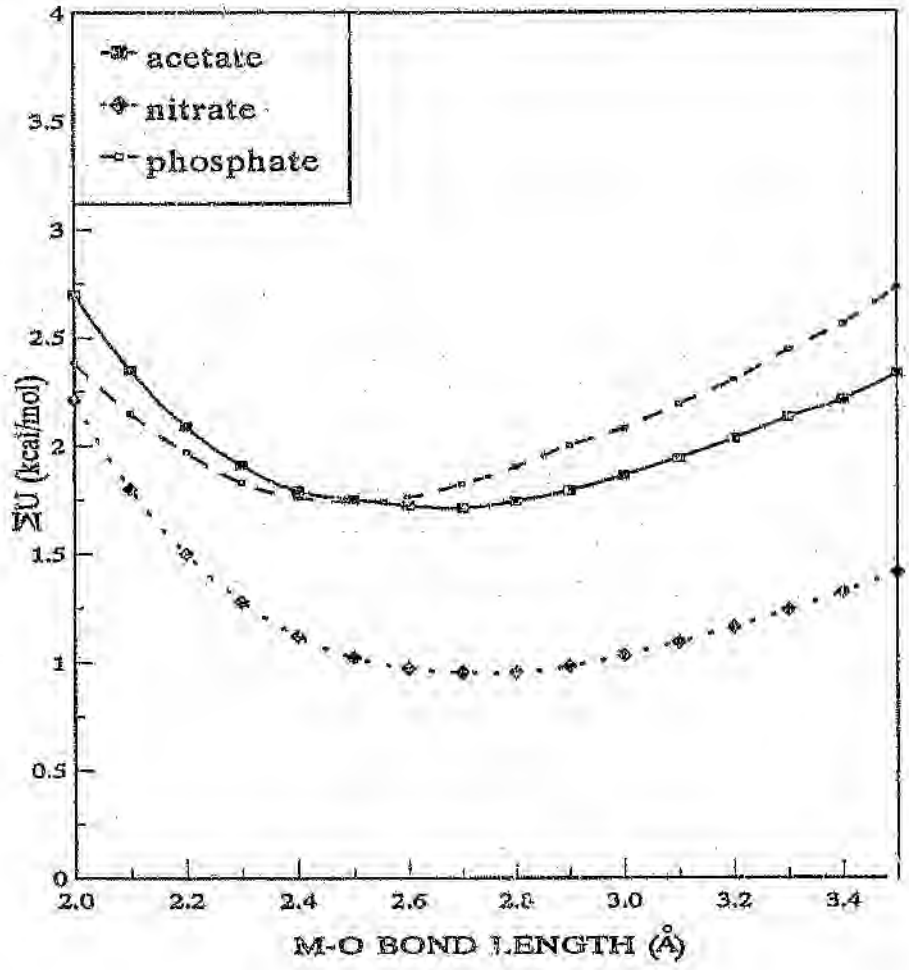

Figure C.10 : Strain energy, ΣU, of isolated acetate, nitrate and phosphate ligands as a function of metal-oxygen bond length and unconstrained O-M-O angles.

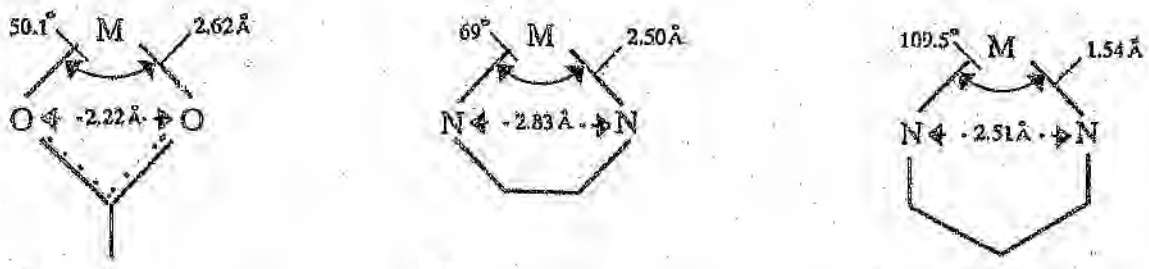

A B C

M-O-C angle = 93° M-N-C angle = 109° M-N-C angle = 109°
O-C-O angle = 123°

Figure C.11 : Lowest strain energy geometry for (A) the four-membered chelate ring, (B) the five-membered chelate ring, and (C) the six-membered chelate ring.
(B) and (C) redrawn from Hancock and Martell (1989).

C.2 BEST-FIT SIZES AND GEOMETRIES OF METAL IONS COORDINATED TO N-DONOR MACROCYCLES

In an attempt to fully understand the effect of N-donor macrocycle flexibility on selectivities exhibited by these structures, an intensive molecular mechanics investigation was carried out on the unsubstituted triaza- and tetraazamacrocycles. For each macrocycle, all possible N-H hydrogen orientations identified and labelled according to the scheme of Bosnich *et al.* (1965) were considered (see Figure A.1). Except where applied constraints are specified, eg. section C.2.1, both coordination geometry of the metal ions and M-N bond length were allowed to vary during scans.

C.2.1 Molecular mechanics calculations using constraints

To compare this molecular mechanics study to previous studies, the planar conformers of every macrocycle were scanned and their planar geometry constrained with an angle bending N-M-N force constant, K_b , of 0.014 kcal.mol^{-1}.deg^{-1} (TRIPOS force field). N-M-N angles were set to either 90° or 180°. Comparison of results is given in Table C.4. Figure C.12 can be consulted for the trans-III and trans-IV conformers of 13-aneN$_4$ and 15-aneN$_4$.

Table C.4 : Best-fit M-N bond lengths for triaza- and tetraaza macrocycles constrained to be trigonal planar and square planar respectively.

	Busch *et al.* (1974)		this work	
Macrocycle	M-N/ Å	deviation from plane[a]/ Å	M-N/ Å	deviation from plane[a]/ Å
9-aneN$_3$	-	-	1.51	0.40
12-aneN$_3$	-	-	1.61	0.35
12-aneN$_4$	1.83	0.41	1.82	0.19
13-aneN$_4$	1.92	0.12	1.97 (trans-III)	0.01
			1.94 (trans-IV)	0.07
14-aneN$_4$	2.07	0.00	2.11 (trans-III)	0.00
			2.08 (trans-IV)	0.00
15-aneN$_4$	2.22	0.14	2.19 (trans-III)	0.11
			2.08 (trans-IV)	0.02
16-aneN$_4$	2.38	0.00	2.32	0.07

[a] plane defined by N-donors

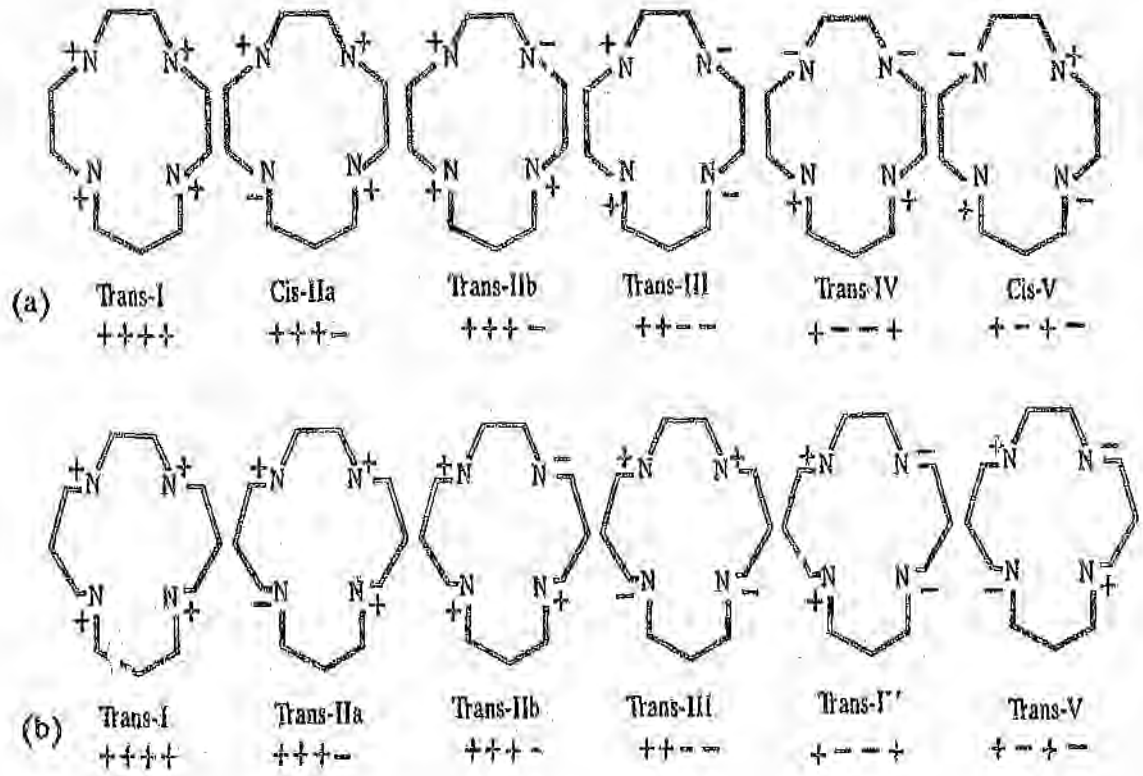

Figure C.12 : The six conformers of (a) 13-aneN$_4$, and (b) 15-aneN$_5$ with respect to the possible orientations of the N-H hydrogen atoms. H-atoms above the plane of the page are assigned +, while those below the plane of the page are assigned - .

C.2.2 9-aneN$_3$ and 12-aneN$_3$ complexes

Two orientations with reference to N-H hydrogens are possible for the triazamacrocycles 9-aneN$_3$ and 12-aneN$_3$ (Figure C.13). MM minimization of the uncomplexed ligands indicated the +++ energy conformer to be much more stable than the ++- . The [333] conformation of 9-aneN$_3$, as depicted by Dale's (1973) notation, was found to yield a lower strain energy than that of the [234] conformation (Hancock, Dobson and Boeyens, 1987). This symmetrical configuration for 9-aneN$_3$, where the chelate rings are all gauche, and the symmetrical [444] configuration for 12-aneN$_3$, where the rings are all chair, were used in initial scans to calculate ideal M-N bond lengths.

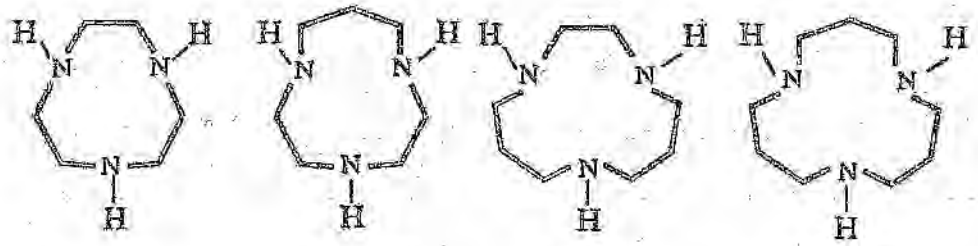

9-aneN$_3$ 10-aneN$_3$ 11-aneN$_3$ 12-aneN$_3$

Figure C.13 : Triazamacrocycles discussed in this section.

In Figure C.14(a) are shown the strain energy (ΣU) versus ideal bond length (r_0) curves for the +++ conformer of 9-aneN$_3$ and 12-aneN$_3$. The broad, flat curve for 9-aneN$_3$ indicates a high tolerance to change in metal ion size, while the narrower curve for 12-aneN$_3$ indicates a lower tolerance level. This may be the reason for the availability in the literature of crystal structures of Cu(II)[1], Pb(II)[2], Re(IV)[3], Pd(II)[4] and Ir(III)[5] complexes of 9-aneN$_3$ where M-N bond lengths range from 2.04 Å to 2.44 Å, and the availability of only Zn(II)[6,7] crystal structures of 12-aneN$_3$ where M-N bond lengths range from 2.00 Å to 2.06 Å. The preferences of 9-aneN$_3$ for larger metal ions and 12-aneN$_3$ for smaller metal ions are shown by the resultant best-fit M-M lengths, 1.80 Å and 1.65 Å respectively, from the curves.

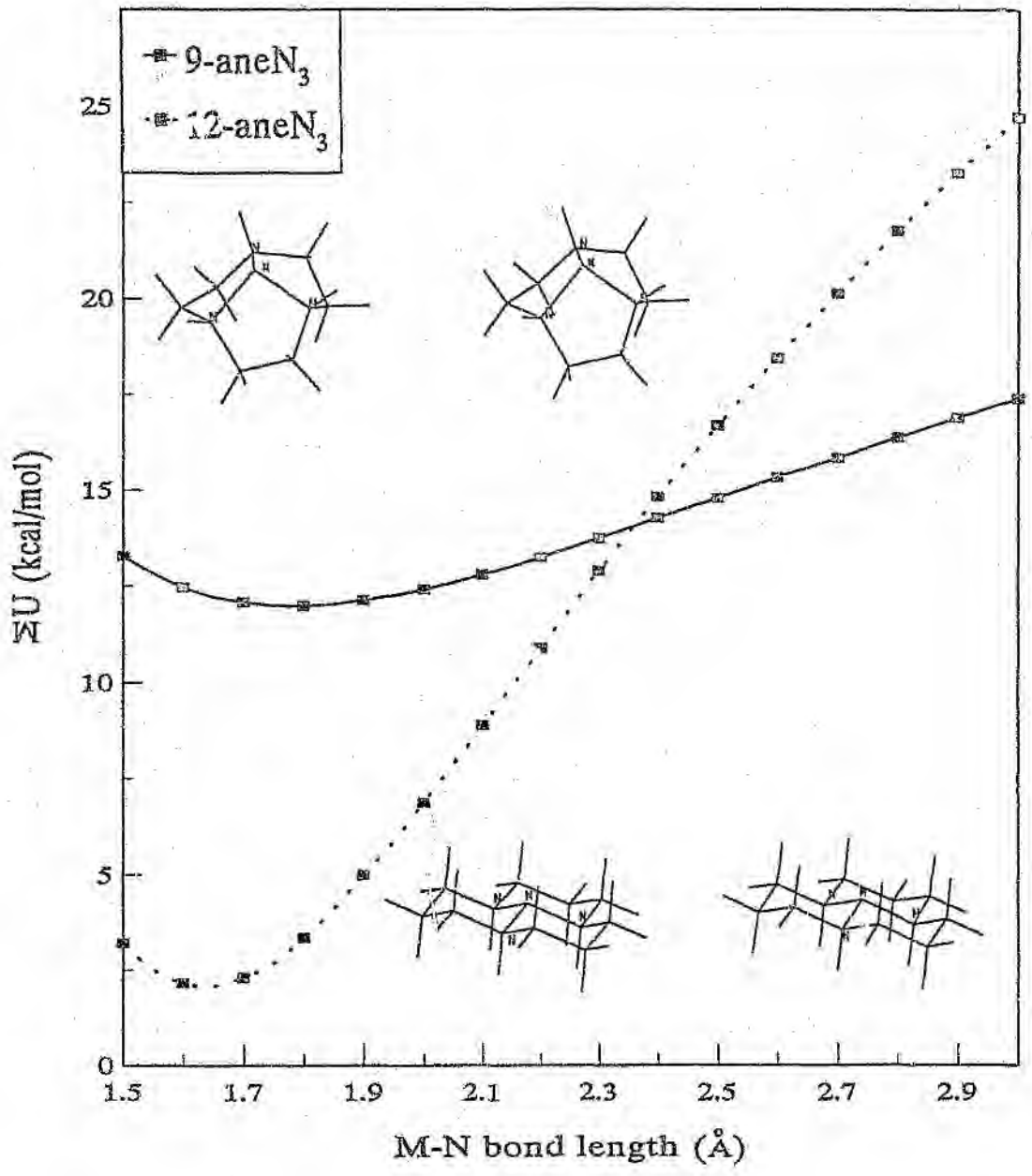

Figure C.14(a) : Total strain energy, ΣU, as a function of ideal M-N bond length for the +++ conformer of 9-aneN$_3$ and 12-aneN$_3$. Lowest energy structures for both are drawn.

Details of the crystal structures mentioned above are given in Table C.5. The smaller ligand experiences five or six coordination, while the larger ligand coordinates tetrahedrally. The coordination geometry calculated here for both triazamacrocycles at their best-fit M-N bond lengths is trigonal pyramidal. The metal lies 0.92 Å away from the N-donor plane in 9-aneN_3 and 0.54 Å away in 12-aneN_3. N-M-N angles in the 12-aneN_3 complex (109.7°) are however larger than those in the 9-aneN_3 complex (96.1°) which corresponds to the tendency of 12-aneN_3 to accommodate smaller tetrahedral metal ions such as Zn(II).

Table C.5 : Crystallographic data on 9-aneN_3 (L1) and 12-aneN_3 (L2) complexes.

Crystal Structure	Coordination Geometry	Ave. M-N/ Å	Ave. N-M-N/ °	Reference
$PbL1(ClO_4)_2$	six-coordinate	2.43	71.6	2
$[ReL1Cl_3]Cl$	pseudo-O_h	2.13		3
$CuL1Br_2$	dist. square pyramidal	2.11	82.9	1
$[PdHL1Br_2]ClO_4$		2.06	82.0	4
$IrL1Cl_3$	dist. O_h	2.06	82.9	5
[ZnL2Br]Br	dist T_d	2.04	104.9	6
$[ZnL2(OH)]_3^{3+}$	dist T_d	2.02	105.5	7

The adoption of the chair-chair-boat (c-c-b) conformation by $Zn(12\text{-ane}N_3)X$, where X = Br^- and OH^-, in two known crystal structures[6,7] instead of the expected ideal chair-chair-chair (c-c-c) conformation warranted further investigation. Results from MM calculations on the c-c-c ([444]) and c-c-b ([2 10]) forms of complexed $12\text{-ane}N_3$ are graphed in Figure C.14(b). Here, the N-M-N angles were constrained at 109.5° to account for tetrahedral metal character by assigning a value of $0.0028 kcal.mol^{-1}.deg^{-1}$ to the N-M-N bending force constant. The c-c-c form, in which N-H hydrogens lie on the opposite side of the N-donors plane to M, is most stable below an M-N bond length of 2.0 Å. The c-c-b form, in which the hydrogens lie on the same side as the metal ion, is most stable at r_0 values below this bond length. Since the average M-N distances in the crystal structures concerned are 2.04 Å and 2.02 Å, it is not unexpected that the c-c-b conformation is the one observed in reality.

Similar calculations were performed on $M(12\text{-ane}N_3)Br$. An extra conformation, c-c-c with N-H hydrogens on the same side of the N-donors plane as the metal, was studied. The curves in Figure C.14(c) show that the axial bromide has no effect on relative conformation stability, and that the c-c-b form still predominates at bond lengths greater than 2.0 Å.

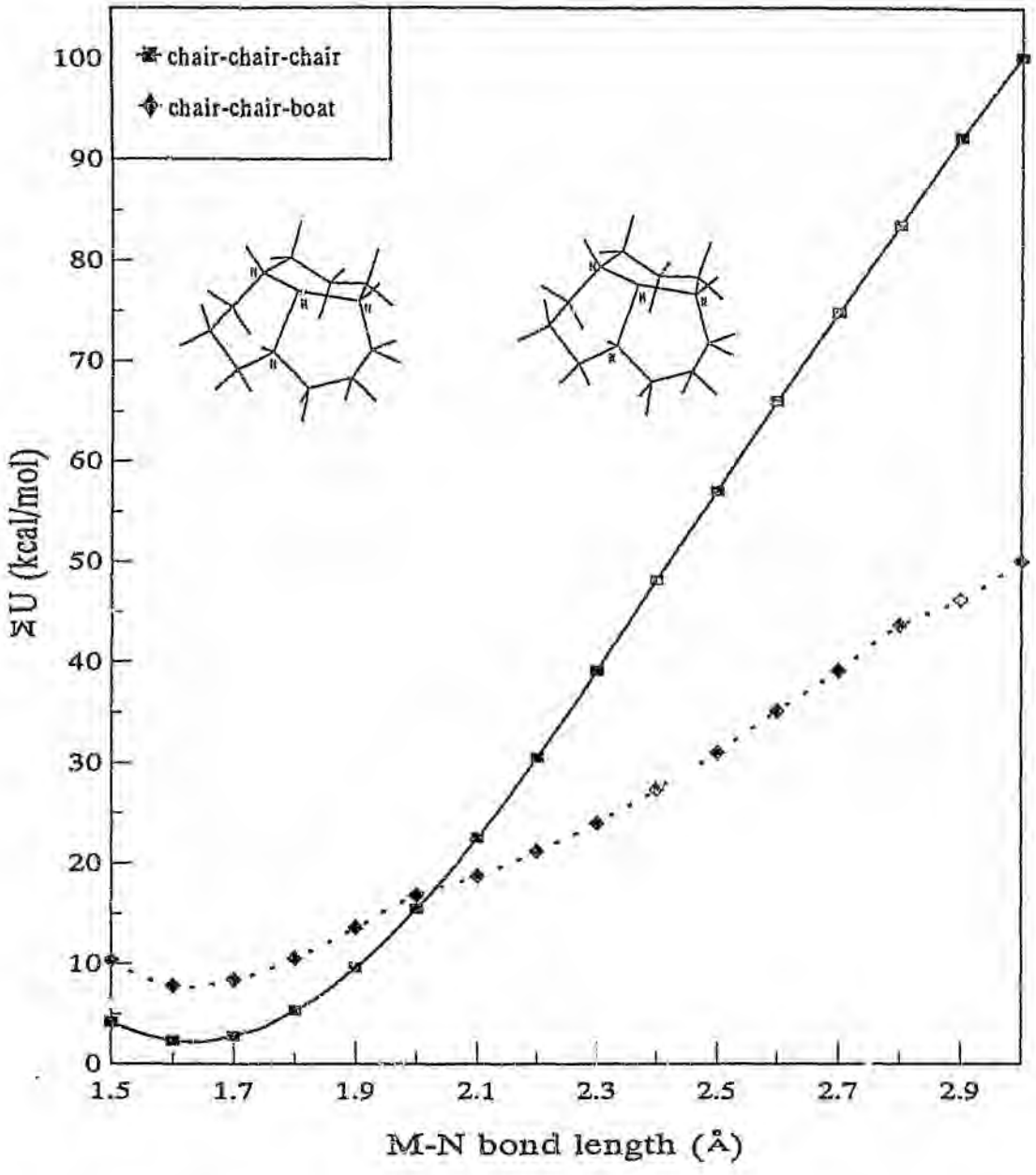

Figure C.14(b) : Total strain energy, ΣU, as a function of ideal M-N bond length for the chair-chair-chair and chair-chair-boat conformations of 12-aneN$_3$. M was constrained to be tetrahedral. In the c-c-c form (see structure in Figure C.14(a)), amine hydrogens lie on the opposite side to M, while in the c-c-b form (illustrated in this figure), they lie on the same side.

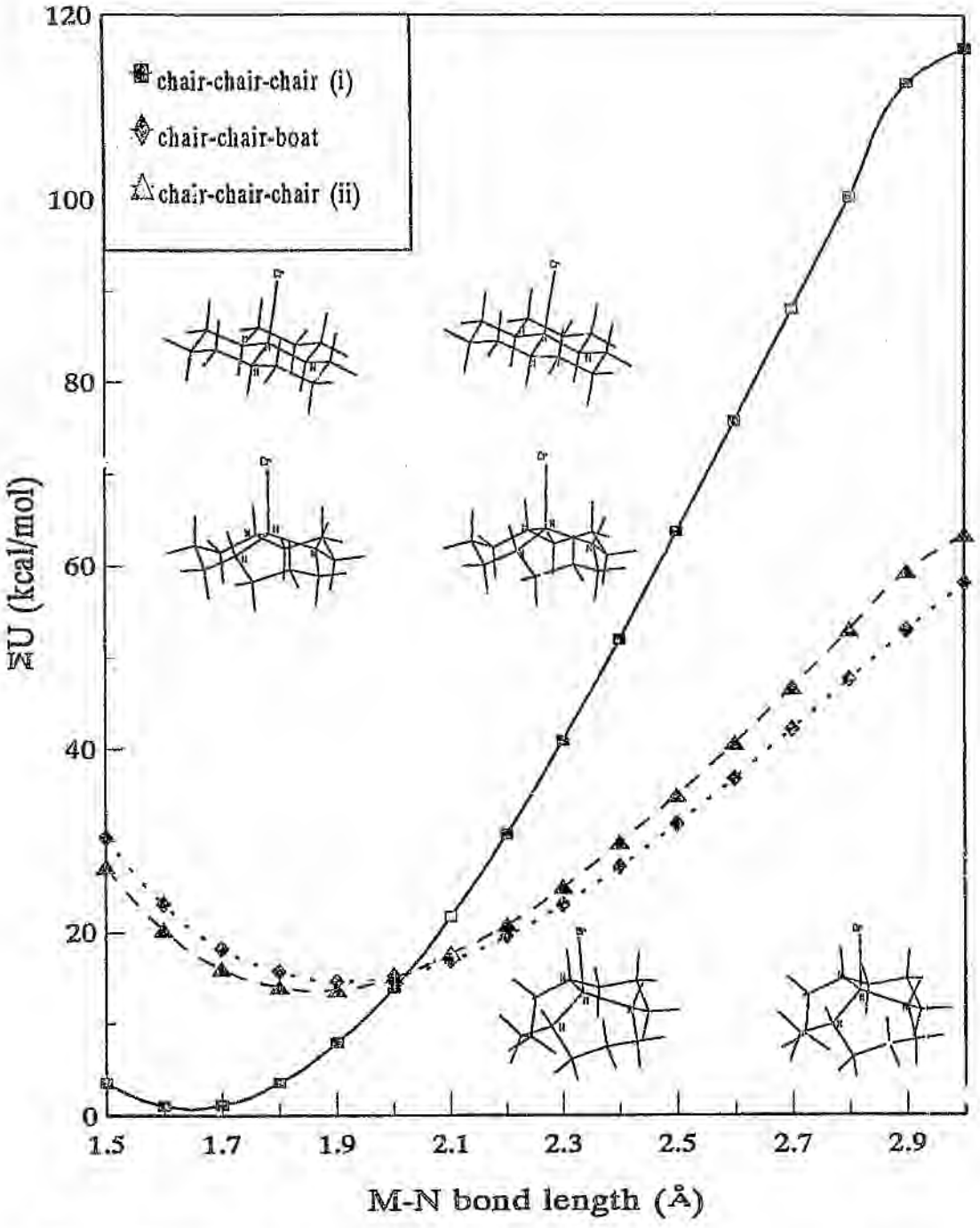

Figure C.14(c) : Total strain energy, ΣU, as a function of ideal M-N bond length for the chair-chair-chair (i), chair-chair-boat and chair-chair-chair (ii) conformations of 12-aneN$_3$Br. M was constrained to be tetrahedral. In the c-c-b (bottom structure) and c-c-c (ii) (middle structure) forms, amine hydrogens lie on the same side as M, while in the c-c-c (i) (top structure) form, they lie on the opposite side.

The popular thought concerning stability constant trends in triazamacrocycles is that the rigidity of these ligands force them to follow the size-match selectivity rule. On inspection of Table C.6, log K values for each ligand do indeed decrease as the size of the metal ion increases from Cu to Cd. The Pb anomaly was explained by Hancock *et al.* (1988) to be the result of stereochemical activity of the inert electron pair of the Pb ion. My study, however, shows that 9-aneN_3 and especially 12-aneN_3 are less rigid than expected. Their best-fit M-N lengths and N-M-N angles agree with the rule of complex stability in relation to chelate ring size, ie. 9-aneN_3 forms five-membered chelate rings when coordinated to a metal ion and therefore prefers larger metal ions, while 12-aneN_3 forms six-membered rings and therefore prefers smaller metal ions. Unfortunately, no reason for this disagreement with experimental data (9-aneN_3 actually binds more tightly to the smaller metal ions Cu and Ni than 12-aneN_3) could be distinguished. Since each ligand contains three secondary amine donor groups, steric effects should predominate and 12-aneN_3 should bind Cu and Ni better than 9-aneN_3.

Table C.6 : Compilation of log K_1 values[a] for complexes of the triazamacrocycles.

	Cu(II)	Ni(II)	Zn(II)	Cd(II)	Pb(II)
ionic radius[b]/ Å	0.57	0.69	0.74	0.95	1.18
log K_1 (9-aneN_3)	17.5	16.24	11.6	9.2	10.8
log K_1 (10-aneN_3)	16.14	14.58	11.28	7.8	8.8
log K_1 (11-aneN_3)	14.4	12.88	10.41		
log K_1 (12-aneN_3)	13.16	10.93	8.75		

[a] references : Chaudhuri and Wieghardt (1987), Kodama and Kimura (1978).

[b] square planar radius for Cu(II); octahedral radii for Ni(II), Zn(II), Cd(II) and Pb(II).

C.2.3 12-aneN$_4$ complexes

The ΣU versus r_0 curve for each of the four possible conformers of 12-aneN$_4$ is seen in Figure C.15. Trans-III (++--) and trans-IV (+--+) conformers are equivalent. The very broad, flat curve for trans-I (+-+++) indicates its probable ability to accommodate the full range of metal ion sizes, provided that they do not require octahedral coordination, since one axial coordination site is blocked off. An example of this conformer is the square pyramidal Cu(II)[8] complex (Table C.7). The relative stability of trans-I compared to the other forms can be attributed to the symmetrical quadrangular [3333] conformation and stable gauche chelate rings it adopts. Between the cross-over points 1.92 Å and 1.98 Å, buckled cis-II (+++-) is the stable conformer. This configuration is found in the Co(III)[9] and blue high-spin Ni(II) (Fabbrizzi, 1977) complexes of 12-aneN$_4$.

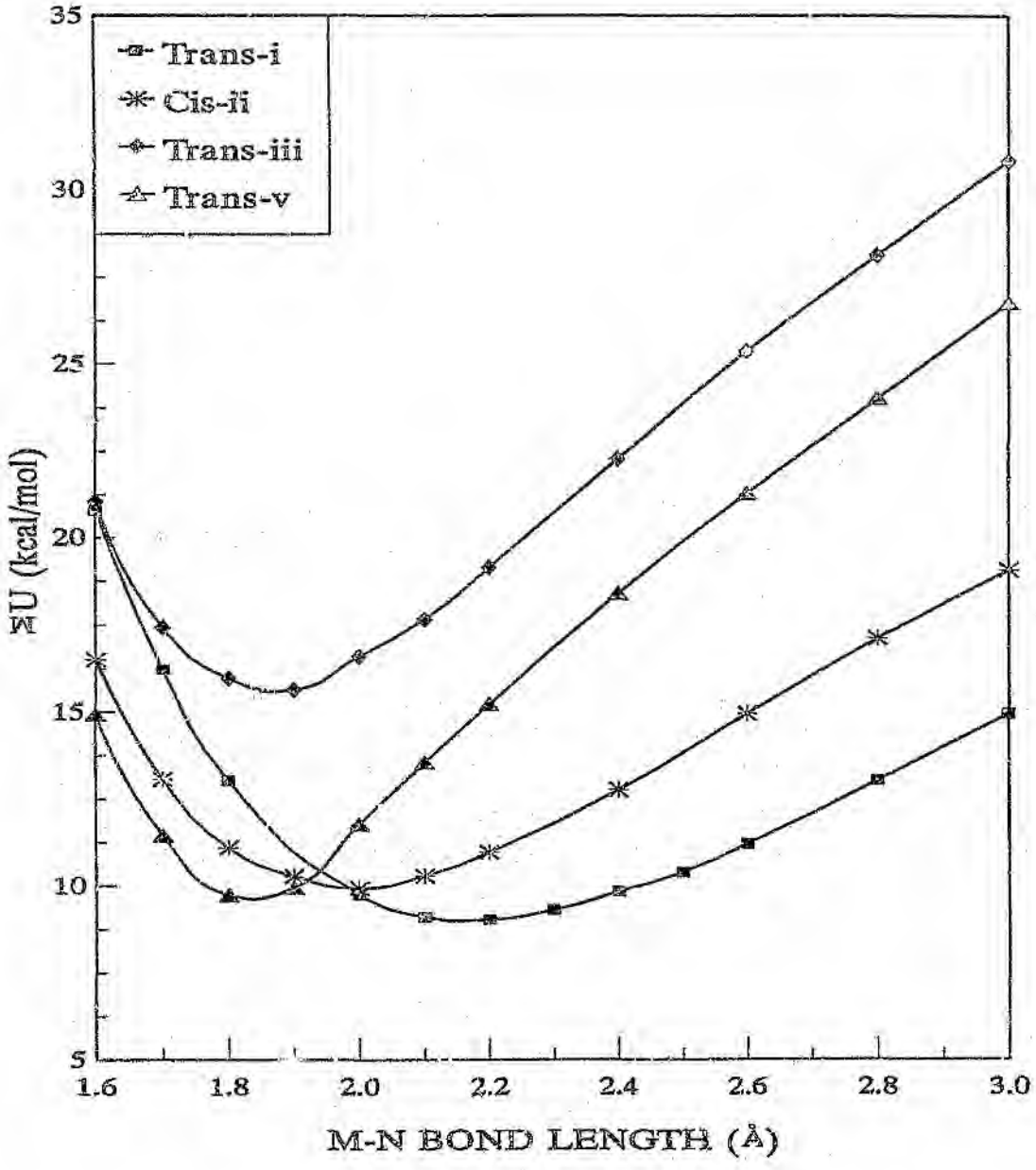

Figure C.15 : Total strain energy, ΣU, as a function of ideal M-N bond length for the four conformers of 12-aneN$_4$

Table C.7 : Crystallographic data on 12-aneN$_4$ (L) complexes.

Crystal Structure	Coordination Geometry	Ave. M-N/ Å	Ave. N-M-N/ °	Deviation from plane[a]/ Å	Reference
[CuLNO$_3$]NO$_3$	square pyramidal	2.02	86.3	0.51	8
[CoL(NO$_2$)$_2$]Cl	cis-O$_h$ (buckled)	1.96	84.8		9

[a] plane defined by N-donors

These results, presented in detail in Table C.8, correlate with previous findings (Thöm *et al.*, 1984). When r_0 is larger than the macrocycle cavity size of 1.82 Å (Table C.4) and octahedral coordination is not required as with Cu(II), the trans-I conformer is adopted. When there is a preference for octahedral geometry such as with Co(III) and high-spin Ni(II), the macrocycle folds. The yellow, square planar, low-spin [Ni(12-aneN$_4$)]$^{2+}$ complex (Fabbrizzi, 1977) has been characterized and predicted to adopt the trans-I configuration. Low-spin Ni(II) should ideally fit into the cavity of the trans-III conformer with its best-fit size of 1.90 Å and therefore assume this form. However, the square planar trans-III conformer has such a large ΣU values when compared to the others, that it seems extremely unlikely that it would occur in any complex. The trans-V (+-+-) conformer, which is also square planar at its lowest energy, is most stable at r_0 values below 1.92 Å and may be the form adopted in the Ni(II) complex.

Table C.8 : Results from MM calculations on conformers of 12-aneN$_4$

Conformer	Ave. r[a]/ Å	Ave. N-M-N angle/ °	ΣU[b]/ kcal.mol^{-1}	Coordination geometry of metal	Deviation from plane/ Å
trans-I (++++)	2.15	82.5[c]	9.01	square pyramidal	0.78
cis-II (+++-)	2.00	87.1	9.94	buckled	-
trans-III (++--)	1.90	87.9	15.63	distorted square planar	0.37
trans-V (+-+-)	1.85	92.6	9.61	distorted square planar	0.12

[a] final (minimised) M-N bond length

[b] strain energy at r

[c] N-M-N angle in five-membered chelate rings

Figure C.16 shows the variation of formation constants for a variety of metal ions as a function of the size of the macrocyclic ring. 12-aneN_4 prefers coordination to larger metal ions, contrary to the "best-fit" hypothesis. This preference can be explained by the results here. Larger metals are allowed to coordinate out of the plane of the N-donors in the trans-I conformer (Figure C.17) which is the most stable conformer at longer M-N bond lengths. Effect of chelate ring size is another factor. The four five-membered chelate rings of 12-aneN_4 favour large metals.

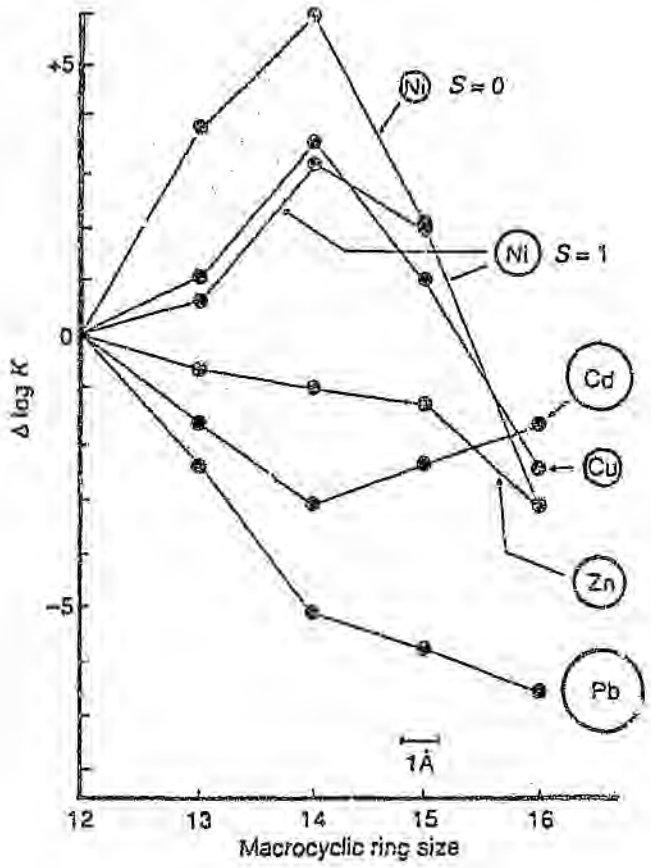

Figure C.16: Variation of complex stability of the tetraazamacrocycles 12-aneN_4 through 16-aneN_4, relative to 12-aneN_4, as a function of macrocyclic ring size. The metal ions are represented as circles of radii proportional to their ionic radii.
Redrawn from Luckay and Hancock, 1991. Stability constants from same reference.

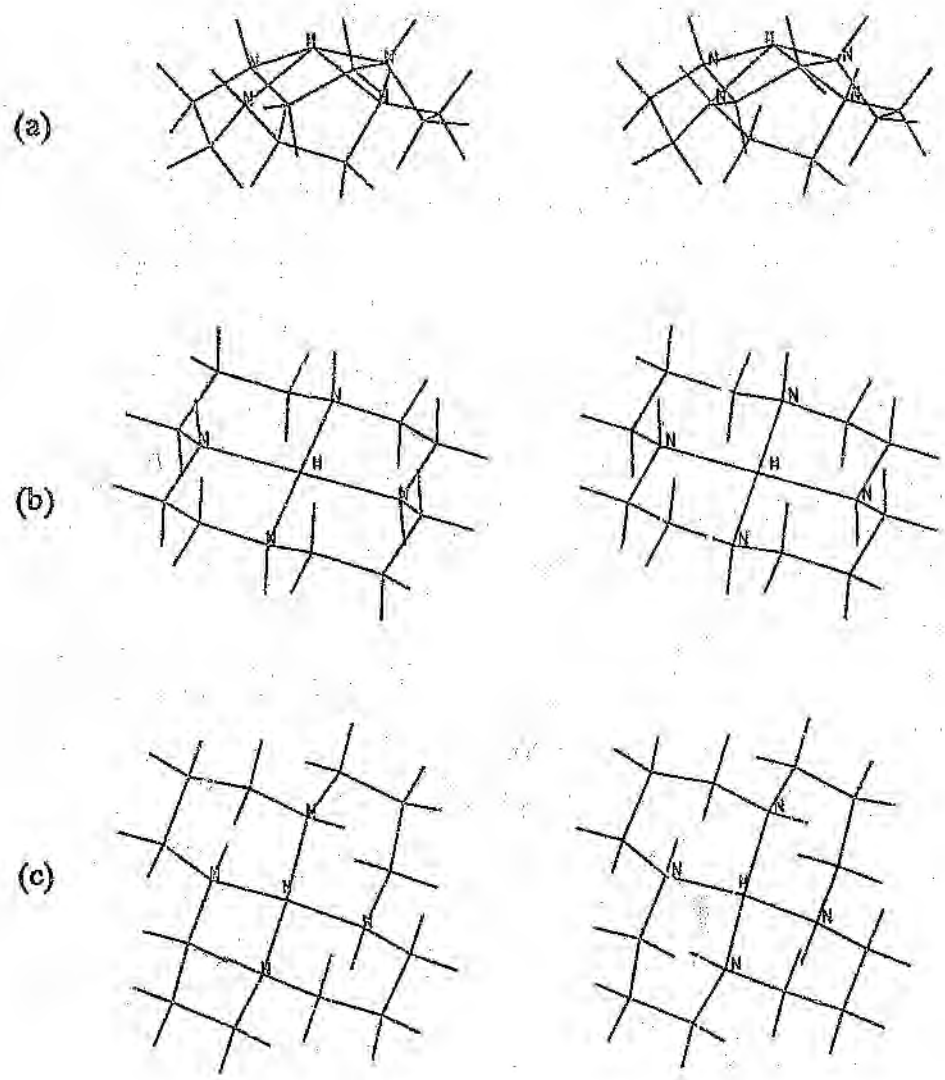

Figure C.17 : Stereoviews of lowest energy conformers of (a) 12-aneN$_4$, (b) 14-aneN$_4$ and (c) 16-aneN$_4$

C.2.4 13-aneN$_4$ complexes

Six conformers of 13-aneN$_4$ are possible (Figure C.12). Results from MM calculations on these conformers are given in Table C.9 and corresponding ΣU versus r_0 curves in Figure C.18. The square-pyramidal trans-IV (+--+) conformer is the most stable over a wide range of M-N bond lengths, ie. from 1.75 Å to 2.60 Å. The other square pyramidal conformer, trans-I (++++), will only predominate at r_0 values greater than 2.60 Å. Thus, with almost all metal ions that can assume square pyramidal geometry, trans-IV configuration is expected. However, the crystal structure of [Cu(13-aneN$_4$O)Br]$^+$ (see Table C.10) was found to match the trans-I form (Thöm *et al.*, 1984). This discrepancy was addressed in the same paper.

With metals that are too small for the 13-aneN$_4$ macrocycle cavity such as low-spin Ni(II)[11], Ni(III)[12] and low-spin Fe(II)[14], the ligand adopts planar geometry. In this case, where the requirement for metal planarity is strong, the planar trans-Ib (+++-) conformer is predicted to be stabilised relative to the trans-III (++--). Martin *et al.* (1987) postulated the presence of these two isomers for the Ni(13-aneN$_4$)$^{2+}$, the +++- being the intermediate. The C-functionalized [Ni(Me$_2$-13-aneN$_4$)]$^{2+}$ complex was reported[11] to have chelate rings in the order chair-gauche-cis-gauche, which is the order found in trans-IIb here.

If the metal ion is larger than the cavity size of 1.97 Å (trans-III) or 1.94 Å (trans-IV) as given in Table C.4, and has a strong preference for remaining octahedral, the cis conformers IIa (+++-) and V (+-+-) will prevail. Examples of such buckled structures are the complexes with high-spin Ni(II)[10], Ru(III)[13] and high-spin Fe(II)[14]. Curves obtained for the cis conformers are so similar that no prediction regarding them can be made. Che *et al.*[13] formulated their Ru(III) structure to be the +++- configuration, while Martin *et al.* (1987) and Hay and Pujari (1986) formulated their complexes, [Ni(13-aneN$_4$)(H$_2$O)2]$^{2+}$ and [Ni(13-aneN$_4$)(en)]$^{2+}$, to be of the form +-+-.

Table C.9 : Results from MM calculations on conformers of 13-aneN_4.

Conformer	Ave. r[a]/ Å	Ave. N-M-N angle/ °	ΣU[b]/ kcal.mol^{-1}	Coordination geometry of metal	Deviation from plane/ Å
trans-I (+++-+)	2.20	80.6[c] 93.2[d]	11.76	square pyramidal	0.73
cis-IIa (+++-)	2.05	86.0 97.9	10.36	buckled	-
trans-IIb (+++-)	1.95	88.1 101.5	9.55	distorted square planar	0.13
trans-III (++--)	2.00	84.2 102.9	10.50	distorted square planar	0.28
trans-IV (+--+)	2.01	86.9 89.1	7.74	square pyramidal	0.44
cis-V (+-+-)	2.00	86.2 103.4	10.48	buckled	-

[a] final (minimised) M-N bond length

[b] strain energy at r

[c] N-M-N angle in five-membered chelate rings

[d] N-M-N angle in six-membered chelate ring

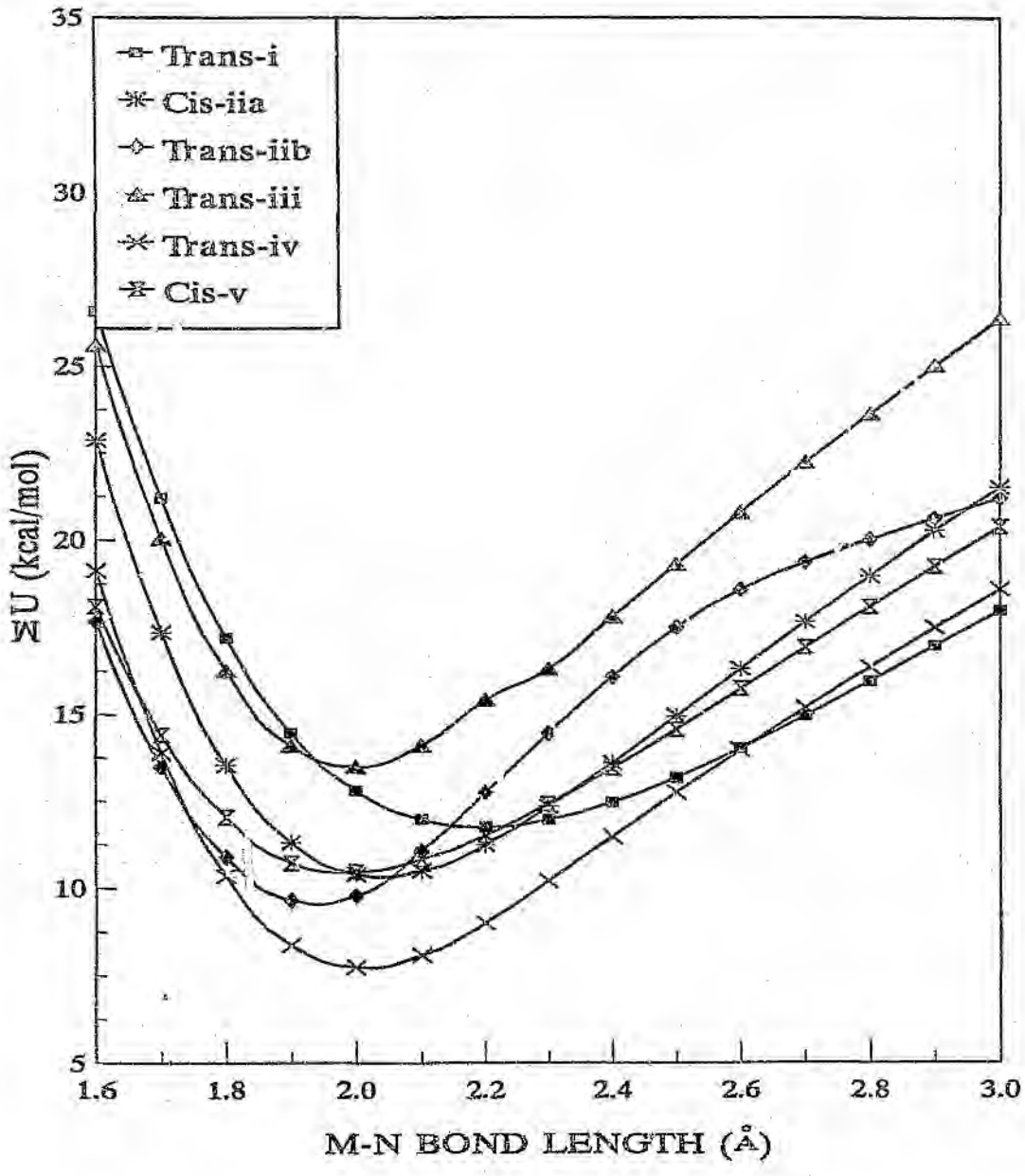

Figure C.18 : Total strain energy, ΣU, as a function of ideal M-N bond length for the six conformers of 13-aneN$_4$.

Table C.10 : Crystallographic data on 13-aneN$_4$ (L) complexes. L^1 is 1,4,7,10 - tetramethyl-13-aneN$_4$.

Crystal Structure	Coordination Geometry	Ave. M-N/ Å	Deviation from plane/ Å	Reference
$[RuL^1Cl_2]ClO_4$	cis-O_h	2.18		13
NiL(NCS)$_2$ (s=1)	cis-O_h	2.12		10
$[Cu(13\text{-}aneN_3O)Br^+$	square pyramidal	2.04	0.47	Thöm *et al.*, 1984
$6[NiL.Br_2]Br$	trans-O_h	1.92		12
$[Ni(Me_2\text{-}L)]^{2+}$ (s=0)	square planar	1.88		11

C.2.5 14-aneN$_4$ complexes

Of the azamacrocycles, cyclam or 14-aneN$_4$ has been the most extensively studied. Hence the many crystal structures available (Table C.11). Planar structures all adopt the trans-III (++--) conformer. Their M-N crystal bond lengths range from 1.97 Å to 2.13 Å. Metals with a strong preference for square planar coordination such as Cu(II)[26] and Pd(II)[29] complex with the ligand in this manner. Diamagnetic, square planar, yellow Ni(II)-cyclam has been characterized in solution by, among others, Ohtaki and Seki (1991), but a crystallographic study has yet to be reported. Buckled cis-V configurations are assumed by high-spin Ni(II)[23] Cr(III)[19], Ru(III)[31], Co(III)[37] and Pb(II)[35], a phenomenon expected for the latter metal only. Both trans and cis-octahedral forms exist for Ir(III) (Monsted *et al.*, 1993), Ni, Cr and Ru, their sizes being on the borderline between cavity size fit and larger than cavity size.

Another large metal, Hg(II)[34], complexes with cyclam in a square pyramidal, trans-I (++++) fashion. Hg is a metal which is not obliged to be octahedral. Ag(II)[36] displays both distorted square planar and octahedral geometries with 14-aneN$_4$. In the square planar structure, Ag is extruded 0.24 Å from the N-donor plane, thus tending towards trans-I conformation. In the octahedral structure, Ag lies in the plane. Both isomers could probably be isolated because the Ag(II) radius is intermediate between that of the smaller transition metals which coordinate in a planar fashion and that of the larger ions which coordinate in square pyramidal.

Table C.11 : Crystallographic data on 14-aneN$_4$ (L) complexes. X = Cl, Br, or NO$_3$.

Crystal Structure	Coordination Geometry	Ave. M-N/ Å	Ave. N-M-N/ °	Reference
$[CrLX_2]^+$	trans-O_h	2.06	85.4[a], 94.6[b]	15, 16, 17, 18
$[CrLCl_2]Cl$	cis-O_h	2.10		19
$[MnLX_2]^+$	trans-O_h	2.03	85.3, 94.7	20
$CoL(ClO_4)_2$ (s=0)	trans-O_h	1.98	85.9, 94.1	21
$NiLX_2$ (s=1)	trans-O_h	2.06		Thöm *et al.*, 1984, Bosnich *et al.*, 1965, 22
$[NiL(H_2O)_2]^{2+}$ (s=1)	cis-O_h	2.10		23
$[NiLCl_2]^+$	trans-O_h	1.97		24
$[CuL(H_2O)_2]^{2+}$	trans-O_h	2.01	85.6, 94.4	25
$[CuL]^{2+}$	square planar	2.04		26
$[ZnL]^{2+}$	trans-O_h	2.11		27, 28
$[PdL]^{2+}$	square planar	2.05		29
$[PdLCl_2]^{2+}$	trans-O_h	2.06		29

$[RuLCl_2]Br$	trans-O_h	2.08	83.4, 96.6	30
$[RuLCl_2]Cl$	cis-O_h	2.11	82.4, 96.1	31
$[ReO(OH)L]^{2+}$	trans-O_h	2.09	83.5, 96.5	32
$[TcLO_2]^+$	trans-O_h	2.13		33
$[HgLCl]^+$	square pyramidal	2.37		34
$PbL(NO_3)_2$	cis-O_h	2.45		35
$AgL(ClO_4)_2$	trans-O_h	2.19		36
	dist. square planar	2.16		

[a] five-membered chelate rings

[b] six-membered chelate rings

In Figure C.19 are seen the univariate scans for the conformers of 14-aneN_4. Detailed results are given in Table C.12. All geometries adopted by the conformers, except cis-V, are square planar. Cis-V only predominates at high r_0 values, a prediction verified by the literature. The lowest energy conformer, trans-III, is diagrammed in Figure C.17.

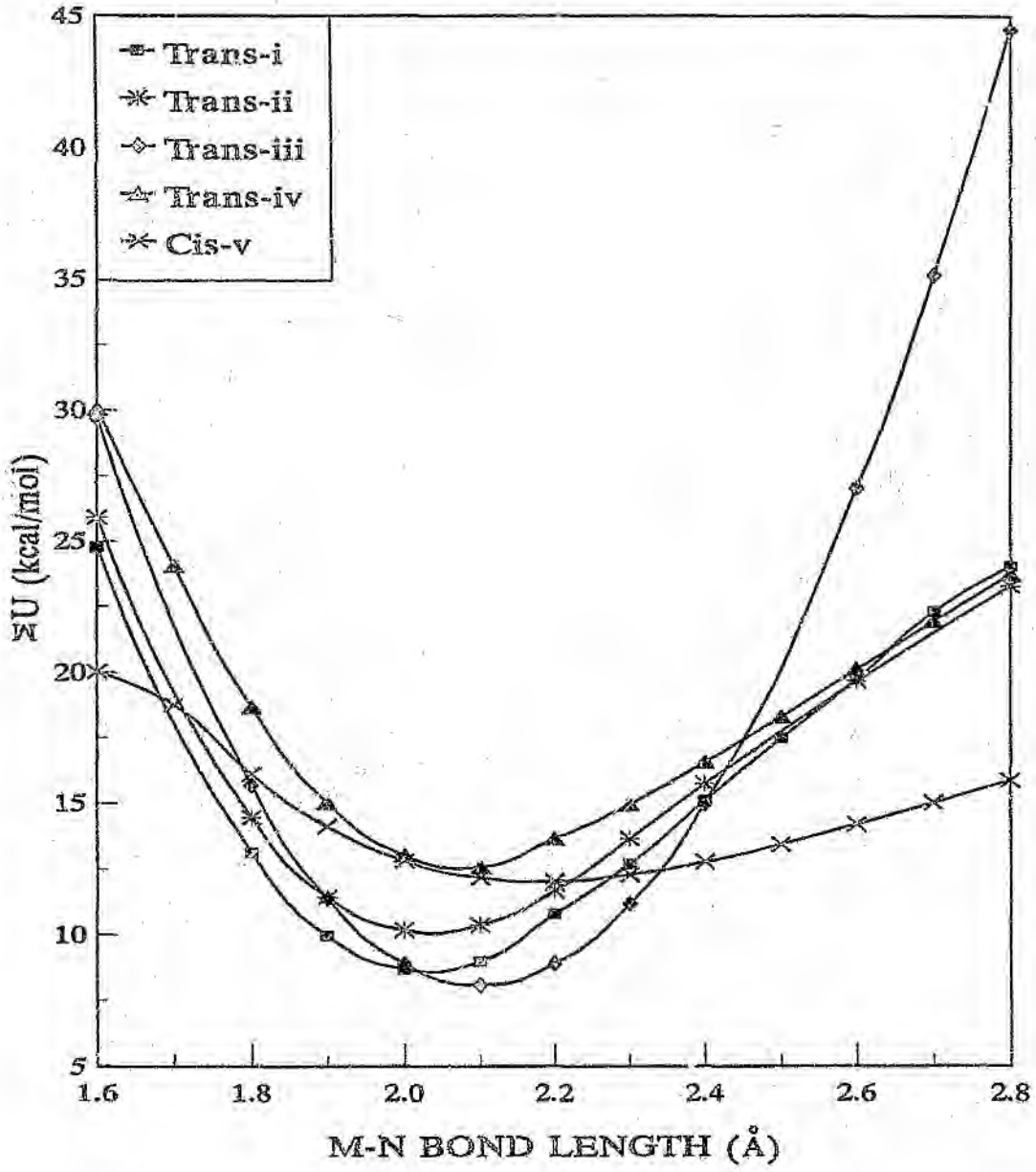

Figure C.19 : Total strain energy, ΣU, as a function of ideal M-N bond length for the five conformers of 14-aneN$_4$

Table C.12 : Results from MM calculations on conformers of 14-aneN$_4$.

Conformer	Ave. r[a]/ Å	Ave. N-M-N angle/ °	ΣU[b]/ kcal/mol	Coordination geometry of metal	Deviation from plane/ Å
trans-I (++++)	2.03	87.6[c] 92.4[d]	8.59	square planar	0.06
trans-II (+++-)	2.04	86.4 93.4	10.06	square planar	0.07
trans-III (++--)	2.11	84.5 95.5	8.07	square planar	0.00
trans-IV (+--+)	2.09	83.4 98.0	12.58	square planar	0.04
cis-V (+-+-)	2.20	80.3 88.1	12.03	buckled	-

[a] final (minimised) M-N bond length

[b] strain energy at r

[c] N-M-N angle in five-membered chelate rings

[d] N-M-N angle in six-membered chelate rings

C.2.6 15-aneN$_4$ complexes

As with 13-aneN$_4$ six conformers of 15-aneN$_4$ are possible. ΣU versus r_0 curves for these conformers are graphed in Figure C.20 and additional information shown in Table C.13. A survey of the literature revealed the availability of only trans-octahedral structures (Table C.14) for the 15-aneN$_4$. M-N bond lengths in these structures indicate that these metals would fit fairly well into the 15-aneN$_4$ macrocyclic cavity whose hole size was calculated to be 2.19 Å (trans-III) and 2.08 Å (trans-IV). Inspection of the experimental curves show that for r_0 values between 1.6 Å and 2.75 Å, planar configurations will likely be adopted. Trans-octahedral geometry is also the geometry found in both high- and low-spin Fe(II) and Cr(III) complexes.

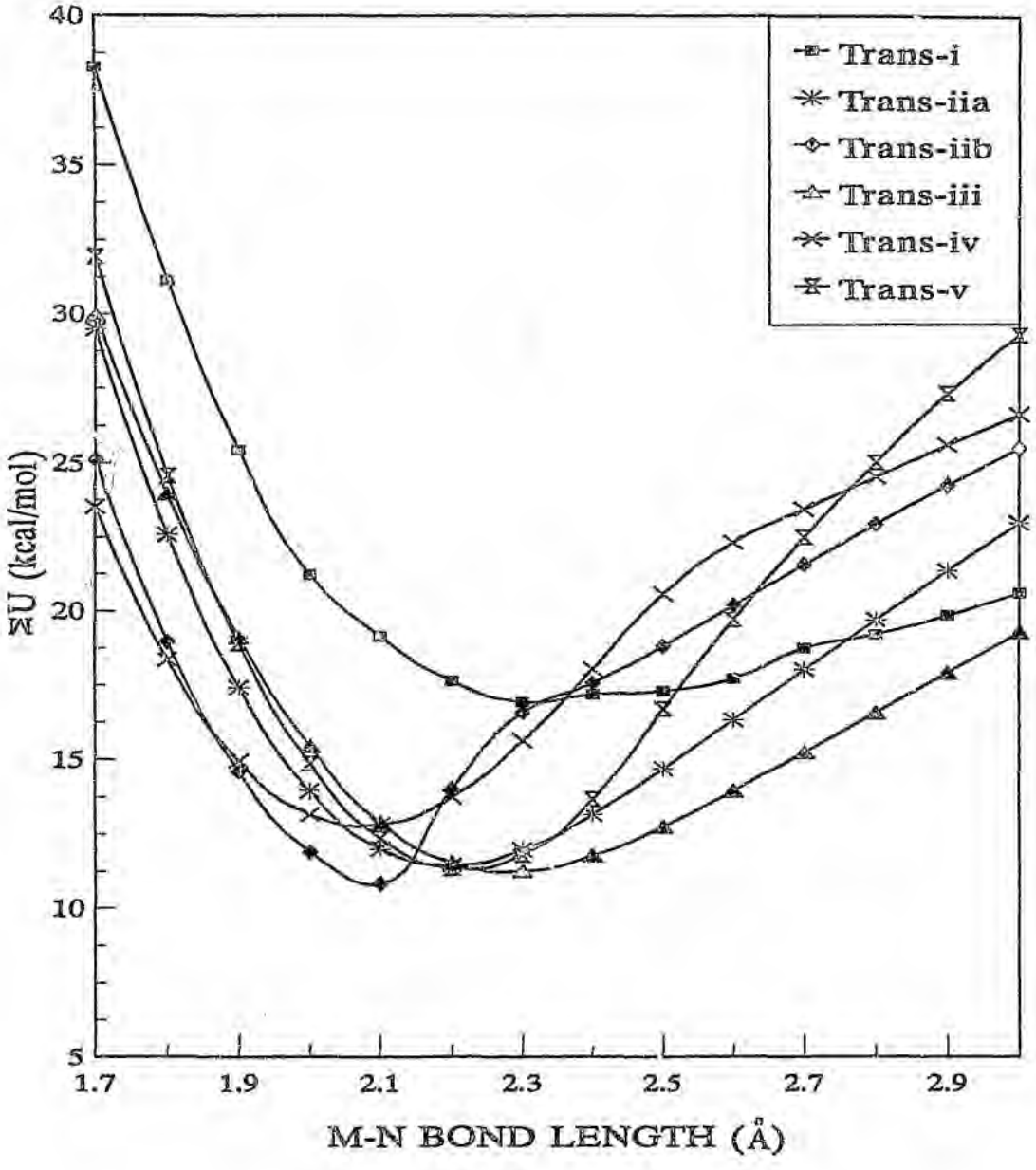

Figure C.20 : Total strain energy, ΣU, as a function of ideal M-N bond length for the six conformers of 15-aneN$_4$

Table C.13 : Results from MM calculations on conformers of 15-aneN$_4$

Conformer	Ave. r[a]/ Å	Ave. N-M-N angle/ °	ΣU[b]/ kcal/mol	Coordination geometry of metal	Deviation from plane/ Å
trans-I (++++)	2.19	81.0[c] 90.7[d]	11.65	square pyramidal	0.41
trans-IIa (+++-)	2.20	80.8 90.0	11.45	square pyramidal	0.45
trans-IIb (+++-)	2.11	84.1 92.3	10.83	square planar	0.10
trans-III (++--)	2.20	78.3 89.1	11.25	square pyramidal	0.59
trans-IV (+--+)	2.09	84.8 92.4	12.82	square planar	0.07
trans-V (+-+-)	2.20	80.8 93.1	11.35	square planar	0.00

[a] final (minimised) M-N bond length

[b] strain energy at r

[c] N-M-N angle in five-membered chelate ring

[d] N-M-N angle in six-membered chelate rings

Table C.14 : Crystallographic data on 15-aneN$_4$ (L) complexes. L^1 is 1,4,8,12 - tetramethyl-15-aneN$_4$.

Crystal Structure	Coordination Geometry	Ave. M-N/ Å	Reference
$CuL(ClO_4)_2$	trans-O_h	2.04	38
$NiLCl_2$ (s=1)	trans-O_h	2.11	22
$ZnL(NCS)_2$	trans-O_h	2.15	39
$[RuL^1O_2](ClO_4)_2$	trans-O_h	2.20	40

The abse of buckled structures results from increased macrocyclic cavity size. This was reasoned by Hung *et al.* (1977) and Richens *et al.*[41] who found that for Co(III) and Cr(III) metals which have a preference for octahedral coordination, cis-folded complexes occur for 12-aneN$_4$, both cis and trans occur for 13-aneN$_4$ and 14-aneN$_4$, but only trans complexes exist for 15-aneN$_4$ and 16-aneN$_4$. These same researchers isolated two isomers for trans -$[Co(15\text{-aneN}_4)Cl_2]^+$. The thermodynamically stable isomer was of configuration +++- or trans-IIb with an MM calculated M-N distance of 2.28 Å. The second isomer had the +-+- or trans-V form with an ideal M-N distance of 2.23 Å.

C.2.7 16-aneN$_4$ complexes

As with 12-aneN$_4$, only four possible conformers of 16-aneN$_4$ are feasible since the trans-III (++--) and trans-IV (+--+) conformers are equivalent. Curves and detailed results are given in Figure C.21 and Table C.15. It can be clearly seen that at low r_0 values (less than 2.1 Å), the tetrahedral trans-V (+-+-) conformer is very much stabilized relative to the remaining conformers. We would thus predict that small tetrahedral cations such as Be(II), B(III) or P(V) would complex most strongly with

16-aneN$_4$. The [4444] conformation assumed by trans-V and its conformational sequence of four chair-form chelate rings is responsible for its low energy. A stereoview of this configuration can be seen in Figure C.17.

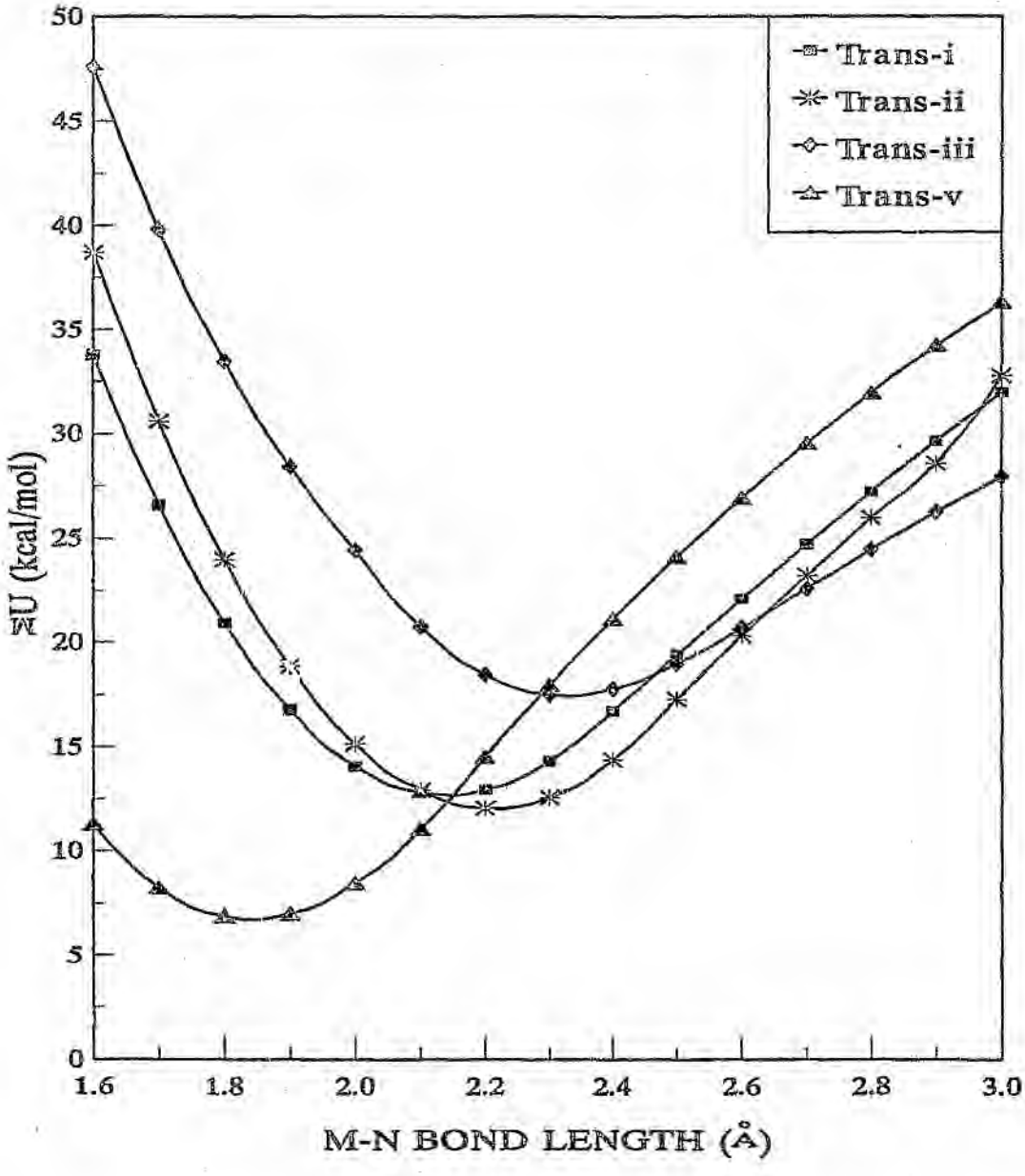

Figure C.21 : Total strain energy, ΣU, as a function of ideal M-N bond length for the four conformers of 16-aneN$_4$.

Table C.15 : Results from MM calculations on conformers of 16-aneN$_4$

Conformer	Ave. r[a]/ Å	Ave. N-M-N angle/ °	ΣU[b]/ kcal/mol	Coordination geometry of metal	Deviation from plane/ Å
trans-I (++++)	2.15	93.6[c]	12.70	distorted square planar	0.26
trans-II (+++-)	2.20	91.2	12.05	dist. sq. planar/ buckled	0.14
trans-III (++--)	2.17	90.3	14.38	distorted square planar	0.26
trans-V (+-+-)	1.85	102.8	6.75	distorted tetrahedral	-

[a] final (minimised) M-N bond length

[b] strain energy at r

[c] N-M-N angle in six-membered chelate rings

The crystal structures of Ni(II)[22] and Cr(III)[42] 16-aneN$_4$ complexes are reported to have the +++- or trans-II configuration. This agrees with the results obtained here. Of the three square planar conformers, the trans-II is the most stable at r_0 values greater than 2.10 Å. Cd(II) and Hg(II)[43] however, have all the N-H groups directed towards one axial ligand, ie. they adopt the trans-I (++++) configuration. This discrepancy can be explained by examining metal to N-donor plane distances for the four structures. The distances for Cd and Hg are much longer than those for Ni and Cr, a result of their larger sizes. Thus, even though trans-II is stabilised relative to trans-I, there will be a tendency towards trans-I when longer M-N bond lengths are required. Pb(II)[43] bonds with the N-donors of 16-aneN$_4$ at distances much larger than the macrocycle cavity size of 2.32 Å (Table C.4), and even though the Pb complex adopts the trans-I form, the preference of Pb to be octahedrally coordinated forces

buckled cis configuration (see Table C.16).

Table C.16 : Crystallographic data on 16-aneN$_4$ (L) complexes.

Crystal Structure	Coordination Geometry	Ave. M-N/ Å	Deviation from plane/ Å	Reference
$NiLCl_2$ (s=1)	trans-O_h	2.18	0.072	22
$[CrLCl_2]ClO_4$	trans-O_h	2.13	0.089	42
$[CdL(NO_3)(H_2O)]^{2+}$	trans-O_h	2.33	0.29	43
$[HgLCl]_2[HgCl_4]$		2.38	0.24	43
$[PbLCl]Cl$, $PbL(NO_3)_2$	cis-O_h	2.54	1.26	43

16-aneN$_4$ forms more stable complexes with smaller metal ions like Cu(II) (log K = 20.92) than with the large metals like Pb(II) (log K = 9.29, Luckay *et al.*, 1991). The principal reason for this selectivity is the inductive effect where Cu binds more tightly to amines than Pb. In addition to this effect, steric factors also act to favour Cu. These steric factors are: (i) the presence of four six-membered chelate rings when 16-aneN$_4$ is complexed, and (ii) the adoption of the stable trans-V conformer which prefers coordination to metals with tendencies to form smaller tetrahedral ions. However, no four-coordinate crystal structures have been recorded to date and attempts with crystallization failed in this project.

MM calculations using metal parameters in the SYBYL 6.0 package were used to predict coordination geometries of Cu(16-aneN$_4$)$^{2+}$ and Pb(16-aneN$_4$)$^{2+}$. Since valencies of six were assigned to the metals when defining them in SYBYL, 1,3-nonbonded interactions replaced N-M-N angle bending constants. Results predict tetrahedral geometry for Cu and trans-I for Pb (Table C.17), which correlates with the work above.

Table C.17: Strain energies for the conformers of $Cu(16\text{-}aneN_4)^{2+}$ and $Pb(16\text{-}aneN_4)^{2+}$.

Metal		trans-I	trans-II	trans-III	trans-V
Cu	ΣU/ kcal.mol^{-1}	16.418	19.511	18.693	5.500
	Ave. Cu-N/ Å	1.947	1.956	1.947	1.909
	Ave. N-Cu-N/ °	94.9	92.4	92.7	102.4
	Coordination geometry	dist. square planar	square planar	square planar	tetrahedral
Pb	ΣU/ kcal.mol^{-1}	15.831	16.485	18.027	17.671

C.3 BEST-FIT SIZES OF METAL IONS COORDINATED TO N-FUNCTIONALIZED MACROCYCLES

In order to gain further insight into ligand design for purposes of diagnostic nuclear medicine and radioimmunotherapy, molecular mechanics minimizations were carried out on azamacrocycles which were N-functionalized with acetate, hydroxyphenyl and hydroxybenzyl groups. The metals of interest here are the lanthanides and Group III's, classified by Pearson (1963) as hard acids. A preliminary thought would thus be to complex them with hard bases like ligands containing neutral and negatively charged oxygen donor atoms. Although macrocycles containing neutral nitrogen donors are less basic, chelating groups can be attached to the nitrogens to improve the coordinating ability of the macrocycle. Full or semi-substitution of amine-attached hydrogens may occur.

Again, all possible conformers for each macrocycle were considered in the calculations. The difference in covalent radii of 0.1 Å between nitrogen and oxygen was used to calculate relative ideal M-O bond lengths. All other experimental data is given in section B.3. See Figure C.22 for ligand structures discussed in this section.

Previous MM calculations by Brecknell *et al.* (1985) and Hay (1991) on lanthanide ion complexes concentrated on optimizing force-field parameters for the metal ions. In both cases, L-M-L bending interactions were replaced with L-L onbonded interactions to circumvent problems in defining angle bending parameters. Fossheim *et al.*, (1990, 1991) examined molecular structures and dynamics of, amongst others, DTPA, TACNTA, DOTA and TETA with Gd(III) by molecular mechanics calculations and molecular dynamics simulations. They were investigating factors which determine stability of these complexes.

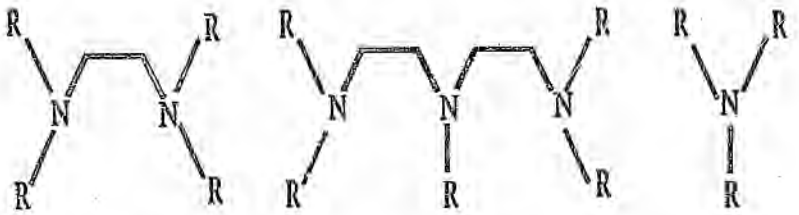

R = acetic acid	EDTA	DTPA	NTA
= propionic acid			NTP
= 2-hydroxyphenyl			NTHP
= 2-hydroxybenzyl			NTHB

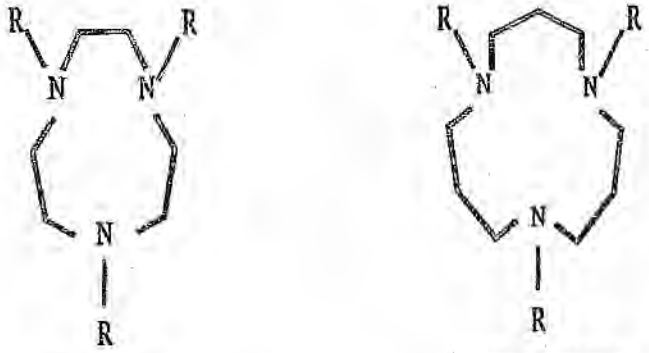

R = acetic acid	TACNTA	TACDTA
= 2-hydroxyphenyl	Q	R
= 2-hydroxybenzyl	V	W

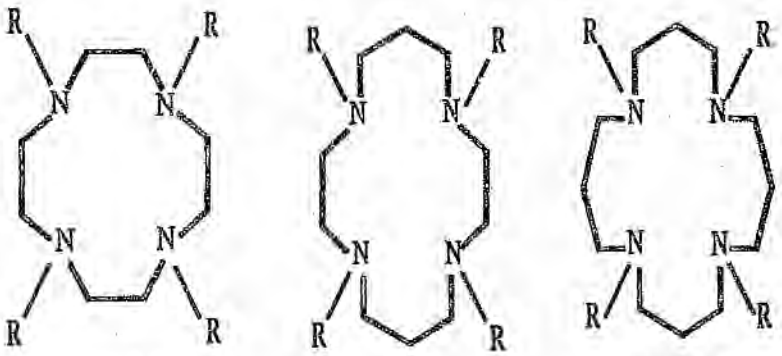

R = acetic acid	DOTA	TETA	HETA
= 2-hydroxyphenyl	S	T	U
= 2-hydroxybenzyl	X	Y	Z

Figure C.22 : Ligands N-functionalized with acetate, hydroxyphenyl and hydroxybenzyl groups.

C.3.1.1 EDTA and DTPA

Since functionalized EDTA and DTPA have also been investigated for medical use, scans on the acyclic ligands EDTA and DTPA were included. Although EDTA forms relatively stable complexes with most metal ions, its open chain backbone often prevents it from completely wrapping around small, hard trivalent metals like Ga(III). The macrocyclic ligand, TACNTA, which will be investigated later, was found to be ideally suited for this purpose. DTPA, although less flexible than EDTA, forms stronger complexes with the lanthanides than does EDTA due to its octadentate nature.

Results are seen in Figure C.23. It would appear that if all donor atoms are used for coordination, eight coordinate DTPA will prefer to bind to larger metal ions (best-fit r(M-N) = 2.23 Å , r(M-O) = 2.16 Å). Six coordinate EDTA prefers smaller metal ions (best-fit r(M-N) =2.02 Å, r(M-O) = 1.97 Å). As expected, angles subtended at the metal are smaller for DTPA (θ(N-M-N) = 81.5°, θ(N-M-O) = 77.8°) than for EDTA (θ(N-M-N) = 86.6°, θ(N-M-O) = 84.8°). Because of the higher coordinating ability of DTPA, it is expected to have a preference for larger metals which require higher coordination numbers. The very broad, flat curve for the EDTA scan reinforces its ability to accommodate the full range of metal ion sizes and may explain its diverse ligating behaviour, while the steeper DTPA curve indicates a preference for specific metals. This finding is not supported by experiment since DTPA is known to complex the full range of metal ions, and with both small and large metals, has larger binding constants than EDTA.

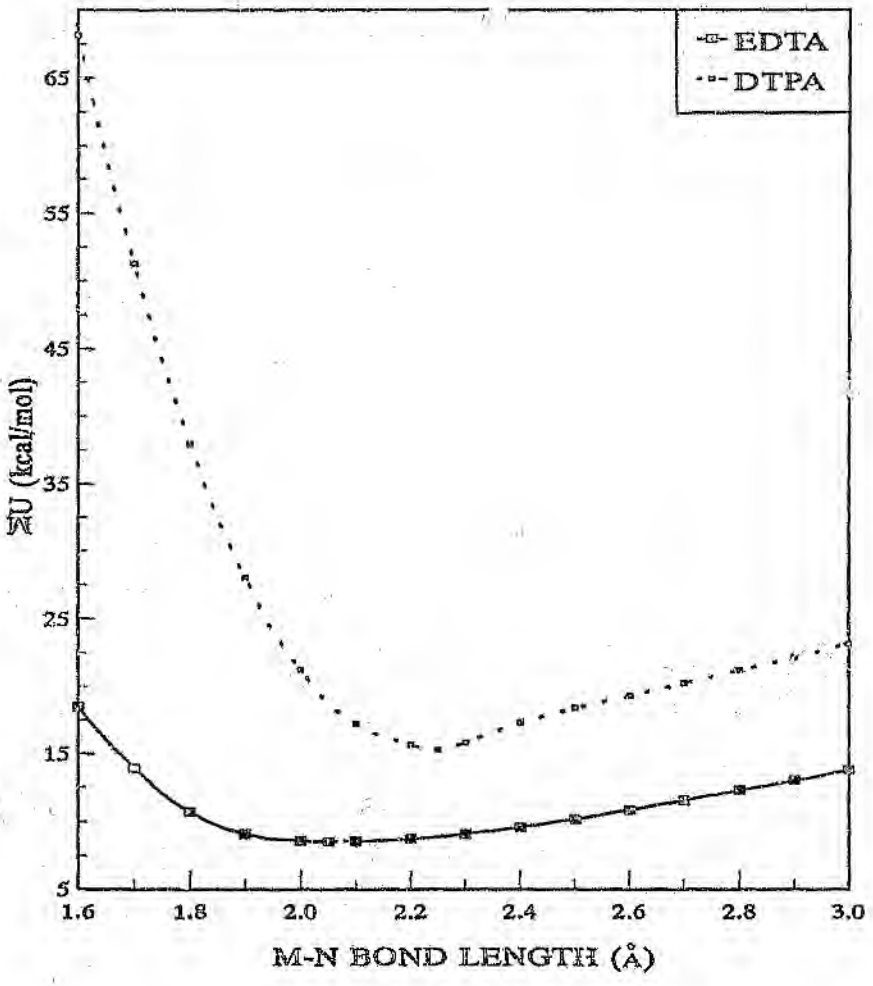

Figure C.23 : Total strain energy, ΣU, as a function of ideal M-L bond length for EDTA and DTPA.

C.3.1.2 NTA and analogues

Hancock and Martell (1989) noted that donor groups with negatively charged oxygen donors, eg. carboxylates, are sterically efficient because the oxygens carry no hydrogen atoms. Thus, ligands which are able to meet the requirements of a large number of carboxylate groups in a sterically efficient arrangement would be best for coordination to the lanthanides and Ca (with chemistry closely allied to that of the lanthanides). NTA is such a ligand. However, its log K, values with Ca(II) and La(III) are relatively low, 7.71 and 12.45 respectively (Martell & Smith). Since the phenolate or hydroxybenzyl pendent donor group may also be sterically efficient, hypothetical ligands NTHP and NTHB were also investigated for ideal metal size. Strain energy curves for NTA and its analogues are shown in Figure C.24. Coordination to all nitrogen and oxygen atoms was assumed.

Calculated best-fit r_0 values agree with the rule connecting chelate ring size to metal ion size. The ligands forming five-membered chelate rings, NTA and NTHP, opt for larger r(M-L) values (r(M-N) = 2.05 Å and 2.08 Å, and r(M-O) = 2.02 Å and 1.94 Å) and smaller N-M-O angles (81.7° and 85.6°). Those forming six-membered rings, NTP and NTHB, opt for smaller r values (r(M-N) = 1.58 Å and 1.67 Å, and r(M-O) = 1.50 Å and 1.61 Å) and N-M-O angles of 127.6° and 118.1°. Coordination geometries found for NTA and NTHP are capped trigonal planar, and for NTP and NTHB, distorted tetrahedral.

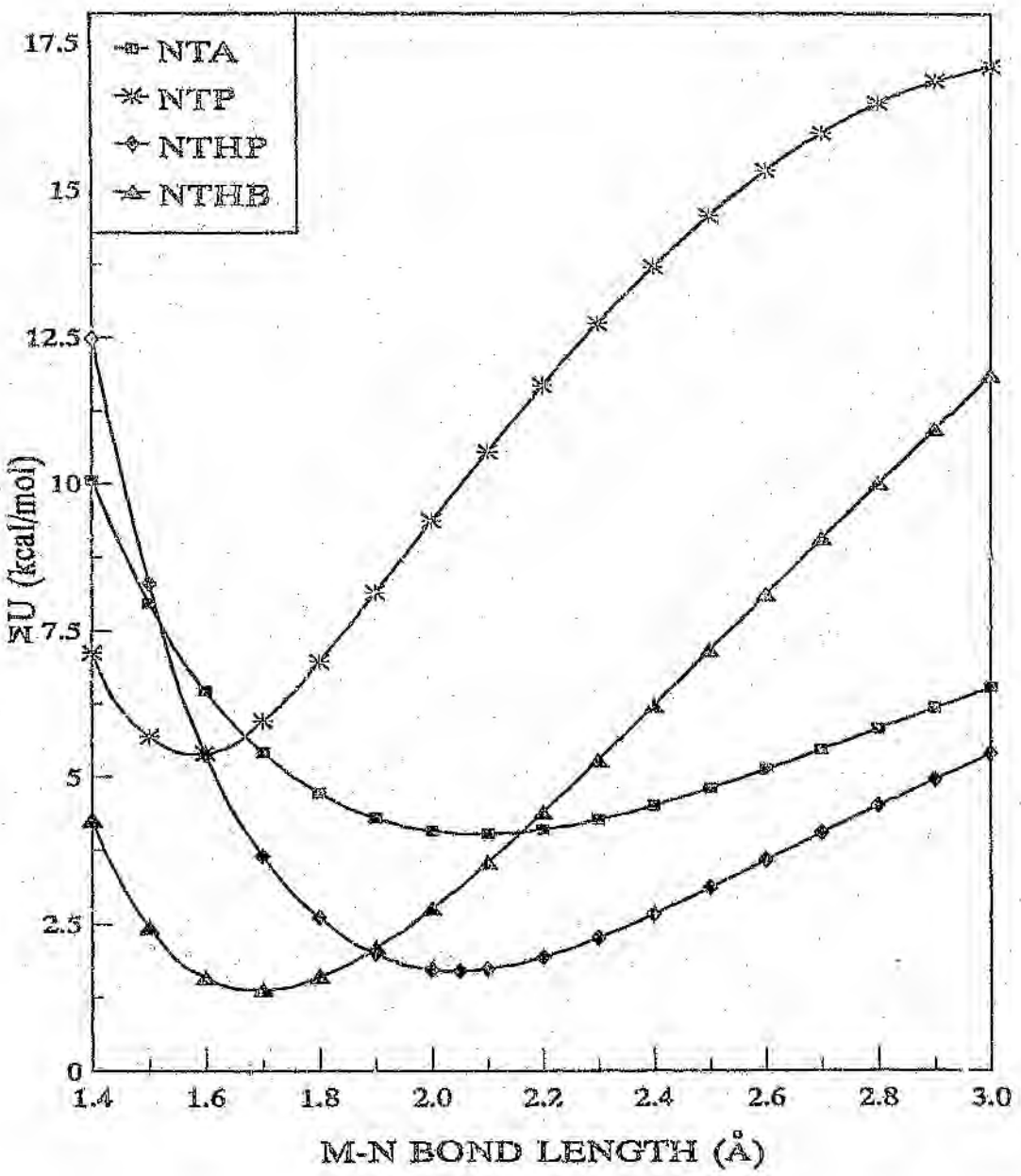

Figure C.24 : Total strain energy, ΣU, as a function of ideal M-L bond length for NTA, NTP, NTHP and NTHB.

The versatile, multidentate capabilities of NTA are evidenced by its diverse coordination complexes and are dependent on the coordination preferences of the particular metal ions. With Ca(II)[38,39], geometries chosen are pentagonal bipyramidal and monocapped trigonal antiprismatic. Zn(II)[39] coordinates octahedrally. Cu(II)[39] assumes both square pyramidal and pentagonal bipyramidal geometries. Results obtained here indicate that if binding structure is dictated entirely by the ligand, NTA would choose to coordinate with smaller Zn and Cu than with Ca. This may add to the reason for the large difference in stability between small Fe(III) (log K_1 = 17.88, Martell *et al.*, 1982) and large Ca(II), the main factor for this stability difference being an inductive effect. Fe(III) has a much higher affinity for negatively charged oxygen donors than Ca(II).

C.3.2 Triacetate triazamacrocycles

C.3.2.1 TACNTA

Two types of complex, I and II[40], exist for TACNTA depending on the orientation of the acetate arms. Type I exhibits a distorted-octahedral environment and type II a distorted-trigonal prismatic. The octahedron is diagrammed schematically below.

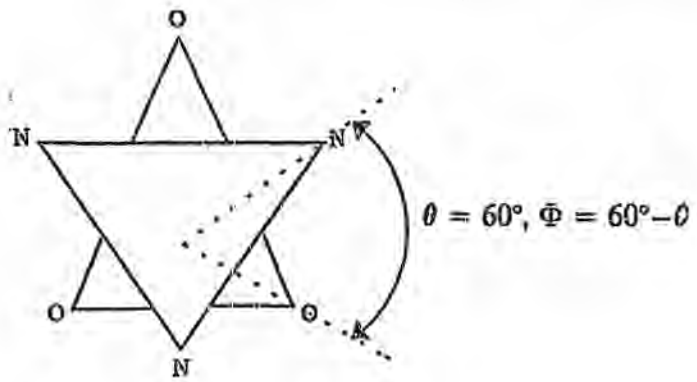

The degree of distortion from regular octahedral arrangement of the N_3O_3 donor set is expressed by a twist angle[41], Φ. Φ is zero for octahedral and 60° for trigonal-prismatic coordination. Since TACNTA is potentially hexadentate bearing three basic groups, its complexation with divalent and trivalent transition metals[40], as well as isotopes ^{111}In and ^{67,68}Ga (Broan *et al.*, 1991), has been studied. Crystal structure data are tabulated below.

Table C.18 : Crystallographic data on TACNTA complexes.

Metal Ion	Coordination Geometry	Ave. M-N/ °	Ave. M-O/ °	Φ/° (Type)	Reference
Ni(III)	pseudo-O_h	1.92	1.92	6.9 (I)	42
Ni(II) (s=1)	pseudo-O_h	2.04	2.08	12.0 (I)	41
Cr(III)	pseudo-O_h	2.06	1.96	11.0 (I)	40
Al(III)	pseudo-O_h	2.06	1.85	9.0 (I)	43, 44
Ga(III)	pseudo-O_h	2.10	1.93	12.4 (I)	Broan *et al.*, 1991, 45
Cu(II)	pseudo-prismatic	2.12	2.11	33.4 (II)	40
Fe(III) (s=1)	pseudo-prismatic	2.18	1.96	35.0 (II)	40

It would appear that the change from type I to type II results from increasing M-N bond distance. When the metal is too large for the cavity, it is forced up out of the N-donor plane causing tension on the M-O bonds which may be relieved by adopting type II configuration. Clarke and Martell (1991) determined stability constants of Fe(III), Ga(III) and In(III) with TACNTA to be 28.3, 30.98 and 26.2 respectively. This trend may be rationalised by the M-N lengths found in these complexes. In the pentagonal bipyramidal structure of [In.HCl.H_2O.TACNTA] (Broan *et al.*, 1991), average M-N distance is 2.31 Å.

Previous MM calculations[92] found 2.0 Å to be the best-fit size for metal ions in both type I and type II TACNTA structures, and type I to be more stable than type II. Results in close agreement were obtained here when octahedral angle constraints were applied (Figure C.25(a)). N-M-N, N-M-O and O-M-O bending angles were set to either 90° or 180° and the K_b(L-M-L) constant given a value of 0.014 kcal.mol^{-1}.deg^{-1}. Type I's lower energy is due to a much lower fixed angle energy needed, as compared to type II, to constrain its angles. When constraints are removed, i.e. all L-M-L constants zeroed, type II becomes more stable than type I at r_0(M-N) values below 2.55 Å (see Figure C.25(b)). Measured twist angles are 8.8° (type I) and 26.9° (type II). This paradox in stability to literature findings occurs when coordination geometry is dictated entirely by the ligand and indicates the controlling influence that the complexed metal may exert on geometry.

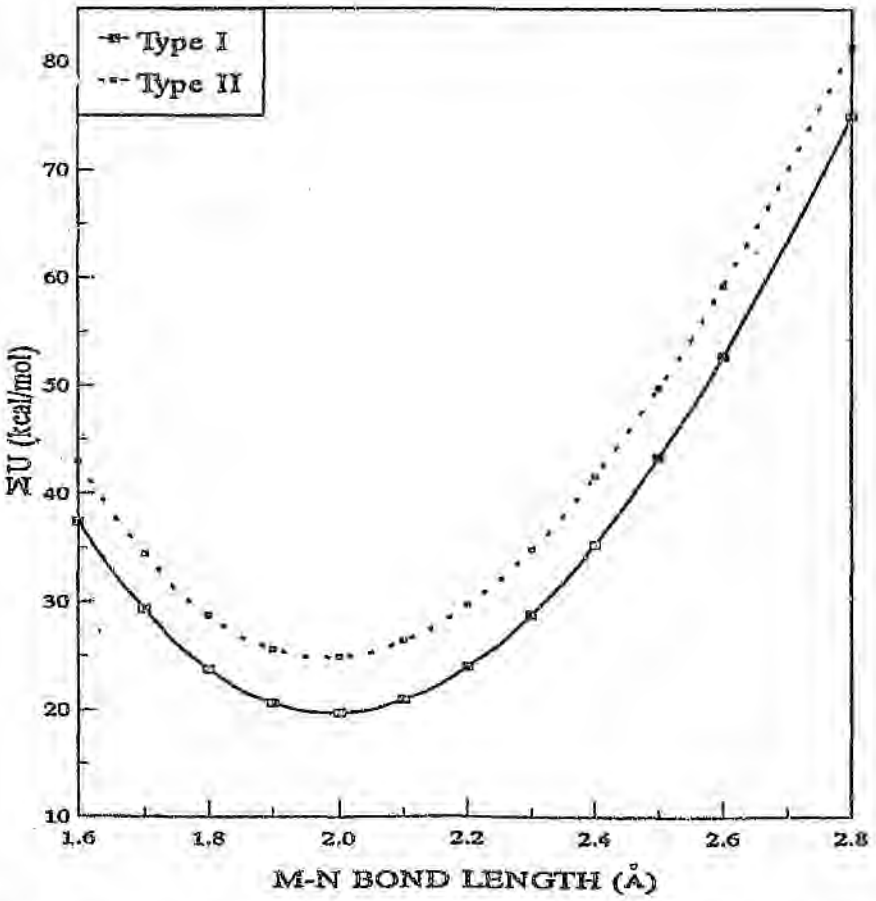

Figure C.25(a) : Total strain energy, ΣU, as a function of ideal M-L bond length for type I and type II configurations of TACNTA using angle constraints.

Minimization of type I and type II complexes of ligands Q and V, which were built from TACNTA, yielded almost identical results for the two configurations. For the Q structures, Φ averages 26.8° and for the V structures, Φ averages 14.1°. Auerbach and Eckert (1990) have solved the crystal structure of V with Cu(II), and found square pyramidal geometry. One phenolate arm was not bound to the metal and was protonated.

C.3.2.2 TACDTA

The search for appropriate hexadentate ligands to bind isotopes for purposes of magnetic resonance imaging led to the synthesis and potentiometric study of TACDTA (Cortes *et al.*, 1990). For the present MM calculations, the existence of the same two types of complex as that found for TACNTA was assumed for TACDTA. Univariate scanning curves are shown in Figure C.25(b). As with TACNTA, type II is stabilised relative to type I, but now the cross-over point is at an r_0 value of 2.2 Å. Measured twist angles are 12.9°(I) and 52.2°(II).

On inspection of ideal metal sizes for the ligands under discussion, it appears that change in chelate ring size does not have the same effect as with the unsubstituted triazamacrocycles. For example, Zn(II) and Cd(II) would be expected to complex better with ligands favouring tetrahedral L-M-L angles, like TACDTA, but Cortes *et al.* (1990) have shown that their binding strengths with TACDTA equal that with TACNTA. They postulated that other factors such as macrocyclic hole size and metal ion-donor atom covalency come into play when considering complexation with different metals.

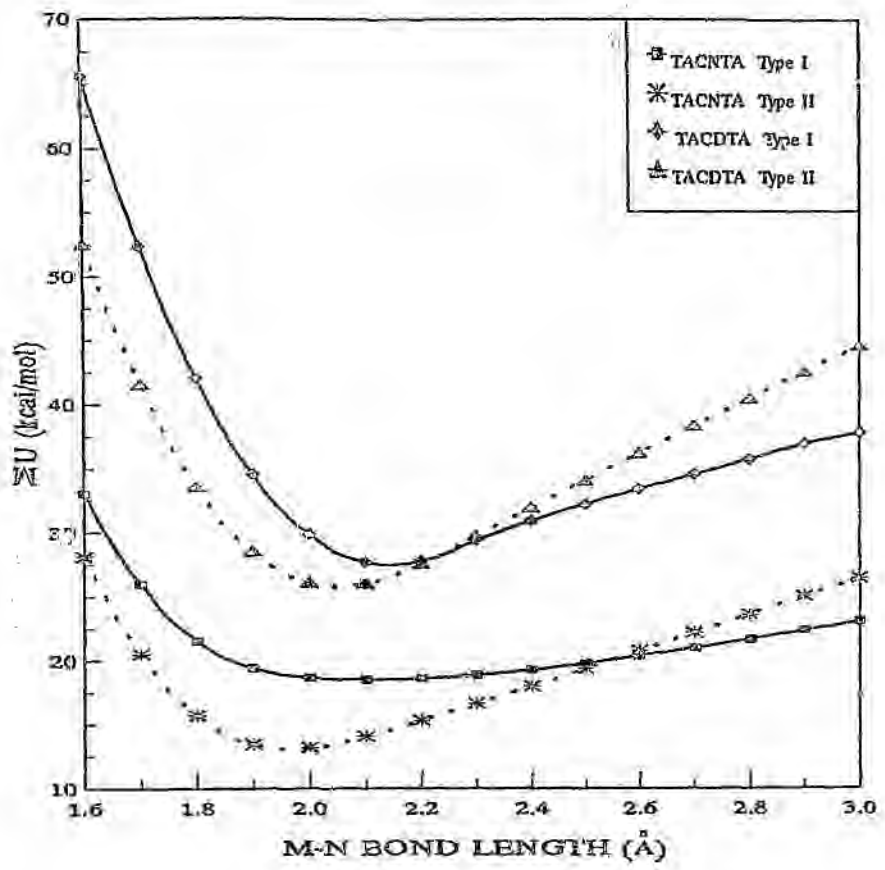

Figure C.25(b) : Total strain energy, ΣU, as a function of ideal M-L bond length for unconstrained TACNTA and TACDTA.

C.3.3 Comparison of conformers for each N-functionalized azamacrocycle

TACNTA and TACDTA are ideal ligands for binding to hexacoordinate Ga(III) and In(III). The tetraazamacrocycles DOTA, TRITA and TETA were concluded by Clarke and Martell (1991a) to be too large to form very stable complexes with such small trivalent metals. These larger ligands may thus be more suitable for octadentate binding to Ca(II) and the Ln(III)'s. Differences in metal size preference for the two series are noted by the log K_1 values for their complexation with Ca(II) and Mg(II). DOTA actually forms the most stable complexes known to date with Ca and the lanthanides.

Table C.19 : Formation constants of the Ca(II) and Mg(II) complexes of a variety of ligands.

Ligand	log K_1[a] (Mg^{2+})	log K_1[b] (Ca^{2+})
TACNTA	8.93	8.81
TACDTA	7.1	6.0
DOTA	11.15	16.37
TRITA	8.18	11.99
TETA	3.01	8.53

[a] 41, Clarke and Martell (1991c)

[b] Cortes *et al.* (1990)

All structures in this section, besides DOTA and TETA, had to be constructed with the SKETCH option of SYBYL because of their unavailability in the literature. Calculations performed here thus focus on prediction rather than interpretation of data. Octadentate coordination was assumed.

C.3.3.1 DOTA and analogues

Four conformers with different nitrogen to pendent donor group orientations may exist for complexes of DOTA, S and X. Scanning of all conformers yielded lowest strain energy values presented in Table C.20. Two observations common to these ligands were noted: (i) Configuration I (++++) is so much more stable than the remaining forms that it is unlikely that any metal complex will assume any other form. Its calculated geometry is distorted square antiprismatic and conformation of the macrocycle ring, [3333]. Dale (1973) found this formation to be the most stable for cyclododecane. (ii) Conformer stability decreases in the order I > II > V > III. Higher strain energies are due primarily to larger angle bending and bond stretching energy values. Disparity in M-L bond lengths may also contribute to steric strain. The lowest energy conformer for each macrocycle can be seen in Figure C.26.

Table C.20 : Minimized strain energies (kcal.mol^{-1}) for conformers of N-functionalized tetraazamacrocycles.

Ligand	Conformer				
	I (++++)	II (+++-)	III (++--)	IV (+--+)	V (+-+-)
DOTA	19.51[a]	55.98	70.75	-	61.36
	(2.38)[e]	(2.22)	(2.19)		(2.19)
S	4.64[a]	40.32	58.22	-	50.89
	(2.24)	(2.23)	(2.23)		(2.29)
X	27.85[a]	76.30	101.54	-	87.09
	(2.50)	(2.39)	(2.29)		(2.27)
TETA	32.05[b]	39.86	41.42	61.88	45.19
	(2.37)	(2.36)	(2.34)	(2.36)	(2.33)
T	14.15[b]	16.11	23.10	34.39	18.83
	(2.38)	(2.38)	(2.39)	(2.38)	.36)
Y	40.60[b]	58.25	61.83	80.07	60.98
	(2.68)	(2.58)	(2.49)	(2.54)	(2.49)
HETA	43.04[c]	50.81	57.00	-	47.93
	(2.50)	(2.57)	(2.53)		(2.54)
U	19.95	25.83	29.03	-	14.93[d]
	(2.50)	(2.51)	(2.50)		(2.49)
Z	48.07[c]	50.02	74.44	-	64.06
	(3.32)	(2.98)	(2.68)		(2.73)

[a] [3333] ring conformation

[b] [77] ring conformation

[c] [1717] ring conformation

[d] [4444] ring conformation

[e] best-fit r(M-N)/ Å

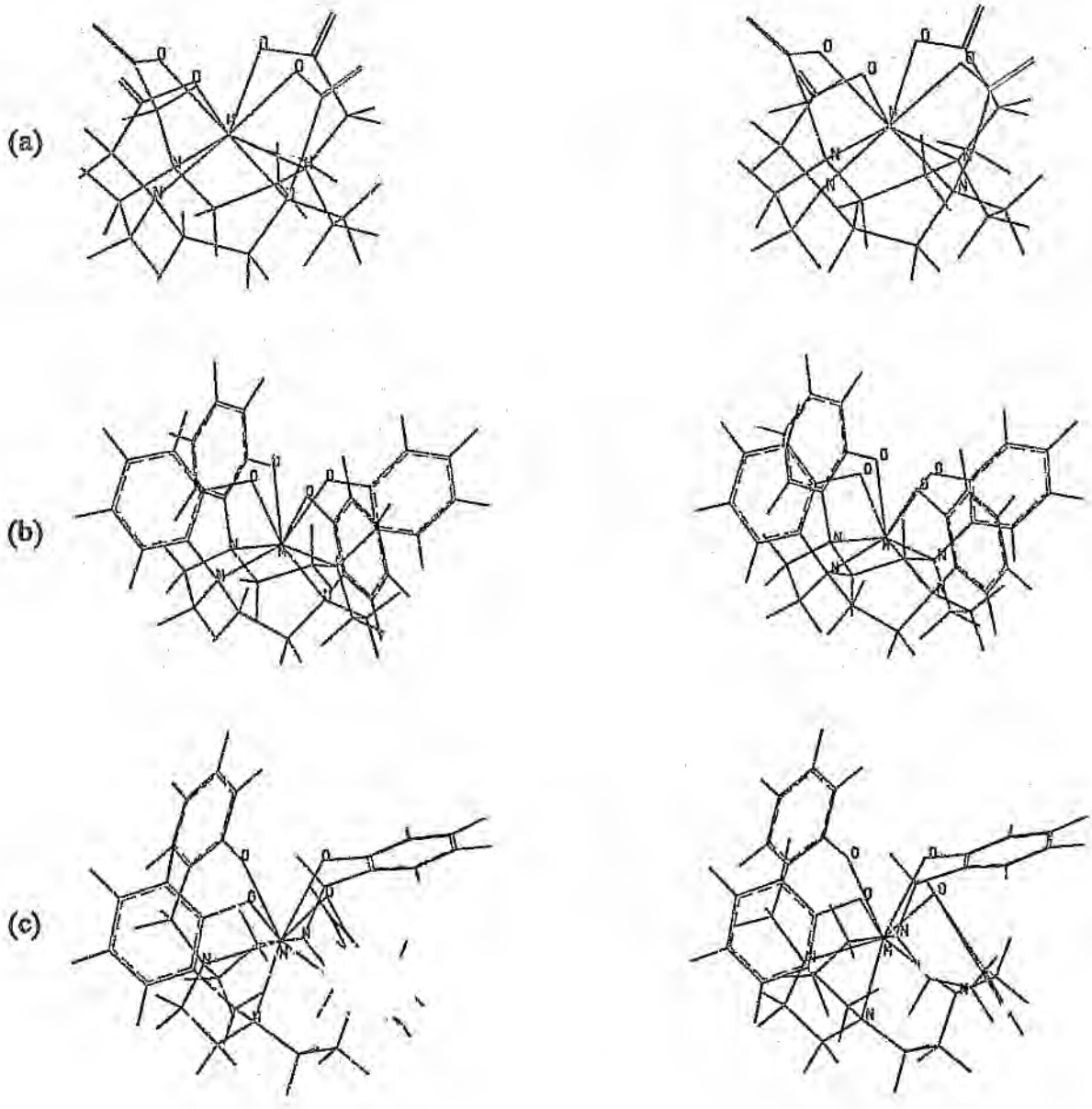

Figure C.26 : Stereoviews of lowest energy conformers of (a) DOTA, (b) S, and (c) K.

No eight-coordinate DOTA complexes appear in the literature. A comparison of the nine-coordinate trans-I structure $[EuDOTA.H_2O]^-$ with the MM calculated trans-I, of which both have the [3333] macrocyclic ring form, indicates that an extra coordinating ligand results in longer M-L bond lengths and smaller L-M-L angles. The geometry adopted by Eu(III) is distorted capped square antiprism. DOTA coordinates octahedrally with the transition metals, Cu(II)[47], Zn(II)[48] and high-spin Ni(II)[47], forming crystals of MH_2DOTA. The metals are in a distorted cis-octahedral geometry bound by four N-atoms and two carboxylates. Conformer I is assumed [illegible] the metal ions lying out of the donor plane and the complexed acetate groups [illegible] positions. A binuclear Cu_2DOTA[49] structure has also been established. A heptacoordinate In(III)[50] structure with 12-aneN_4 and only three pendent acetates has been characterized where trans-I configuration and capped trigonal prismatic geometry were adopted. The MM-derived prediction that conformer I will predominate for DOTA complexes thus seems to be correct.

Aime *et al.* (1992) and Hoeft *et al.* (1993) studied structures and dynamics of Ln(III) DOTA complexes in solution and discovered the presence of two isomeric forms, major and minor, which differ in the layout of the acetate arms (see diagram below). This situation is similar to that with TACNTA. Relative torsion angles indicate that the calculated trans-I form described here is the antiprismatic major isomer.

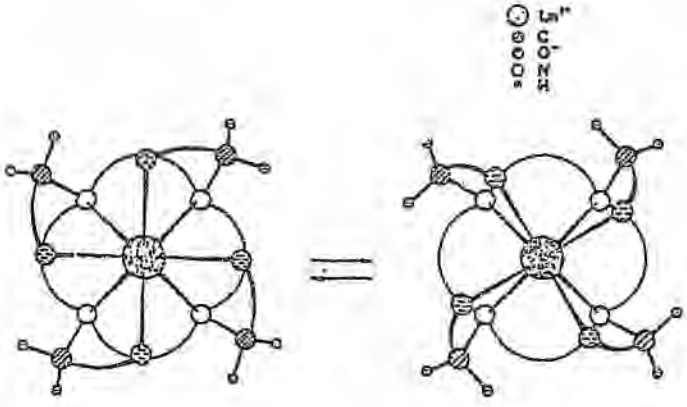

Figure C.27: The two isomers of DOTA differing in the orientation of the acetate arms. Redrawn from Aime et al. (1992).

C.3.3.2 TETA and analogues

Five conformers may exist for complexes of TETA, T and Y. As with DOTA and its analogues, conformer I for each ligand experiences the least amount of steric strain (Table C.20). Distorted dodecahedron geometry and [77] macrocycle conformation prevail. Energy differences between conformers, especially for T, are not as marked as those for DOTA, etc. This was also observed with 12-aneN$_4$ and 14-aneN$_4$, , where trans-I for 12-aneN$_4$ clearly predominated, while 14-aneN$_4$ experienced much overlapping of conformers. The instability of conformer IV for all three ligands, despite its low energy [3344] form (Dale, 1973), is again due to high angle bending strain. Lowest energy conformers are diagrammed in Figure C.28.

The crystal structure[51] of [TbTETA]$^-$, where Tb(III) is eight-coordinate, reveals properties correctly predicted by this MM work. Its geometry is distorted dodecahedron, the four carboxylic pendent arms lie on the same side of the ring, and [77] conformation is maintained. Average M-N distances and L-M-L angles are smaller than those obtained for the minimum energy structure from the trans-I curve. As with DOTA, crystallographic data is available for both mononuclear[52] and binuclear[49] Cu(II)-TETA complexes. With CuH$_2$TETA[52], Cu is again six-coordinate but this time is contained in the macrocyclic cavity. Two pendent acetato groups coordinate in trans positions. In the binuclear complex[49], Cu lies outside the cavity in a square pyramidal fashion. Unlike ZnH$_2$DOTA, where Zn is in a cis-octahedral arrangement, trans-octahedral geometry is adopted in ZnH$_2$TETA[48]. The configuration assumed by TETA in these complexes where the metal is planar is trans-III, and occurs because of the better fit between cavity and metal ion size. In a heptacoordinate structure with In(III)[50], trans-I is again found.

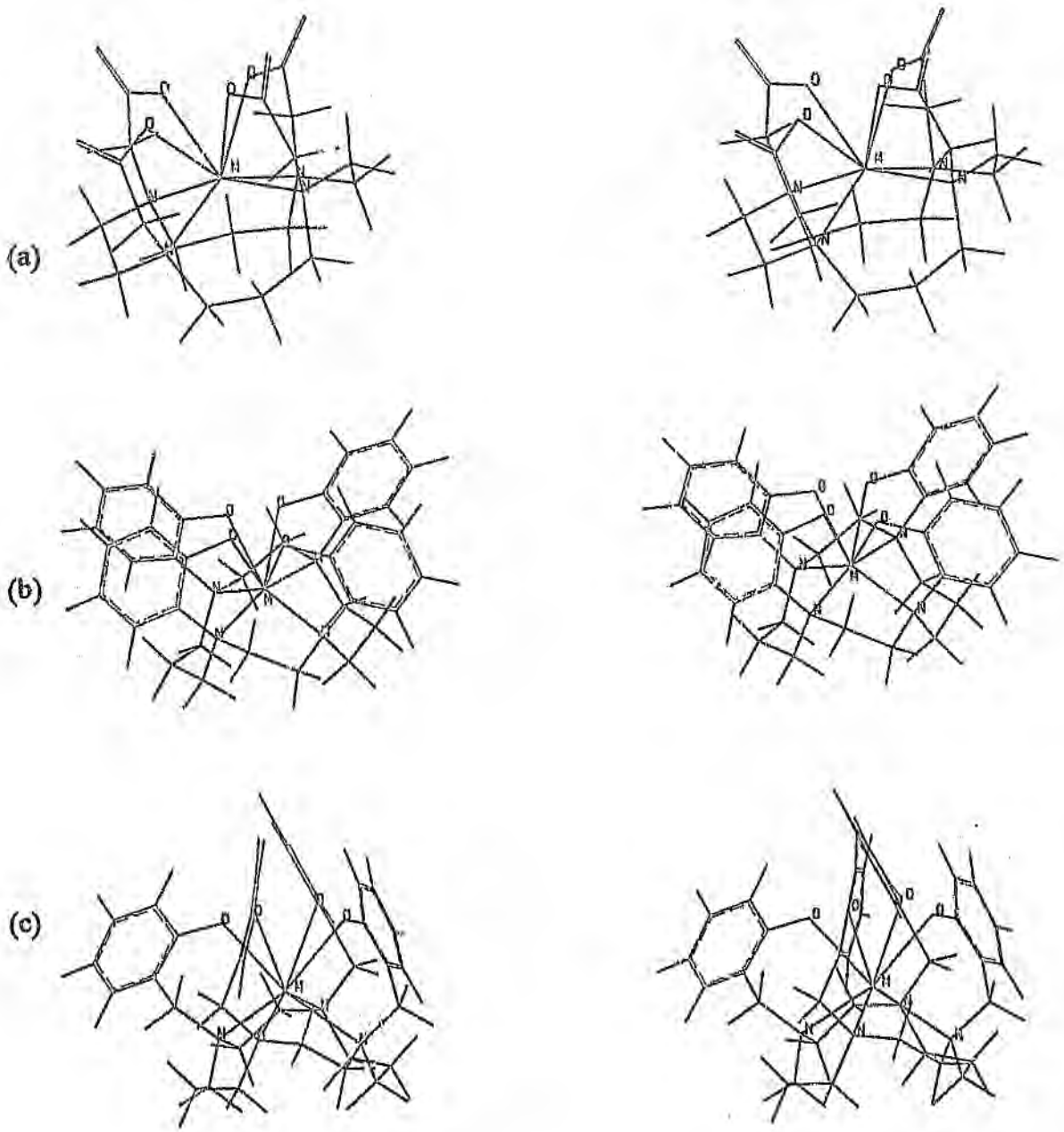

Figure C.28 : Stereoviews of lowest energy conformers of (a) TETA, (b) T, and (c) Y.

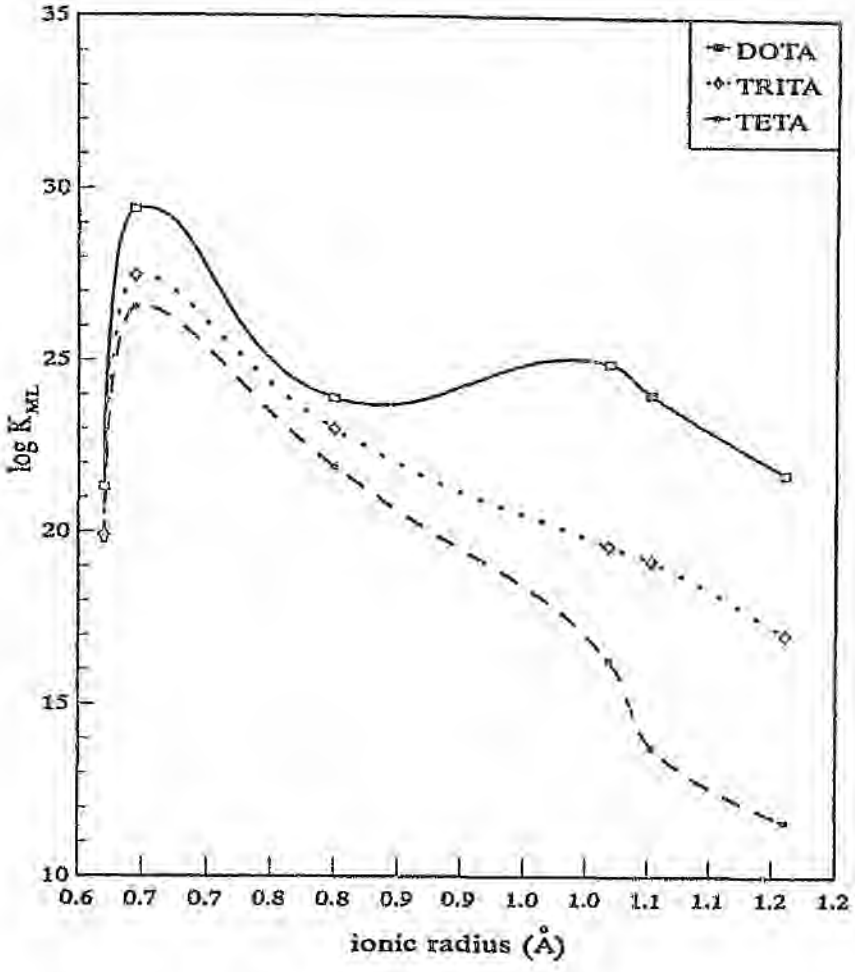

Figure C.29 : Variation of log stability constants with various metal ions for the macrocyclic series DOTA, TRITA and TETA.
Log K_{ML} values from Clarke and Martell (1991d) and Cox et al. (1989).
Effective octahedral (Ga, Fe, In) and 8-coordinate (Y, Gd, La) ionic radii from Shannon (1976).

Figure C.29 shows the variation of log K with the various metal ions of interest in this section for DOTA, TRITA and TETA. Stability constants vary with ligand in the order DOTA > TRITA > TETA and generally decrease with increasing metal ion size. The high stabilities of the Fe(III) complexes are partly due to the small Fe(III)'s fit into the N-macrocyclic cavities when it is octahedrally coordinated. Again the inductive effect is the main reason for these high stabilities. Small, highly charged

Fe(III) has a high affinity for negative oxygen donor groups. When octa- or nona-coordination occurs, as with Y, Gd and La, the larger sizes of the metals make N-planar complexation impossible. Elevation of the metals likely leads to destabilisation relative to in-plane octahedral geometry (Clarke & Martell, 1991d). The stability of DOTA complexes is partially assigned to the low repulsion energy of its square antiprismatic conformation. TETA lanthanide chelates conform to dodecahedral geometry which exhibits a higher repulsion energy (Loncin *et al.*, 1986).

C.3.3.3 HETA and analogues

Minimized strain energies obtained whilst scanning HETA, U and Z are shown in Table C.20. Again, energy differences between the four conformers of each ligand are not extreme. Most stable energy forms are I ([1717]) for HETA and Z, and V ([4444]) for U. The latter configuration was also calculated to be the most stable for 16-aneN_4, as was the trans-III form calculated to be the least stable.

In general, conformers which have two pendent donor groups both above and below the macrocyclic plane defined by the N-donors are unstable. This is likely the result of steric repulsion experienced by the groups when the metal is forced to remain in the cavity. Compression of the metal in such conformers results in longer than expected ideal r(M-O) values. These effects decrease with an increase in macrocycle size. In the HETA, U and Z configurations, no compression of r(M-L) and lengthening of r(M-O) bonds occur. Basal nitrogens are at distances far enough apart so as not to cause steric strain between their attached groups. Rigidity of these N-substituted structures makes no allowance for preferred metal geometries. However, positioning of all pendent groups on one side of the N-plane does allow for metal movement up out of the plane leading to relief of strain for both M-N and M-O bonds. Thus the stability of trans-I conformers with larger r(M-L) lengths, specifically for the small 12-aneN_4 series.

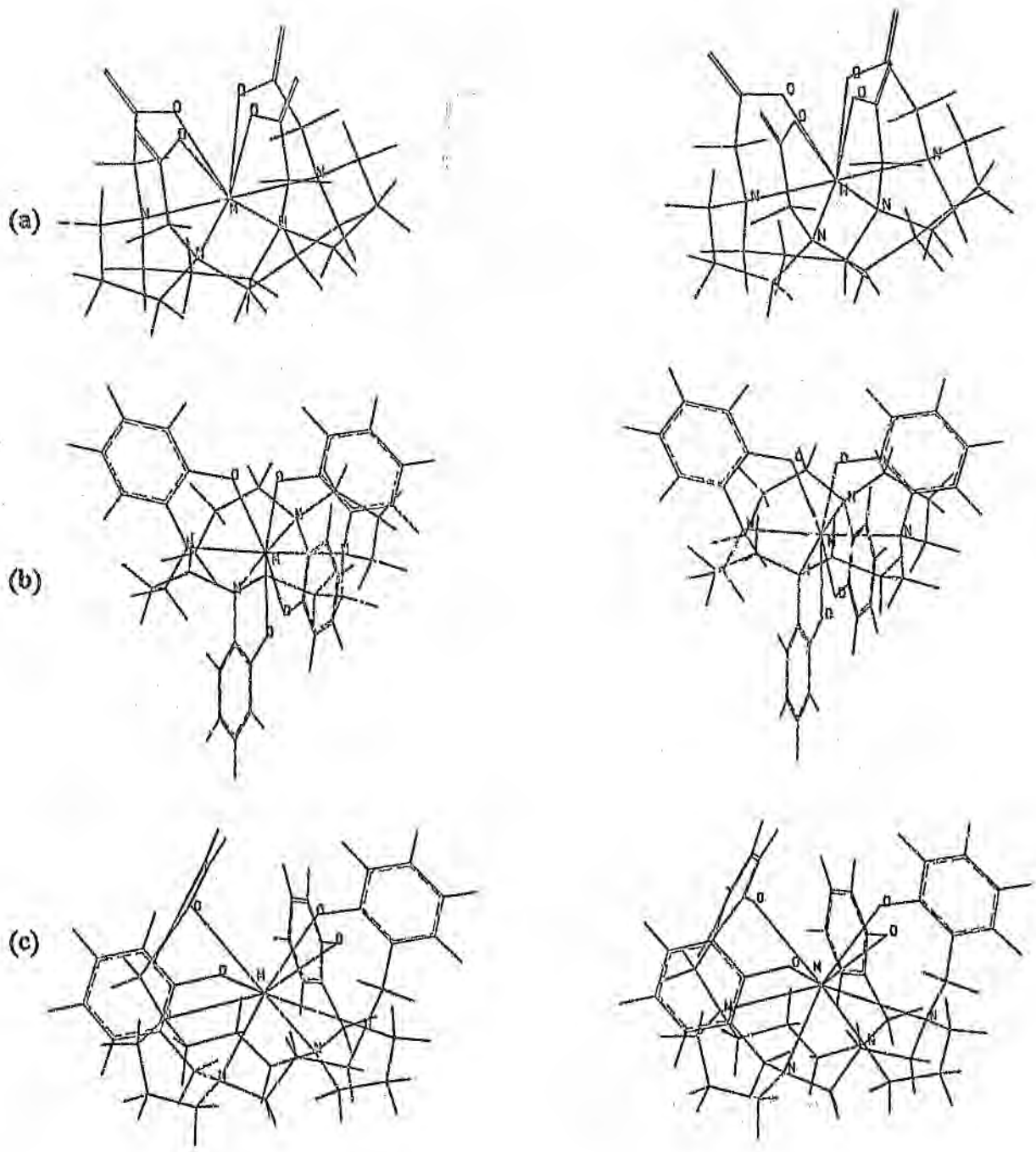

Figure C.30 : Stereoviews of lowest energy conformers of (a) HETA, (b) U, and (c) Z.

C.3.4 Effect of pendent donor group - acetate, hydroxyphenyl, hydroxybenzyl

Examination of Tables C.21 and C.22 where lowest energy conformers for each ligand are compared reveals the expected increase in ideal M-N bond length when moving from unsubstituted to substituted chelates. In other words, an increase in potential coordinating ability from three- to six-coordinate or from four- to eight-coordinate should result in an increase in the metal ion size favoured since larger metals are able to accommodate more donor atoms.

As was established by MM in section C.2 of this dissertation, as macrocycle size increases, ie. from 9-aneN_3 to 12-aneN_3, and from 12-aneN_4 to 16-aneN_4, best-fit metal size decreases. The principal reason for this trend is the increase in the size of the chelate rings formed from five-membered to six-membered. MM, however, shows the opposite trend with macrocycles bearing hard oxygen donor groups. It appears that "ligand size-match" selectivity is followed. Thus, the chelate ring size effect falls away with larger coordination numbers. This is logical since an increase in coordination will inevitably lead to a decrease in L-M-L angle size and an increase in preferred M-L distance. This phenomenon is pronounced with HETA and its analogues. An extremely low value of 62.2° is obtained for N-M-O angles in six-membered chelate rings. Note that complete hexadentate coordination with the triaza series and octadentate coordination with the tetraaza series were used in the calculations.

For each base ligand, best-fit r(M-N) and r(M-O) values generally decrease from pendent donor group hydroxybenzyl to acetate to hydroxyphenyl. This can probably be attributed to added flexibility permitted by the linking -CH_2- group in the former two pendent arms. Other pendent donor groups such as phosphinic acid have been tried (Parker *et al.*, 1992). Complexes with phosphinic acid donors were expected to be more kinetically stable than those with carboxylic acid donors.

Results emphasize the rigidity placed on macrocycles when functionalized with donor ligands. Folding of macrocycles is prevented by the arrangements assumed by

coordinated donor atoms.

Table C.21 : Comparison of ideal r(M-L) and θ(L-M-L) values for unsubstituted and substituted triazamacrocycles. Lowest energy conformer results.

Ligand	Type	Ave. r(M-N)/ Å	Ave. r(M-O)/ Å	Ave. N-M-N/ °	Ave. N-M-O/ °
9-aneN_3	-	1.80	-	96.1	-
TACNTA	I	2.09	2.01	85.2	83.2
	II	1.94	1.87	90.3	88.1
Q	I = II	1.95	1.84	91.8	92.4
V	I = II	2.00	1.91	89.2	103.3
12-aneN_3	-	1.65	-	109.7	-
TACDTA	I	2.13	2.07	109.1	81.8
	II	2.03	1.97	104.3	84.0
R	I	2.01	1.91	106.3	88.1
W	I	2.26	2.21	104.2	94.2

Table C.22 : Comparison of ideal r(M-L) and θ(L-M-L) values for unsubstituted and substituted tetraazamacrocycles. Lowest energy conformer results.

Ligand	Conformer	Ave. r(M-N)/ Å	Ave. r(M-O)/ Å	Ave. N-M-N/ °	Ave. N-M-O/ °
12-aneN$_4$	I	2.15	-	82.5	-
DOTA	I	2.38	2.31	78.1	72.9
S	I	2.24	2.14	82.2	79.4
X	I	2.50	2.41	76.2	84.3
14-aneN$_4$	III	2.11	-	84.5[a]	-
				95.5[b]	
TETA	I	2.37	2.32	79.7	72.9
				93.2	
T	I	2.38	2.29	78.0	72.6
				96.6	
Y	I	2.68	2.62	70.6	79.8
				89.0	
16-aneN$_4$	V	1.85	-	102.8	-
HETA	I	2.50	2.42	90.0	70.3
U	V	2.49	2.41	90.1	70.9
Z	I	3.32	3.18	80.1	62.2

[a] N-M-N angle in five-membered chelate rings

[b] N-M-N angle in six-membered chelate rings

C.4 STRUCTURAL FACTORS AFFECTING SELECTIVITY IN MONENSIN AND RELATED POLYETHER ANTIBIOTICS

C.4.1 Previous molecular mechanics calculations

In their endeavour to correlate structural features with the selectivity of monensin for Na^+ over K^+, Pangborn *et al.* (1987a) performed MM calculations on rings D and E (see Figure A.5), isolated from each monensin complex. They constrained torsion angles and obtained qualitative results indicating a distortion of the molecule from its low-energy conformation when coordinated to the larger K^+ ion. To obtain more realistic conclusions, MM calculations in this dissertation encompassed the entire molecule and avoided the fixing of torsion angles.

C.5.2 Optimization of TRIPOS force field

C.5.2.1 Covalent assumption

For monensin complexed with K , initial calculations (SYBYL Version 5.5) using the ionic bonding approach led to unsatisfactory structure reproduction. Collapse of the minimised structure occurred and appeared to result from the strong attraction of the single positive charge on the alkali-metal for the single negative charge at the carboxylate end of the molecule. This prompted the use of a covalent bonding model where bonds are explicitly described. The M-O bond was given a low force constant value of 28.8 kcal/mol.Å^2 and the O-M-O angle, a zero force constant. O--O nonbonded interactions were also not taken into account. Angles M-O-C and M-O-H were both given ideal values of 109.5° and K_θ values of 0.0044 kcal/mol.deg^2. The twist constant for the H-O-C-C torsion was decreased from 1.2 to 0.2 kcal/mol.deg^2. Torsion constants involving the M-O bonds were set to zero. The K-O bonds were made more covalent by reducing the electrostatic charge on the metal to 0.6 and assigning each of the six nearest oxygens a formal charge of 0.067. The two

carboxylate oxygens were given a charge of -0.5.

Root mean square deviation (RMSD) results comparing initial structures to final minimised structures are shown in Table C.23. The poor performance of the ionic model can be noted. Although better reproduction was obtained in case (c) than in (b), formal charges in the former case are unrealistic and bring into question the validity of the computed electrostatic charges. Identical calculations on Na monensin indicated that, under these conditions, the TRIPOS force field was better equipped to accommodate the Na structure. r(M-O) values employed were 2.72 Å and 2.43 Å respectively for K-O and Na-O. Total minimized strain energies obtained for cases (b) and (d) were 40.269 kcal.mol^{-1} and 46.034 kcal.mol^{-1}. The difference in energy was attributed entirely to electrostatics.

Table C.23 : Complexed monensin minimization results as a function of M formal charge.

	Formal charge		RMSD			
	M	coordinated O	M-O bonds	O-M-O angles	M-O-C angles	M-O torsions
K^+ complex						
(a)	+1	0	0.033	22.097	13.292	28.032
(b)	+0.6	0.067	0.128	9.216	4.766	14.738
(c)	+0.4	0.1	0.086	5.695	3.985	11.046
Na^+ complex						
(d)	+0.6	0.067	0.078	4.164	3.209	7.382

Another approach adopted was that of the covalent assumption without electrostatic effects, ie. atomic charges were ignored. In recent MM work on potassium crown ethers, Hay *et al.* (1993) have suggested the use of a value of trigonal planar 123.5° for the M-O-C angle instead of tetrahedral 109.5°. This value was substituted into the changed TRIPOS force field mentioned above. All other parameters, except electrostatic charges which were removed, were left unchanged. To evaluate the effect of steric hindrance on complex stability, complexed monensin and nigericin were scanned and their strain energies calculated as a function of varying metal ion size. Their Na crystal structure coordinates (Duax *et al.*, 1980 and reference 65) served as base coordinates. The formation of hydrogen bonds in these polyethers is essential since they link the carboxylate ends of the molecules to their A rings (see Figure C.31), thus producing the cavity in which the cation fits for coordination. To prevent disruption of these bonds and subsequent structure collapse, the bonds were constrained at their literature values during minimizations.

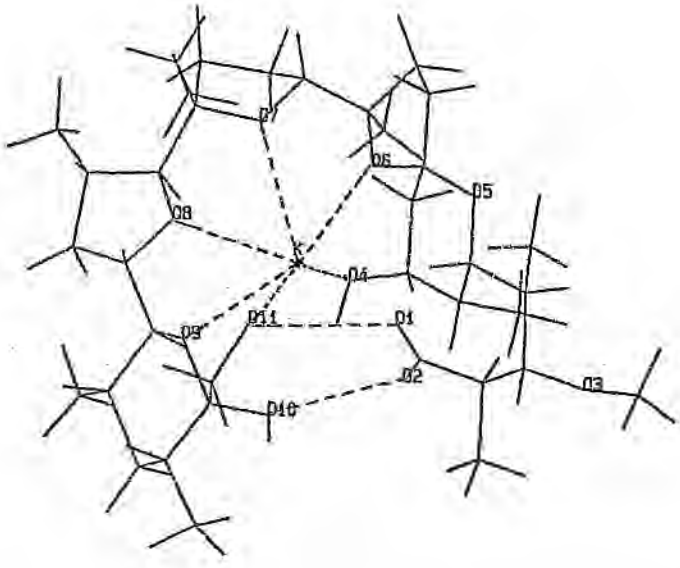

Figure C.31 : The K monensin crystal structure showing intramolecular hydrogen bonding and cation coordination. Reference: Pangborn et al. (1987a)

The resultant monensin curve in Figure C.32 corroborates its selectivity preference for Na over K. It displays a steeper increase in strain energy after an r_0 value of 2.4 Å than does the curve for nigericin. Complexed monensin will thus be destabilised with larger metal ions. Although nigericin is known to be more specific for K than for Na, results here predict that at higher M-O values, it will be non-specific. Structure reproduction (Figure C.33) improved when compared to the minimised structures obtained above.

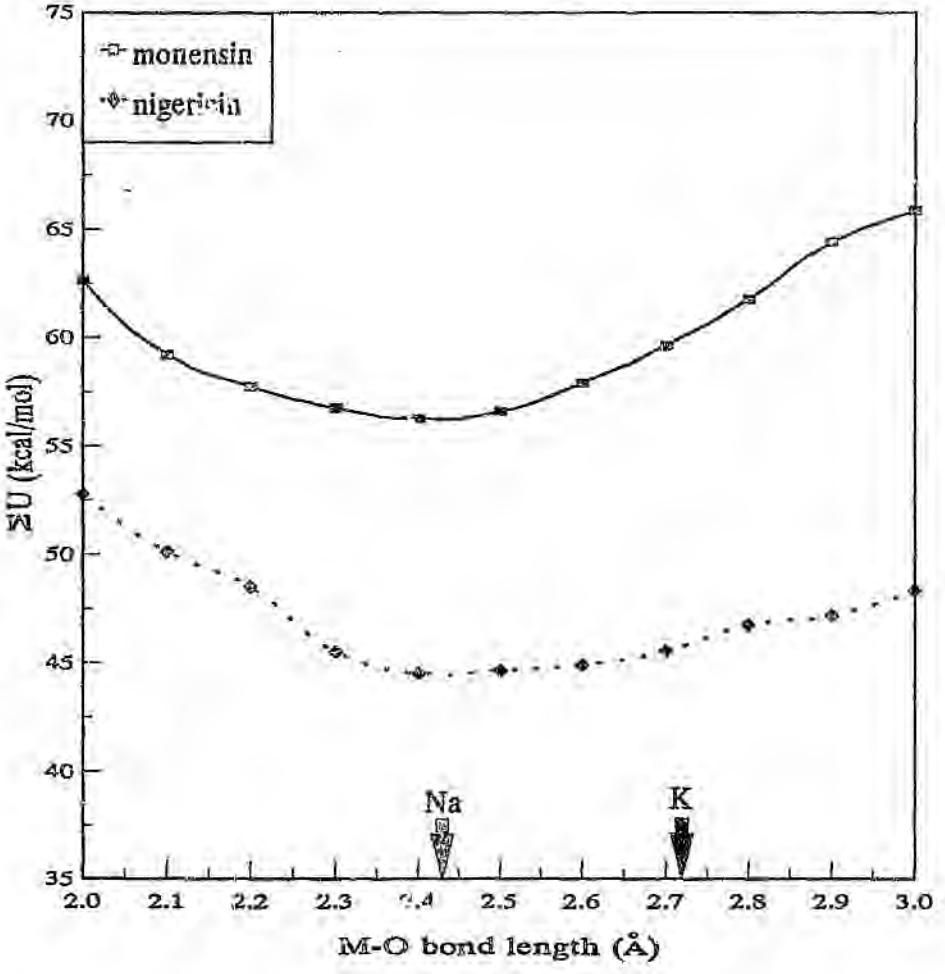

Figure C.32 : Total strain energy, ΣU, as a function of ideal M-O bond length for the polyether antibiotics, monensin and nigericin. Covalent bonding was assumed, electrostatics was ignored and hydrogen bonding was constrained.

(a)

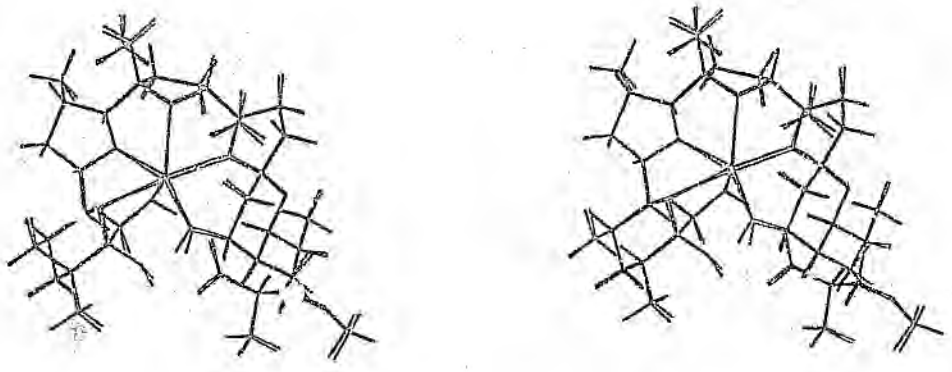

(b)

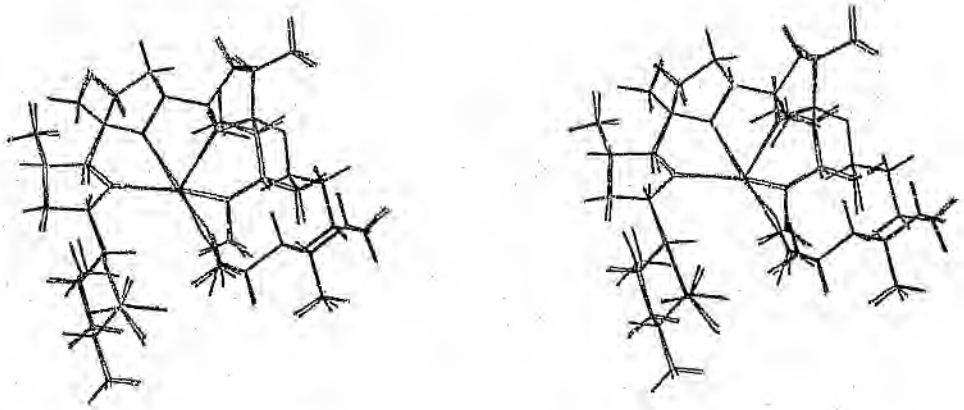

Figure C.33 : Stereoviews of initial and final energy minimized structures of (a) M^+-monensin and (b) M^+-nigericin. Ideal M-O value = 2.43 Å. RMSD of internal coordinates of all atoms: (a) 0.143 and (b) 0.173.

C.4.2.2 Ionic assumption

The initial calculations discussed in the previous section were performed using SYBYL Version 5.5. Although satisfactory structure reproduction was reached with the covalent bonding approach, it was decided to adopt the more realistic ionic model in future investigations where an improved SYBYL Version 6.0 would be employed.

Electrostatic parameters

Since electrostatic interactions are important in biological systems, these parameters were investigated closely. The SYBYL modeling package makes available two methods and variations thereof for the computation of partial atomic charges: Del Re's (1[illegible] method and Gasteiger's (1980) method of partial equalization of orbital [illegible]ty. MM calculations on uncomplexed and complexed monensin u[illegible] resulted in similar minimized structures, and Gasteiger's charge calculation [illegible] chosen for further minimizations. In this ionic model approach, formal charges of +1, 0, and -0.5 were respectively assigned to the alkali-metal, coordinated oxygens and carboxylate oxygens.

Seibel and Kollman (1990) suggested that for charged or highly polar molecules, models where charge is independent of conformation and polarization is unaccounted for, are highly inadequate. This may explain the problems encountered in this work with the allocation of partial charges. Also, the ionic approach is inherently a bad model, with coulombic interactions between charges centred at nuclear positions yielding a very poor approximation of reality

Originally the dielectric constant, D was set to unity. To weaken long-range coulombic effects and so take into account the critical role played by solvents in antibiotic activity, the dielectric was varied. The cut-off distance for electrostatic interactions was kept at the default value of 8.00 Å. Values in Table C.2 show the sensitivity of strain energy to a change in dielectric constant. RMSD values of internal coordinates for all atoms in the molecule were obtained using the MATCH option in

SYBYL. *D* had a marked effect on Na monensin reproduction. When set to a constant value, the displacement of Na from its original position increased by about tenfold. The collapse of structures during refinement due to the strong electrostatic attraction between metal ions and carboxylate oxygens appeared to be prevented by the use of this charge attenuation option. Unlike 18-crown-6 and its alkali-cation complexes which display relative conformational stabilities dependent on dielectric constant (Wipff *et al.*, 1982), conformational flexibility of the monensin complexes was found to be independent of this factor. To predict more accurately the effect of solvent polarity on conformational dynamics, a solution study such as that made by Painter *et al.* (1982) on the polyether antibiotic, lasalocid A, is required.

Table C.24 : K- and Na-monensin minimization results as a function of dielectric constant, D.

D	ΣU/ kcal.mol^{-1}		RMSD[a]		Displ.[b]/ Å	
	K	Na	K	Na	K	Na
r_{ij}[c]	-31.300	-46.088	0.348	0.240	0.444	0.162
$2r_{ij}$	4.578	14.231	0.221	0.218	0.461	0.106
$4r_{ij}$	19.402	19.572	0.268	0.219	0.396	0.115
1	-114.438	-143.580	0.289	0.363	0.532	1.411
2	-36.192	-45.590	0.274	0.346	0.520	1.479
4	0.616	-4.086	0.232	0.418	0.470	1.398

[a] root mean square deviation of internal coordinates of all atoms

[b] displacement of metal from initial structure position to final structure position

[c] *D* proportional to the distance between atoms i and j

Nonbonding parameters

The TRIPOS force field was found to be inadequate when dealing with the 6-12 potential parameters for alkali-metal ions. Li, Na and K are assigned identical van der Waals radii (R) and well depths (ε). Several researchers have determined nonbonded parameters for these metals, values being specific to the force field used. Lifson *et al.* (1983) employed a Lennard-Jones potential of the form $2\varepsilon(r^*/r)^9 - 3\varepsilon(r^*/r)^6$ in their work on polylactone macrocycles, and resorted to a "learned guess" of ε and r^* which led to satisfactory calculation results. Grootenhuis and Kollman (1989) derived the 6-12 potential parameters by varying them to reproduce experimental interaction energies and metal-oxygen distances as calculated by *ab initio* methods for alkali cation-water complexes. Twyford (1993), in his work on simulating the dynamics of alkali-metal ions in solution with SYBYL, found nonbonded parameters using a method similar to that of Grootenhuis *et al.* (1989). He used crystal ionic radii (Shannon, 1976) as a basis for calculations. These latter parameters, referred to here as parameter set 1, were used as a starting point for parameterization of the TRIPOS force field in this study.

At fixed, chosen ε values, van der Waals radii for K and Na were varied and several of their complexes, including monensin, 18C6, DB18C6, DB30C10, valinomycin and A204A, minimized. Initial and final structures were then compared visually and RMSD values obtained. Since no relationship appeared to exist between R and RMSD, a simplex optimization method could not be employed and force constants had to be fitted using a trial and error procedure. Monensin results from two R and ε parameter sets are shown in Table C.25. With all parameters tried, difficulty was met in preventing the Na^+ ion in the minimized molecules from being displaced too far away from its initial position.

Table C.25 : Nonbonded parameters for Na and K, and corresponding monensin complex reproduction.

	Metal ion	R/ Å	ε/ kcal.mol^{-1}	RMSD[a]	Displ.[b]/ Å
Parameter set 1	Na	1.3	0.2	0.363	1.411
	K	1.7	0.35	0.289	0.532
Parameter set 2	Na	1.75	0.2	0.443	0.825
	K	1.75	0.35	0.306	0.482

[a] root mean square deviation of internal coordinates of all atoms

[b] displacement of metal from initial structure position to final structure position

When an earlier SYBYL version was employed, one of the central causes of structure collapse was the disruption of hydrogen bonds (shown in Figure C.31). Better accountability for hydrogen bonding in SYBYL Version 6.0 improved structure reproduction. The default scaling term of 0.7 was found to yield the most favourable results. The lack of a hydrogen bonding function in the MHB force field (McDougall *et al.*, 1978) forced the discontinuance of this force field in these calculations.

Other variables such as minimization procedure, minimizer termination option and interaction cut-off points were maintained at TRIPOS force field default values. Attempts to solve these MM calculations with the MM2 force field (Allinger, 1976) were unsuccessful. Problems encountered were thought to be due to the poor minimizer of MM2.

C.4.3 Comparison with previous molecular mechanics studies

It can be seen from the above results that parameter optimization for this study of polyether antibiotics is complicated. Indeed, with the ionic bonding approach, no common parameter set was found which yielded superior structure reproduction for every compound tested. To assess the performance of the TRIPOS force field on alkali-metal complexes, molecular mechanics calculations were carried out on 18-crown-6 and valinomycin. Both have been previously subjected to such calculations. Their structures are illustrated in Figure C.34. Coordination to alkali-metals is via oxygen donors, the metals being enclosed within a cavity. The cyclic nature of these ligands allow for the presence of a preformed cavity whereas the acyclic polyether antibiotics rely on hydrogen bonding for cavity formation. Results obtained here were compared to those from previous molecular modeling studies.

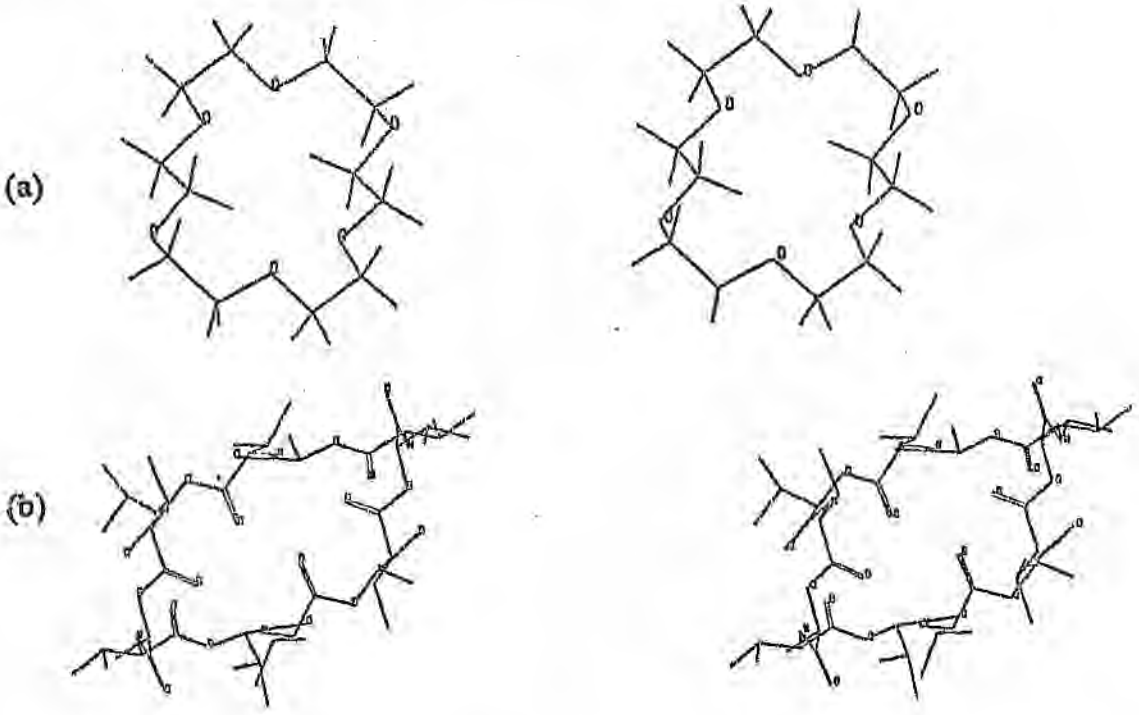

Figure C.34 : The structures of (a) 18-crown-6 and (b) valinomycin. H-atoms have been omitted for (b).

C.4.3.1 18-crown-6

As starting geometries for the MM calculations on the crown ether and its cation complexes, literature X-ray data were used[59-61].

The flexibility of 18C6 allows it to adopt different conformations when complexing different species. Recent molecular dynamics studies by Leuwerink *et al.* (1993) predict correctly conformations assumed in the solid state: D_{3d} for the K^+ and Rb^+ complexes, an irregular C_1 conformation for the Na^+ complex, and C_i for the free crown. Conformations are thus sensitive to metal ion radius. Bigger ions offer a closer fit to the cavity size of the stable D_{3d} form, while smaller ions cause the molecule to adopt a form which allows for closer approach of the ion and donor atoms. (See Figure C.35.) These were also the findings of Wipff *et al.* (1982) who calculated relative conformer energies via MM. Using their procedure, strain energies of the same conformers were calculated with the TRIPOS force field. Nonbonding parameters were taken from set 1, and the dielectric constant set to unity (see previous section). A comparison of results is given in Table C.26.

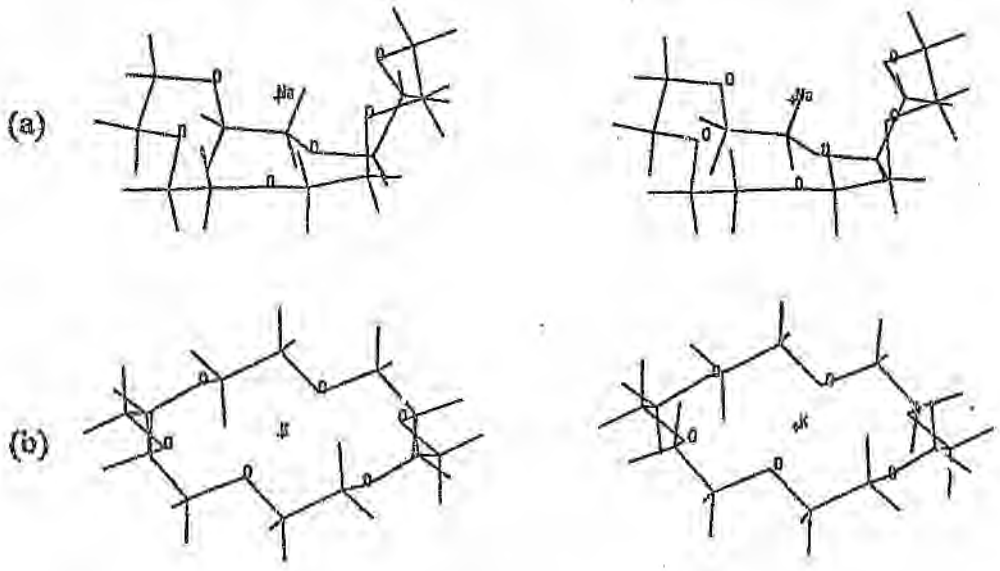

Figure C.35 : Structures of (a) $[Na(18C6)]^+$ and (b) $[K(18C6)]^+$. The Na^+ complex is in the C_1 conformer, and the K^+ complex in the D_{3d} conformer.

Table C.26 : Summary of total energies (kcal.mol^{-1}) of 18C6 uncomplexed and complexed.

	Conformation		
	D_{3d}	C_i	C_1
uncomplexed crown			
Wipff *et al.*[a]	193.3	181.4	202.3
this work[b]	60.643	47.383	70.508
K^+ complex			
Wipff *et al.*[a]	119.6	134.7	126.7
this work	-16.296[c]	25.781	-13.877
Na^+ complex			
Wipff *et al.*[a]	114.6	137.6	111.5
this work	-16.333	6.823	-27.245[d]

[a] charge of -0.6 on coordinated oxygens

[b] RMSD: D_{3d} = 0.132, C_i = 0.170, C_1 = 0.125

[c] RMSD = 0.0928

[d] RMSD = 0.304

Yamabe *et al.* (1979) and Wipff *et al.* (1982) concluded from their research that relative solvation made the largest contribution to the selectivity of 18C6 for certain cations. Thus, hydration energies must be taken into account when examining specificities. The reaction energy, ΔE, for

$$M_1^+(H_2O)_6 + M_2^+/\text{crown} \rightarrow M_2^+(H_2O)_6 + M_1^+/\text{crown} \qquad (1)$$

was calculated to be -15.7 kcal.mol^{-1}, where M_1 = K, M_2 = Na, $-E_T(K^+(H_2O)_6)$ = 65.4 and $-E_T(Na^+(H_2O)_6)$ = 89.2 (Wipff *et al.*, 1982). This is in agreement with

experimental stabilization energies which indicate the crown ether's preference, in aqueous solution, for K^+. In the present study, ΔE for reaction (1) was calculated to be -14.4 kcal.mol^{-1}. The cation hydration energies of -81.5 for K and -106.6 for Na were taken from Twyford (1993).

The TRIPOS force field yielded satisfactory results with regard to the above calculations. The same order in conformation energies as that found in the literature was obtained, and 18C6's relative affinity for K^+ over Na^+ was affirmed.

C.4.3.2 Valinomycin

Valinomycin is one of the most extensively studied ionophores. It is a cyclic depsipeptidic antibiotic which selectively enhances potassium permeability across membranes. Its K^+/Na^+ selectivity ratio is actually the largest known to date. Gresh and Pullman (1985) used *ab initio* to calculate interaction energies between the alkali-metal ions and valinomycin. T' energies were attained by placing the ions at variable locations within the cav' the potassium ionophore. To obtain the correct order of prefere. 'al binding, determined experimentally, they also took desolvation energies of the ions into consideration. Their final affinity sequence was of the order: $Rb^+>K^+>Cs^+>Na^+$. Masui and Kushick (1985) used molecular mechanics in their investigation. Again, K^+-valinomycin was the base complex. Their selectivity preference order was: $Cs^+>Rb^+>K^+>Na^+>Li^+$. High strain energies for the Na^+ and Li^+ complexes were attributed to the rigidity of the valinomycin central cavity which does not allow for accommodation of smaller ions.

Calculations with the TRIPOS parameters incorporated both K^+- and Na^+-valinomycin crystal structures[62,63]. Strain energy values obtained were 3.793 kcal.mol^{-1} for K^+ and 0.629 kcal.mol^{-1} for Na^+. As with 18C6, ΔE for the reaction

$$M_1^+(H_2O)_6 + M_2^+/\text{valinomycin} \rightarrow M_2^+(H_2O)_6 + M_1^+/\text{valinomycin},$$

where M_1 = K and M_2 = Na, was evaluated and found to be -22.14 kcal.mol^{-1}.

Although these results correlate with affinities in the literature, structure reproduction of the Na^+ complex was not good. Figure C.36 shows initial and minimized structures of the valinomycin compounds. The distance moved by K^+ during minimization was 0.083 Å, while that moved by Na^+ was much greater at 1.821 Å. Respective RMSD values for K- and Na-valinomycin were 0.242 and 0.357.

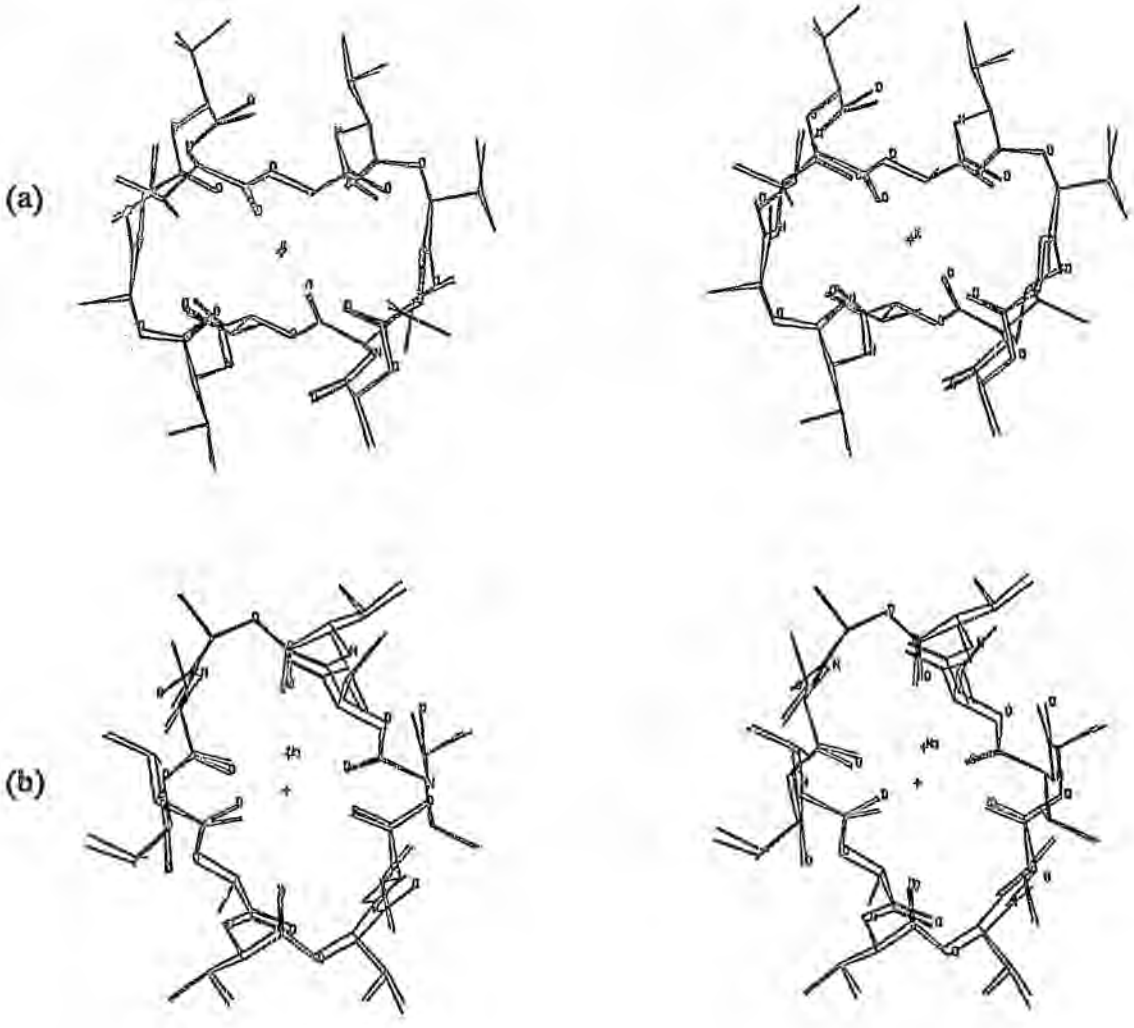

Figure C.36 : Stereoviews of initial and final energy minimized structures of (a) K^+-valinomycin and (b) Na^+-valinomycin.

C.4.4 Application to monensin and related polyether antibiotics

Predicted selectivities for monensin and related polyether antibiotics, obtained using the ionic assumption, are presented in this section. However, it must be remembered that calculated strain energy values are sensitive to the force field used, especially where flexible ligands such as these are concerned. Mis-parametrization may thus lead to inconsistent conclusions.

With reference to the equation in section A.4.3,

$$\Delta G_{ML} = \Delta G_{M(desolv)} + \Delta G_{L(desolv)} + \Delta G_{L(conf)} - \Delta G_{int}$$

ΔG_{int} values were obtained for several polyether antibiotics from energy minimizations. These, together with calculated ΔG_{ML} values, are presented in Table C.27. $\Delta G_{M(desolv)}$ quantities were again taken from Twyford (1993). Ligand and complex solvation energies were assumed to be negligible. Since these molecules did not appear to vary much in conformation when proceeding from the uncomplexed to the complexed state, $\Delta G_{L(conf)}$ was also not considered. The cavity in which the cation sits thus appears to be preformed before coordination. Structural formulae for the relevant ligands can be seen in Figure A.5. Crystal structure data were used as starting coordinates for the minimizations.

Table C.27 : Calculated ΔG values for monensin and related polyether antibiotics. Nonbonded parameter set 1, dielectric constant=1, Gasteiger-Marsilli charge calculations.

Ligand	Metal ion	ΔG_{int}/ kcal.mol^{-1}	ΔG_{MI}/ kcal.mol^{-1}	ΔE^a/ kcal.mol^{-1}	Reference[b]
monensin A	K^+	-114.438	32.938	3.842	Pangborn *et al.*, 1987a
	Na^+	-143.580	36.780		Duax *et al.*, 1980
monensin B	Na^+	-146.280	39.480		64
nigericin	Na^+	-135.602	28.802		65
A204A	K^+	-117.883	36.383	0.139	66
	Na^+	-143.322	36.522		Pangborn *et al.*, 1987b

[a] calculated as in section C.4.3 with M_1 = K and M_2 = Na

[b] crystal structure data

Although the positive ΔE value for monensin A correlated with the selectivity preference of the ligand for Na^+ over K^+, ΔE obtained for A204A incorrectly predicted the same pattern. On comparison of the different energies comprising ΔG_{int}, electrostatic energy was again found to be the central cause of strain energy difference between K and Na complexes.

Walba and Hermsmeier (1985) have shown that monensin B has diminished affinity for both K^+ and Na^+ relative to monensin A, but is still more selective for Na^+ over K^+. The fact that small structural changes, such as that between monensin A and B,

can have a measurable effect on binding makes proper parametrization of the force field in MM calculations even more vital. Energy results obtained here for Na monensin A and Na monensin B gave no clear indication as to which structural factors cause cation discrimination.

The effect of variance in dielectric constant and van der Waals parameters on ΔE is seen in Table C.28. Although improved structure reproducibility was gained with parameter set 2 and $\varepsilon = 4r_{ij}$, especially with the Na complexes, ΔE values for monensin were negative. With 18C6 and valinomycin, their very high preferences for K^+ over Na^+ always led to calculations yielding negative ΔE's. Where differences in specificity were less marked, as with monensin, it was obvious that the force field failed.

Table C.28 : Calculated ΔE^a, RMSD and metal displacement values as a function of nonbonded parameters and dielectric constant, D.

D		Ligand	Metal ion	RMSD	Displ./ Å	ΔE/ kcal.mol^{-1}
1	Parameter set 1	monensin A	K^+	0.289	0.532	3.842
			Na^+	0.363	1.411	
		A204A	K^+	0.323	0.149	0.139
			Na^+	0.367	0.553	
	Parameter set 2	monensin A	K^+	0.306	0.482	-15.092
			Na^+	0.443	0.825	
		A204A	K^+	0.320	0.132	-21.735
			Na^+	0.255	0.169	
$4r_{ij}$	Parameter set 1	monensin A	K^+	0.268	0.396	-25.47
			Na^+	0.219	0.115	
		A204A	K^+	0.227	0.086	-19.596
			Na^+	0.273	0.196	
	Parameter set 2	monensin A	K^+	0.230	0.416	-26.413
			Na^+	0.336	0.663	
		A204A	K^+	0.230	0.093	-24.688
			Na^+	0.274	0.368	

[a] calculated as in section C.4.3 with M_1 = K and M_2 = Na

D. CONCLUSIONS

The preference of ligands, which upon complexation form four-membered chelate rings, for larger metal ions, as witnessed by the abundance of stable calcium-acetate complexes of highly variable coordination number, is consolidated with molecul mechanics calculations. The previously established trend, observed for five- and six-membered chelate rings, has proved valid for four-membered rings. The larger the chelate ring size, the smaller the metal selected, and vice versa.

This effect may assist in the explanation of metal ion discrimination by carboxylate, acetate and phosphate groups in biochemical systems.

The effect of conformational flexibility of unsubstituted azamacrocycles on macrocycle selectivity is noted. Flexible ligands are able to fulfil specific geometric requirements of certain small metal ions, thus explaining literature selectivities, crystal structures and conformations in solution. The mode of complexation is governed by the same principles as open-chain polyamines, the chelate ring size effect. To achieve selectivity based on cavity size, more rigid macrocycle structures are required.

Complexation of nitrogen-substituted open-chain ligands with metal ions also complies with the chelate ring size effect. However, nitrogen-substituted azamacrocycles, which are less flexible than their unsubstituted counterparts seem to follow the "cavity size-match" selectivity rule. Due to their higher coordinating ability, these macrocycles are able to accommodate larger metals, especially when cavity size is too small. Pendent donor groups enhance donor atom basicity, prevent ligand folding thus stiffening the macrocyclic ring and improving preorganization, and introduce steric crowding into the coordination sphere of small metals thus denying them access to solvent molecules. Here, steric requirements of the ligand alone governs stereochemistry of

the complex. DOTA, with its preformed internal cavity of eight donor sites is well suited to wrap around lanthanide(III) and Group(III) metal ions, leading to the establishment of safe and effective contrast agents for nuclear MRI.

Agreement between predicted and experimental data shows that the TRIPOS force field performs satisfactorily with univariate scanning of simple open-chain and macrocyclic ligands. Setting the donor atom-metal-donor atom angle bending constant to zero so that stereochemistry depends entirely on coordination geometry of the metal appears to be justified.

The force field does not perform efficiently in the reproduction of polyether antibiotic structures when the ionic bonding situation is assumed. This results in errors in thermodynamic predictions for sodium and potassium complexes, which are likely due to intrinsic faults of the force field. Modifications to the force field include the parameterization of van der Waals parameters and the dielectric function. These lead to moderately enhanced structure reproduction. Electrostatic effects, including the improper allocation of partial atomic charges, are thought to be the main cause of poor TRIPOS performance. When electrostatic effects are ignored and covalent bonding between metal and donor atoms is assumed, structure reproduction is good and the correct prediction of metal selectivity for monensin is obtained.

Aime,S., Botta,M., Ermondi,G. (1992). *Inorg. Chem.*, 31, 4291.

Ahlström,P., Teleman,O., Kördel,J., Forsén,S., Jönsson,B. (1989). *Biochem.*, 28, 3205.

Allinger,N.L. (1976). *Adv. Phys. Org. Chem.*, 13, 1.

Artz,S.P., Cram,D.J. (1984). *J. Am. Chem. Soc.*, 106, 2160.

Auerbach,U., Eckert,U., Wieghardt,K., Nuber,B., Weiss,J. (1990). *J. Inorg. Chem.*, 29, 938.

Bernhardt,P.V., Comba,P. (1991). *Helv. Chim. Acta.*, 74, 1834.

Bernhardt,P.V., Comba,P. (1992). *Inorg. Chem.*, 31, 2638.

Bond,A.M., Hambley,T.W., Mann,D.R., Snow,M.R. (1987). *Inorg. Chem.*, 26, 2257.

Bond,A.M., Hambley,T.W., Snow,M.R. (1985). *Inorg. Chem.*, 24, 1920.

Bosnich,B., Mason,R., Pauling,P.J., Robertson,G.B., Tobe,M.L. (1965). *J. Chem. Soc., Chem. Commun.*, 97.

Bowen,J.P., Cory,M. (1991). *"Encyclopaedia of Pharmaceutical Technology."* Vol.3, 167, Marcel Dekker Inc., N.Y.

Boyd,R.H., Breitling,S.M., Mansfield,M. (1973). *Am. Inst. Chem. Eng. J.*, 19, 1016.

Brecknell,D.J., Raber,D.J., Ferguson,D.M. (1985). *J. Mol. Struct. (Theochem.)*, 124, 343.

Broan,C.J., Cox,J.P.L., Craig,A.S., Kataky,R., Parker,D., Harrison,A., Randall,A.M., Ferguson,G. (1991). *J. Chem. Soc. Perkin Trans. 2*, 87.

Brooks,B.R., Bruccoleri,R.E., Olafson,B.D., States,D.J., Swaminathan,S., Karplus,M. (1983). *J. Comput. Chem.*, 4, 187.

Brubaker,G.R., Johnson,D.W. (1984). *Coord. Chem. Rev.*, 53, 1.

Burkert,U., Allinger,N.L. (1982). *ACS Monograph 177, American Chem.Soc.*, Washington,D.C.

Cabbiness,D.K., Margerum,D.W. (1969). *J. Am. Chem. Soc.*, 91, 6540.

Cacheris,W.P., Nickle,S.P., Sherry,A.D. (1987). *Inorg. Chem.*, 26, 958.

Chaudhuri,P., Wieghardt,K. (1987). *Progr. Inorg. Chem.*, 35, 329.

Clark,M., Cramer III,R.D., van Opdenbosch,N. (1989). *J. Comput. Chem.*, 10, 8, 982.

Clarke,E.T., Martell,A.E. (1991a). *Inorg. Chim. Acta*, 181, 273.

Clarke,E.T., Martell,A.E. (1991b). *Inorg. Chim. Acta,* 186, 103.

Clarke,E.T., Martell,A.E. (1991c). *Inorg. Chim. Acta,* 190, 27.

Clarke,E.T., Martell,A.E. (1991d). *Inorg. Chim. Acta,* 190, 37.

Cohen,N.C., Blaney,J.M., Humblet,C., Gund,P., Barry,D.C. (1990). *J. Med. Chem.,* V33, 3, 883.

Comba,P. (1993). *Coord. Chem. Rev.,* 123, 1.

Corey,E.J., Bailar,J.C. (1959). *J. Am. Chem. Soc.,* 81, 2620.

Cortes,S., Brucher,E., Geraldes,C.F.G.C., Sherry,A.D. (1990). *Inorg. Chem.,* 29, 5.

Cotton,F.A., Wilkinson,G. (1980). *"Advanced Inorganic Chemistry,"* 4th ed., John Wiley & Sons, Inc. New York, 132.

Cox,J.P.L., Jankowski,K.J., Kataky,R., Parker,D., Beeley,N.R.A., Boyce,B.A., Eaton, M.A.W., Millar,K., Millican,A.T., Harrison,A., Walker,C. (1989). *J. Chem. Soc., Chem. Commun.,* 797.

Cram,D.J., Kaneda,T., Helgeson,R.C., Brown,S.B., Knobler,C.B., Maverick,E., Trueblood,K.N. (1985). *J. Am. Chem. Soc.,* 207, 3645.

Dale,J. (1973). *Acta Chem. Scand.,* 27, 1115 & 1130.

De Hayes,L.J., Busch,D.H. (1973). *Inorg. Chem.,* 12, 1505.

Del Re,G. (1958). *J. Chem. Soc.,* 4031.

Deutsch,E., Libson,K., Jurisson,S., Lindoy,L.F (1983). *Progr. Inorg. Chem.,* 30, 75.

Dostrovsky,I., Hughes,E.D., Ingold,C.K. (1946). *J. Chem. Soc.,* 173.

Drew,M.G.B., Hollis,S., Yates,P.C. (1985). *J. Chem. Soc. Dalton Trans.,* 1829.

Drew,M.G.B., Santos,M.A. (1993). *Structural Chem.,* 4, 5.

Duax,W.L., Smith,G.D., Strong,P.D. (1980). *J. Am. Chem. Soc.,* 102, 6725.

Fabbrizzi,L. (1977). *Inorg. Chem.,* 16, 2667.

Ferguson,D.M., Raber,D.J. (1989). *J. Am. Chem. Soc.,* 111, 4371.

Fossheim,R., Dahl,S.G. (1990). *Acta Chem. Scand.,* 44, 698.

Fossheim,R., Dugstad, H., Dahl,S.G. (1991). *J. Med. Chem.,* 34, 819.

Gasteiger,J., Marsili,M. (1980). *Tetrahedron,* V36, 3219.

Geddes,A.J., Sheldrick,B., Stevenson,W.T.J. (1974). *Biochem. and Biophys. Res. Commun.,* V60, 1245.

Goldman,S., Bates,R. (1972). *J. Am. Chem. Soc.,* 94, 1476.

Gollogly,J.R., Hawkins,C.J. (1969). *Inorg. Chem.,* 8, 1168.

Gresh,N., Pullman,A. (1985). *"Metal Ions in Biological Systems,"* V19, Ch. 12, Marcel Dekker Inc., N.Y.

Grootenhuis,P.D.J., Kollman,P.A. (1989). *J. Am. Chem. Soc.*, 111, 2152.

Gundertofte,K., Palm,J., Pettersson,I., Stamvik,A. (1991). *J. Comp. Chem.*, V12, 2, 200.

Hancock,R.D. (1986). *Pure and Appl. Chem.*, V58, 11, 1445.

Hancock,R.D. (1989). *Progr. Inorg. Chem.*, 37, 187.

Hancock,R.D. (1990). *Acc. Chem. Res.*, 23, 253.

Hancock,R.D. (1992). *J. Chem. Ed.*, 69, 615.

Hancock,R.D., Dobson,S.M., Boeyens,J.C.A. (1988). *Inorg. Chim. Acta.*, 133,

Hancock,R.D., Evers,A., Ngwenya,M.P., Wade,P.W. (1987). *J. Chem. Soc.,Chem. Commun.*, 1129.

Hancock,R.D., Martell,A.E. (1989). *Chem. Rev.*, V89, 8, 1875.

Hancock,R.D., McDougall,G.J. (1980). *J. Am. Chem. Soc.*, 102, 6551.

Hancock,R.D., Nakani,B.S., Marsicano,F. (1983). *Inorg. Chem.*, 22, 2531.

Hancock,R.D., Shaikjee,M.S., Dobson,S.M., Boeyens,J.C.A. (1988). *Inorg. Chim. Acta*, 194, 229.

Hay,B.P. (1991). *Inorg. Chem.*, 30, 2876.

Hay,B.P., Rustad,J.R., Hostetler,C.J. (1993). *J. Am. Chem. Soc.*, 115, 11158.

Hay,R.W., Pujari,M.P. (1986). *J. Chem. Soc. Dalton Trans.*, 1485.

Hebrant,M., Pointud,Y., Juillard,J. (1991). *J. Phys. Chem.*, 95, 3653.

Henrick,K., Tasker,P.A., Lindoy,L.F. (1985). *Progr. Inorg. Chem.*, 33, 1.

Hill,T.L. (1946). *J. Chem. Phys.*, 14, 465.

Hoeft,S., Roth,K. (1993). *Chemische Berichte*, 126, 869.

Hughes,M.N., Birch,N.J. (1982). *Chemistry in Britain*, March, 196.

Izatt,R.M., Pawlak,K., Bradshaw,J.S. (1991). *Chem. Rev.*, 91, 1721.

Jorgensen,W.L., Tirado-Rives,J. (1988). *J. Am. Chem. Soc*, 110, 1657.

Kodama,M., Kimura,E. (1978). *J. Chem. Soc. Dalton.*, 1081.

Lauffer,R.B. (1987). *Chem. Rev.*, 87, 901.

Lehn,J.M. (1978). *Acc. Chem. Res.*, 11, 49.

Leuwerink,F.T.H., Harkema,S., Briele,W.J., Feil,D. (1993). *J. Comp. Chem.*, V14, 899.

Lifson,S., Felder,C.E., Shanzer,A. (1983). *J. Am. Chem. Soc.*, 105, 3866.

Lifson,S., Warshel,J. (1968). *J. Chem. Phys.*, 49, 5116.

Lindoy,L.F. (1989). "*The Chemistry of Macrocyclic Ligand Complexes,*" Cambridge University Press, Cambridge.

Loncin,M.F., Desreux,J.F., Merciny,E. (1986). *Inorg. Chem.*, 25, 2646.

Luckay,R.C., Hancock,R.D. (1991). *J. Chem. Soc. Dalton Trans.*, 1491.

Lutz,W.K., Fruh,P.U., Simon,W. (1971). *Helv. Chim. Acta*, 54, 2768.

Lutz,W.K., Winkler,F.K., Dunitz,J.D. (1971). *Helv. Chim. Acta*, 54, 1103.

Martell,A.E., Smith,R.M. (1974-77, 1982, 1989). "*Critical Stability Constants,*" Plenum, New York.

Martin,A.M., Billo,E.J., Grant,K.J. (1986). *Inorg. Chem.*, 25, 4904.

Martin,L.Y., De Hayes,L.J., Zompa,L.F., Busch,D.H. (1974). *J. Am. Chem. Soc.*, 96, 4046.

Masut,R.A., Kushick,J.N. (1985). *J. Comp. Chem.*, V6, 148.

Mathias,C.J., Sun,Y., Ccunett,J.M., Philpott,G.W., Welch,M.J., Martell,A.E. (1990). *Inorg. Chem.*, V29, 8, 1475.

May,P.M., Bulman,R.A. (1983). *Prog. Med. Chem.*, 20, 226.

McDougall,G.J., Hancock,R.D., Boeyens,J.C.A. (1978). *J. Chem. Soc. Dalton Trans.*, 1438.

McMurray,W., Begg,R. (1959). *Arch. Biochem. Biophys.*, 84, 546.

Meyers,R.T. (1978). *Inorg. Chem.*, 17, 952.

Monsted,L., Monsted,O., Nord,G., Simonsen,K. (1993). *Acta Chem. Scand.*, 47, 439.

Momany,F.A., McGuire,R.F., Burgess,A.W., Scheraga,H.A. (1975). *J. Phys. Chem.*, 79, 2361.

Moore,D.A., Fanwick,P.E., Welch,M.J. (1989). *Inorg. Chem.*, 28, 1504.

Ohtaki,H., Seki,H. (1990). *J. Macromol. Sc. Chem.*, A27, 1305.

Paine,G.H., Scheraga,H.A. (1985). *Biopolymers.*, 24, 1391.

Painter,G.R., Pollock,R., Pressman,B.C. (1982). *Biochemistry*, 21, 5613.

Painter,G.R., Pressman,B.C. (1985). "*Metal Ions in Biological Systems,*" Vol. 19, Ch. 9, Marcel Dekker Inc., New York.

Pangborn,W., Duax,W., Langs,D. (1987a). *J. Am. Chem. Soc.*, 109, 2163.

Pangborn,W., Duax,W., Langs,D. (1987b). *Acta Cryst.*, C43, 890.

Parker,D. (1990). *Chem. Soc. Rev.*, 19, 271.

Parker,D., Pulukkody,K., Norman,T.J., Harrison,A., Royle,L., Walker,C. (1992). *J. Chem. Soc., Chem. Commun.*, 19, 1441.

Pearson,R.G. (1963). *J. Am. Chem. Soc.*, 85, 3533.

Pedersen,C.J. (1967). *J. Am. Chem. Soc.*, 89, 2459.

Pinkerton,M., Steinrauf,L.K. (1970). *J. Mol. Biol.*, 49, 533.

Pressman,B.C. (1965). *Proc. Natl. Acad. Sci. USA*, 53, 1076.

Pressman,B.C., de Guzman,N.T. (1975). *Ann. N. Y. Acad. Sci.*, 264, 373.

Ripka,W. (1988). *New Scientist*, June.

Sargeson,A.M. (1984). *Pure Appl. Chem.*, 56, 1603.

Seibel,G.L., Kollman,P.A. (1990). "*Comprehensive Medicinal Chemistry*," Vol. 4, 18.2, 125, Pergamon Press, N.Y.

Shannon,R.D. (1976). *Acta Cryst.*, A32, 751.

Shinkai,S., Koreishi,H., Ueda,K., Arimura,T., Manabe,O. (1987). *J. Am. Chem. Soc.*, 109, 6371.

Smith,P.W., Still,W.C. (1988). *J. Am. Chem. Soc.*, 110, 7917.

Smith,G.D., Strong,P.D., Duax,W.L. (1978). *Acta Cryst.*, B34. 3436.

Steinrauf,L.K., Czerwinski,E.W., Pinkerton,M. (1971). *Biochem. Biophys. Res. Commun.*, V45, 5, 1279.

Stetter,H., Frank,W. (1976). *Aangew. Chem. Int. Ed. Engl.*, V15, 11, 686.

Taylor,R.W., Kauffman,R.F., Pfeiffer,D.R. (1982). "*Polyether Antibiotics. Naturally Occurring Acid Ionophores*," Vol. 2., Ch. 4, Marcel Dekker Inc., N.Y.

Thöm,V.J., Fox,C., Boeyens,J.C.A., Hancock,R.D. (1984). *J. Am. Chem. Soc.*, 106, 5947.

Thöm,V.J., Hancock,R.D. (1985). *J. Chem. Soc. Dalton Trans.*, 1877.

Thöm,V.J., Hosken,G.D., Hancock,R.D. (1985). *Inorg. Chem.*, 24, 3378.

TRIPOS Associates, 1699 S. Hanley Road, St. Louis, MO, SYBYL 5.5 and SYBYL 6.0. (1992, 1993).

Twyford,J.G. (1993). *Private Communication.*

Wade,P.W. (1989). *Ph. D. thesis.*

Walba,D.M., Hermsmeier,M. (1985). *J. Chem. Soc., Chem. Commun.*, 383.

Walba,D.M., Hermsmeier,M., Haltiwanger,R.C., Noordik,J.H. (1986). *J. Org. Chem.*, 51, 245.

Weiner,P.K., Kollman,P.A. (1981). *J. Comput. Chem.*, 2, 287.

Weiner,P.K.,Profeta,S.,Jr.,Wipff,G.,Havel,T.,Kuntz,I.D.,Langridge,R.,Kollman,P.A. (1983). *Tetrahedron*, 39, 1113.

Weiner,S.J., Kollman,P.A., Case,D.A., Singh,U.C., Ghio,C., Alagona,G., Profeta,S., Weiner.P. (1984). *J. Am. Chem. Soc.*, 106, 765.

Westheimer,F.H., Mayer,J.E. (1946). *J. Chem. Phys.*, 14, 733.

Westley,J.W. (1977). *Adv. in Applied Microbiology*, 22, 177.

White,D.N.J. (1977). "*Computers & Chemistry*," Vol. 1, 225, Pergamon Press, U.K.

White,D.N.J., Ruddock,J.N., Edgington,P.R. (1989). "*Computer-Aided Molecular Design*," Ch. 2, IBC Technical Services Ltd., London.

Williams,R.P.J. (1983). *Pure and Appl. Chem.*, 55, 35.

Wipff,G., Weiner,P., Kollman,P. (1982). *J. Am. Chem. Soc.*, 104, 12, 3249.

Yamabe,T., Hori,K., Akagi,K., Fukui,K. (1979). *Tetrahedron*, V35, 1065.

F. CRYSTAL STRUCTURE REFERENCES

1 Bereman,R.D., Churchill,M.R., Schaber,P.M., Winkler,M.E. (1979). *Inorg. Chem.*, 18, 3122.

2 Wieghardt,K., Kleine-Boymann,M. Nuber,B., Weiss,J., Zsolnai,L., Huttner,G. (1986). *Ibid.*, 25, 1647.

3 Bolm,G., Wieghardt,K., Nuber,B., Weiss,J. (1991). *Ibid.*, 30, 3464.

4 Margulis,T.N., Zompa,L.J. (1992). *Inorg. Chim. Acta*, 201, 61.

5 Gajhede,M., Simonsen,K., Skov,L.K. (1993). *Acta Chem. Scand.*, 47, 271.

6 Schaber,P.M., Fettinger,,J.C., Churchill,M.R., Nalewajek,D., Fries,K. (1988). *Inorg. Chem.*, 27, 1641.

7 Kimura,E., Shiota,T., Koike,T., Shiro,M., Kodama,M. (1990). *J. Am. Chem. Soc.*, 112, 5805.

8 Clay,R., Murray-Rust,P., Murray-Rust,J. (1979). *Acta Cryst., Sect. B.*, 35, 1894.

9 Iitaka,Y., Shina,M., Kimura,E. (1974). *Inorg. Chem.*, 13, 2886.

10 Martin,L.Y., Sperati,C.R., Busch,D.H. (1977). *J. Am. Chem. Soc.*, 99, 2968.

11 Waters,J.M., Whittle,K.R. (1972). *J. Inorg. Nucl. Chem.*, 34, 155.

12 Miyamae,H., Yamauchi,K., Yamashita,M. (1991). *J. Chem. Soc. Dalton Trans.*, 2921.

13 Che,C., Tang,W., Wong,W., Lam,H., Lai,T. (1990). *Ibid.*, 2077.

14 Watkins, Jr.,D.D., Riley,D.P., Stone,J.A., Busch,D.A. (1976). *Inorg. Chem.*, 15, 387.

15 Lisgarten,J.N., Palmer,R.A., Hemmings,A.M., Gazi,D.M. (1990). *Acta Cryst., Sect. C.*, 46, 396.

16 Floresvelez,L.M., Sosarivadeneyra,J., Sosatorres,M.J Rosaleshoz,M.J., Toscano,R.A. (1991). *J. Chem. Soc. Dalton Trans.*, 3243.

17 Dealwis,C.G., Janes,R.W., Palmer.R.A., Lisgarten,J.N., Maes,D., Flint,C.D., Gazi,D.M. (1992). *Acta Cryst., Sect. C*, 48, 1754.

18 Chattopadhyay,T.K., Palmer,R.A., Lisgarten,J.N., Wyns,L., Gazi,D.M. (1992). *Ibid.*, 48, 1756.

19 Forsellini,E., Bombieri,G., Parasassi,T., Sosa,M.E., Tobe,M.L. (1986). *Ibid.*,

42, 563.

20 Daugherty,R.A., Glerup,J., Goodson,P.A., Hodgson,D.J., Michelsen,K. (1991). *Acta Chem. Scand.*, 45, 244.

21 Endicott,J.F., Lilie,J., Kuszaj,J.M., Ramaswamy,B.S., Schmonsees,W.G., Simic,M.G., Glick,M.D., Rillema,D.P. (1977). *J. Am. Chem. Soc.*, 99, 429.

22 Ito,T., Kato,M., Ito,H. (1984). *Bull. Chem. Soc. Jpn.*, 57, 2641.

23 Barefield,E.K., Bianchi,A., Billo,E.J., Connolly,P.J., Paoletti,P., Summers,J.S., Van Derveer,D.G. (1986). *Inorg. Chem.*, 25, 4197.

24 Ito,T., Sugimoto,M., Toriumi,K., Ito,H. (1981). *Chem. Lett.*, 1477.

25 Emsley,J., Arif,M., Bates,P.A., Hursthouse,M.B. (1990). *J. Mol. Struct.*, 220, 1.

26 Tasker,P.A., Sklar,L. (1975). *Cryst. Mol. Struct.*, 5, 329.

27 Tyson,T.A., Hodgson,K.O., Hedman,B., Clark,G.R. (1990). *Acta Cryst. C.*, 46, 1638.

28 Alcock,N.W., Berry,A., Moore,P. (1992). *Ibid.*, 48, 16.

29 Toriumi,K., Yamashita,M., Ito,H., Ito,T. (1986). *Ibid.*, 42, 963.

30 Walker,D.D., Taube,H. (1981). *Inorg. Chem.*, 20, 2828.

31 Che,C., Kwong,S., Poon,C., Lai,T., Mak,T.C.W. (1985). *Ibid.*, 24, 1359.

32 Tsang,B.W., Reibenspies,J., Martell,A.E. (1993). *Ibid.*, 32, 988.

33 Zuckman,S.A., Freeman,G.M., Troutner,D.E., Volkert,W.A., Holmes,R.A., Van Derveer,D.G., Barefield,E.K. (1981). *Ibid.*,20, 2386.

34 Alcock,N.W., Curzon,E.H., Herron,N., Moore,P. (1979). *J. Chem. Soc. Dalton Trans.*, 1987.

35 Alcock,N.W., Herron,N., Moore,P. (1979). *Ibid.*, 1486.

36 Ito,T., Ito,H., Toriumi,K. (1981). *Chem. Lett.*, 1101.

37 Lai,T.F., Poon,C.K. (1976). *Inorg. Chem.*, 15, 1562.

38 Fabbrizzi,L., Mealli,C., Paoletti,P. (1979). *J. Chem. Res.*, 170, 2041.

39 Ito,T., Kato,M., Ito,H. (1984). *Bull. Chem. Soc. Jpn.*, 57, 2634.

40 Mak,T.C.W., Che,C., Wong,K. (1985). *J. Chem. Soc. Chem. Commun.*, 986.

41 Richens,D.T., Adzamli,I.K., Leupin,P., Sykes,A.G. (1984). *Inorg. Chem.*, 23, 3065.

42 Bang,E., Eriksen,J., Monsted,O. (1987). *Acta Chem. Scand., Ser. A.*, 41, 506.

43 Alcock,N.W., Curzon,E.H., Moore,P. (1984). *J. Chem. Soc. Dalton Trans.*, 2813.

44 Whitlow,S.H. (1972). *Acta Cryst. Sect. B.*, 28, 1914.

45 Oliver,J.D., Barnett,B.L., Strickland,L.C. (1984). *Ibid.*, 40, 377.

46 Wieghardt,K., Bossek,U., Chaudhuri,P., Herrmann,W., Menke,B.C., Weiss,J. (1982). *Inorg. Chem.*, 21, 4308.

47 Van der Merwe,MJ., Boeyens,J.C.A., Hancock,R.D. (1985). *Ibid.*, 24, 1208.

48 Van der Merwe,MJ., Boeyens,J.C.A., Hancock,R.D. (1983). *Ibid.*, V22, 24, 3490.

49 Jyo,A., Kohno,T., Terazono,Y., Kawano,S. (1990). *Anal. Sci.*, 6, 629.

50 Bossek,U., Hanke,D., Wieghardt,K. (1993). *Poyhedron*, 12, 1.

51 Jyo,A., Kohno,T., Terazono,Y., Kawano,S. (1990). *Anal. Sci.*, 6, 323.

52 Spirlet,M.R., Rebizant,J., Desreux,J.F., Loncin,M.F. (1984). *Inorg. Chem.*, 23, 359.

53 Riesen,A., Zehnder,M., Kaden,T.A. (1986). *Helv. Chim. Acta*, 69, 2067.

54 Riesen,A., Zehnder,M., Kaden,T.A. (1991). *Acta Cryst.*, C47, 531.

55 Riesen,A., Zehnder,M., Kaden,T.A. (1986). *Helv. Chim. Acta*, 69, 2074.

56 Riesen,A., Kaden,T.A., Ritter,W., Mäcke,H.R. (1989). *J. Chem. Soc., Chem. Commun.*, 460.

57 Spirlet,M.R., Rebizant,J., Loncin,M.F., Desreux,J.F. (1984). *Inorg. Chem.*, 23, 4278.

58 Riesen,A., Zehnder,M., Kaden,T.A. (1988). *Acta Cryst.*, C44, 1740.

59 Dunitz,D.J., Dobler,M., Seiler,P., Phizackerley,R.P. (1974). *Acta Cryst.*, B30, 2733.

60 Seiler,P., Dobler,M., Dunitz,J.D. (1974). *Ibid.*, B30, 2744.

61 Dobler,M., Dunitz,J.D., Seiler,P. (1974). *Ibid.*, B30, 2741.

62 Hamilton,J.A., Sabeson,M.N., Steinrauf,L.K. (1981). *J. Am. Chem. Soc.*, 103, 5880.

63 Steinrauf,L.K., Hamilton,J.A., Sabeson,M.N. (1982). *Ibid.*, 104, 4085.

64 Barrans,Y., Alleaume,M., Jeminet,G. (1982). *Acta Cryst.*, B38, 1144.

65 Barrans,Y., Alleaume,M., David,L. (1980). *Ibid.*, B36, 936.

66 Jones,N.D., Chaney,M.O., Chamberlin,J.W., Hamill,R.L., Chen,S (1973).

J. Am. Chem. Soc., 95, 3399.

Author: Chantson, Tracy Elizabeth.
Name of thesis: A molecular mechanics study of ligands for selective complexation of metal ions in medical applications.

PUBLISHER:
University of the Witwatersrand, Johannesburg
©2015

LEGALNOTICES:

Copyright Notice: All materials on the University of the Witwatersrand, Johannesburg Library website are protected by South African copyright law and may not be distributed, transmitted, displayed or otherwise published in any format, without the prior written permission of the copyright owner.

Disclaimer and Terms of Use: Provided that you maintain all copyright and other notices contained therein, you may download material (one machine readable copy and one print copy per page)for your personal and/or educational non-commercial use only.

The University of the Witwatersrand, Johannesburg, is not responsible for any errors or omissions and excludes any and all liability for any errors in or omissions from the information on the Library website.